SIMULATION STUDIES ON ROGOWSKI COIL BASED CURRENT MEASUREMENT SYSTEM CONSIDERING PARTIALLY DISTRIBUTED PARAMETER MODEL

By MANDIP KAMI

Course affiliated to
Faculty of Engineering and Technology
Department of Electrical Engineering
Jadavpur University
Kolkata, West Bengal 700032

2022

SIMULATION STUDIES ON ROGOWSKI COIL BASED CURRENT MEASUREMENT SYSTEM CONSIDERING PARTIALLY DISTRIBUTED PARAMETER MODEL

A dissertation submitted in partial fulfilment of the requirements for the degree of

Master of Electrical Engineering

In

Electrical Measurement and Instrumentation

By

MANDIP KAMI

Roll No: M4ELE22011

Registration Number: 154001 of 2020-21

Under the Guidance of

Prof. Sugata Munshi

And

Associate Prof. Biswajit Bhattacharyya

Course affiliated to
Faculty of Engineering and Technology
Department of Electrical Engineering
Jadavpur University
Kolkata, West Bengal 700032

2022

M.E. (ELECTRICAL ENGINEERING)

Course affiliated

Faculty of Engineering and Technology

Jadavpur University

Kolkata, West Bengal 700032

CERTIFICATE OF RECOMMENDATION

*This is to certify that the thesis entitled "***Simulation Studies On Rogowski Coil Based Current Measurement System Considering Partially Distributed Parameter Model***" By SRI* MANDIP KAMI (M4ELE22011)*, submitted to the Jadavpur University Kolkata, West Bengal for the award of Master of Electrical Engineering in Electrical Measurement and Instrumentation is a record of Bonafede research work carried out by him in the Department of Electrical Engineering, under my supervision. I believe that this thesis fulfils part of the requirements for the award of degree of Master of Electrical Engineering during the academic session 2020- 2022. The results embodied in the thesis have not been submitted for the award of any other degree elsewhere.*

.....	.....
PROF Dr. SASWATI MAZUMDAR	PROF.SUGATA MUNSHI
HEAD ELECTRICAL ENGG. DEPT.	ELECTRICAL ENGG DEPT
JADAVPUR UNIVERSITY	JADAVPUR UNIVERSITY
.....	.....
Associate Prof. BISWAJIT BHATTACHARYYA	PROF. CHANDAN MAJUMDER
ELECTRICAL ENGG DEPT	DEAN-FACULTY OF ENGINEERING
JADAVPUR UNIVERSITY	AND TECHNOLOGY
	JADAVPUR UNIVERSITY

M.E. (ELECTRICAL ENGINEERING)

Course affiliated

Faculty of Engineering and Technology

Jadavpur University

Kolkata, West Bengal 700032

CERTIFICATE OF APPROVAL

This foregoing thesis is hereby approved as a credible study of an engineering subject carried out and presented in a manner satisfactorily to warranty its acceptance as a prerequisite to the degree for which it has been submitted. It is understood that by this approval the undersigned do not endorse or approve any statement made or opinion expressed or conclusion drawn therein but approve the thesis only for purpose for which it has been submitted.

Committee of final examination ----------

For evaluation of Thesis

DECLARATION OF ORIGINALITY AND COMPLIANCE OF ACADEMIC ETHICS

I hereby declare that this thesis contains literature survey and original research work by the undersigned candidate, as part of his **M.E. (ELECTRICAL ENGINEERING)** studies during academic session 2020-2022. All information in this document has been obtained and presented in accordance with academic rules and ethical conduct.

I also declare that, as required by this rules and conduct, I have fully cited and referred all material and results that are not original to this work.

NAME: **MANDIP KAMI**

ROLL NUMBER: **M4ELE22011**

THESIS TITLE

"Simulation Studies On Rogowski Coil Based Current Measurement System Considering Partially Distributed Parameter Model"

SIGNATURE: DATE:

Acknowledgment

Most real spirit is to achieve a goal through a way of perfection. The achievement, which I have gain, cannot be possible without the cooperation of numerous personalities.

I am very much thankful to various personalities who helps me a lot for structuring my thesis. At the outset, I would like to express my thanks to Prof. Sugata Munshi and Associate prof. Biswajit Bhattacharyya for their guidance, supervision during this research work. As a guide, their advice always encourages me and helps me a lot to and out suitable way for successful completion of this work. Their idea, observations help me to enrich my knowledge.

I express my heartfelt thanks to all the faculty members of the Electrical Measurement and Instrumentation Section, Department of electrical Engineering, Jadavpur University for their advice, support, encouragement and valuable comments.

I am grateful that I got lovely opportunity to study in one of the best universities and under some of the best faculties, it really changed my life.

I am sincerely thankful to all my friends, without whom, this journey would not be this much pleasant.

I am also grateful to my family for their blessing, advice and moral support. I want to dedicate this work to them which could not be fulfilled without their love and blessing.

Mandip Kami

Contents

Chapter 3: Investigation and Results

Chapter 1: INTRODUCTION

INTRODUCTION

In industries and plants, the most used devices for sensing alternating current, and scaling it down to the level compatible with measuring instruments and relays are current transformers (CT). This type of devices has primary and secondary ends where the primary winding carries the current to be measured and the secondary winding feeds the measuring instrument or the protective relay. Most frequently the CT does not have an explicit primary winding. The conductor carrying the current to be sensed, forms the single-turn primary, and passes through the aperture of the CT core. A current transformer is primarily described by its current ratio from primary to secondary. A 500 A/ 5 A CT will provide a current of 5A in its secondary when 500 A current flows through the primary of the CT. Other specifications of the CT are the VA burden and some indication of the type (metering or protection) and the accuracy. The CT can experience a large inrush current in the primary side when it is connected to the primary of surge protection system of any plants. The high frequency current with large magnitude flowing through the primary leads to non-uniform distribution of flux in the primary, which results in instant magnetic saturation of the core. So due to these above reasons the current transformer is not preferable for the applications such in the fields like precision welding system, surge or lightning system, hydro generator sudden short circuit testing [1], arc-furnace current measurement systems [2] and the systems where the possibility of high speed current occurs. The alternative sensors for measurement of current in the above stated systems are Rogowski coil, Neel Effect toroidal current sensor [3], Hall Effect sensors [4]. For high amplitude and high-speed current the Rogowski coil has the better preference due its less bulky construction and the less cost.

Designing of a Rogowski coil based current measuring system involves the mathematical modeling simulation studies taking in to account all the parameters of the sensor together with those of the associated circuitry and systems, e.g., parameters of the connecting cable, the measuring instrument, etc. Rogowski coil is to be modeled considering all the possible factors (e.g., parasitic) that can create problems in different locations.

In this thesis the performance of a Rogowski coil based current measurement system has been studied considering two different types of models, namely lumped parameter type and distributed parameter type, through simulation in PSPICE. A recording device (oscilloscope) is considered as for measuring output of the system, practical values of co-axial cable parameters (characteristic

impedance, delay time), and oscilloscope parameters (input resistance and capacitance) are considered for the study.

Chapter 2: AN INSIGHT OF ROGOWSKI COIL

2.1 Introduction

The Rogowski coil named after *Walter Rogowski* a German physicist is a representative of several devices that measure large currents. A Rogowski coil is an electrical device that measures alternating currents or high frequency currents like in surge protection system, arc furnace system, leakage current of semiconductor devices in inverter or rectifiers and in short circuit testing electric generators. In this chapter the basic construction, working principle for sensing the current has been discussed. The different types of integration methods have also been discussed so as to get output voltage proportional to input current. Finally, the shielding of Rogowski coil has also been discussed.

Fig 2.1: Flexible Rogowski Coil

2.2 Working of Rogowski Coil

The Rogowski coil consists of a wire wound on in the form of helix around the air core uniformly. The coil has a cross section area of A_x, mean outer diameter of D, inner diameter of d with N numbers of turns. A current carrying conductor passes through the aperture of the coil as shown in Fig. 2.2.

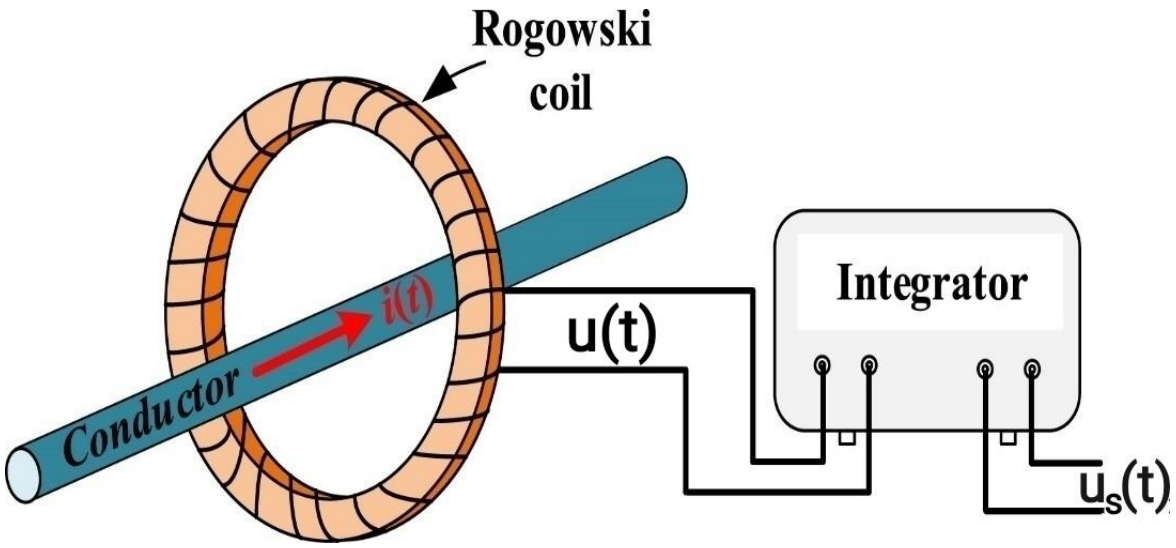

Fig 2.2: Basic construction of Rogowski coil

Due to time varying current carrying by conductor a voltage e(t) gets induced in the coil.

$$e(t) = -M\frac{di(t)}{dt} \qquad \ldots (2.1)$$

The voltage of output terminals of Rogowski coil i.e., open circuit voltage will be defined by$u(t)$.

$$u(t) = -e(t) = M\frac{di(t)}{dt} \qquad \ldots (2.2)$$

To get the output voltage replica of input current an integrator has to be connected at the output side. So, after connecting the integrator the output voltage will be$u_s(t)$.

$$u_s(t) = K_i \int u(t)\, dt$$

$$u_s(t) = K_i M i(t) \qquad \ldots (2.3)$$

Where M is mutual coupling between current carrying conductor and the coil.

By Ampere's circuited law the above relation is proved in the following.

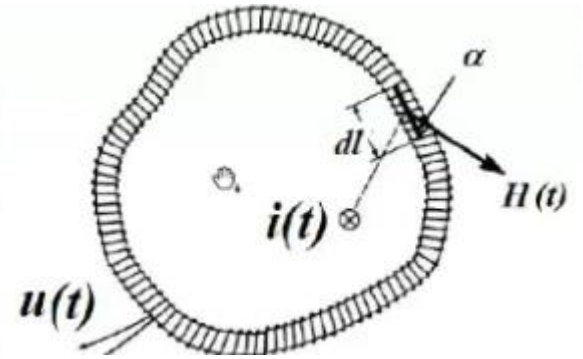

Fig 2.3: Enclosed Rogowski Coil

The relation between the current enclosed by R-coil core and magnetic field intensity along axis of the coil is given by ampere's circuital law as shown below.

$$i(t) = \oint H(t) \cos\alpha . dl \qquad \ldots (2.4)$$

Where $H(t)$ is vector in space,

$H(t)$is converted to $B(t)/\mu_0$ due to non-magnetic material core,

dl is a small element of length along loop with n turn/meter i.e., uniformly distributed turns and cross-sectional area in a section of length dl ,

No. of turns is n dl,

Angle between dl and $H(t)$ is α, the magnetic flux linkage of the section

$$d\psi(t) = \mu_0 H(t) A_x \mathrm{n} dl \cos\alpha$$

Where $d\psi(t)$is the flux linkage of the small element of dl

So, flux linkage of entire length of coil is-

$$\psi(t) = \int d\psi(t) = \mu_0 A_x \mathrm{n} \oint H(t) \cos\alpha dl$$

From Eqn. (2.4) we get

$$\psi(t) = \mu_0 A_x n i(t) = M i(t)$$

Irrespective of shape of core emf is statically induced in the coil so the coil output is:

$$u(t) = \frac{d\psi(t)}{dt} = M \frac{di(t)}{dt}$$

So, $$u_s(t) = K_i \int u(t) = K_i M i(t) \qquad \ldots (2.5)$$

where, K_i is integration constant of the integrator.

The Rogowski coil does not get affected due to external current carrying conductor, as according to ampere's circuital law Rogowski coil works on the closed contour i.e., the current has to pass from aperture of the coil to induced emf in the coil.

$\oint H(t) \cos\alpha dl = i(t)$, for current passing through aperture

$\oint H(t) \cos\alpha \, dl = 0$, otherwise.

2.3 Lumped Equivalent Circuit of Rogowski Coil

In the below Fig. 2.4 lumped equivalent circuit of Rogowski coil is represented by the rectangular broken line which is followed by terminating resistance R_t and an integrator.

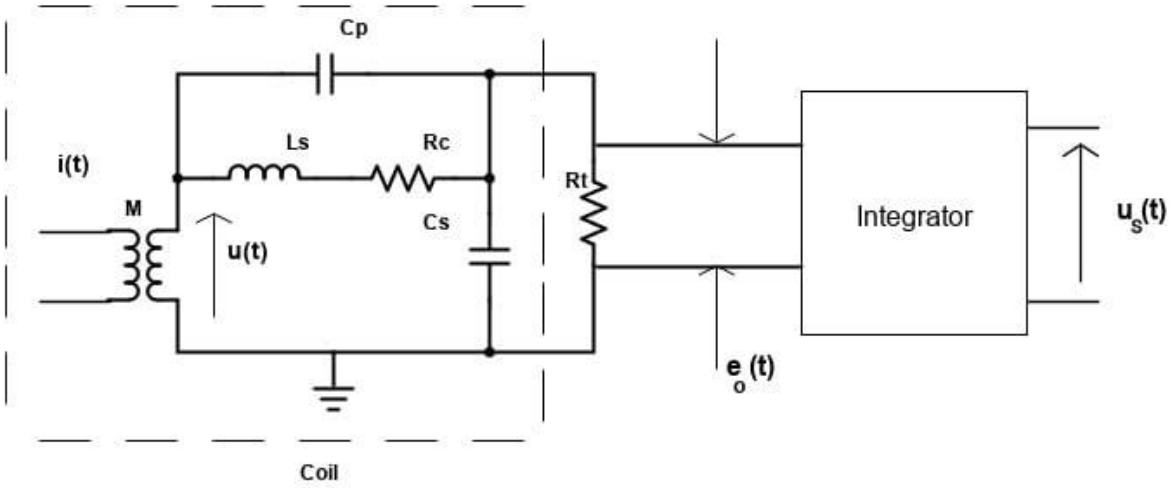

Fig 2.4: Lumped Equivalent Circuit of Rogowski Coil with integrator

Here the derivation of output gain G(s) which is the ratio of Laplace transform of integrator output $u_s(t)$ and Laplace transform of input current i(t) to the Rogowski coil.

M : Mutual inductance between coil and the current carrying conductor

R_c : Coil resistance

L_s : Self inductance of the coil

C_s : Shunt capacitance of the coil

C_p : Inter-turn capacitance

R_t : Terminating resistance

Self-impedance of the coil,

$$Z_s = \frac{\frac{1}{sC_p}(R_c + sL_s)}{(R_c + sL_s + \frac{1}{sC_p})} = \frac{(R_c + sL_s)}{(s^2 L_s C_p + sR_c C_p + 1)} = \frac{N(s)}{D(s)}$$

Terminating impedance of the coil,

$$Z_t = \frac{\frac{R_t}{sC_s}}{R_t + \frac{1}{sC_s}} = \frac{R_t}{1 + sC_sR_t} = \frac{R_t}{D_1(s)}$$

Now using voltage divider rule across R_t we get,

$$\frac{E_o(s)}{U(s)} = \frac{Z_t}{Z_s + Z_t} = \frac{\frac{R_t}{D_1(s)}}{\frac{N(s)}{D(s)} + \frac{R_t}{D_1(s)}} = \frac{R_t\, D(s)}{N(s)D_1(s) + R_t\, D(s)}$$

$$= \frac{R_t(s^2L_sC_p + sR_sC_p + 1)}{N(s)D_1(s) + R_t\, D(s)}$$

$$= \frac{R_t(s^2L_sC_p + sR_cC_p + 1)}{(R_c + sL_s)(1 + sC_sR_t) + (s^2L_sC_pR_t + sR_cC_pR_t + R_t)}$$

C_p is very small,

$$\therefore \frac{Z_t}{Z_s+Z_t} \approx \frac{R_t}{R_c+sL_s+sC_sR_tR_c+s^2L_sC_sR_t}$$

$$= \frac{R_t}{s^2L_sC_sR_t + s(L_s + C_sR_tR_c) + R_c + R_t}$$

$$= \frac{{}^1\!/_{L_sC_s}}{s^2 + s\frac{(L_s+C_sR_tR_c)}{L_sC_sR_t} + \frac{R_c+R_t}{L_sC_sR_t}}$$

$$= \frac{{}^1\!/_{L_sC_s}}{s^2 + 2\left({}^1\!/_{L_sC_s}\right) \times \frac{1}{2}\left(\frac{L_s}{R_t} + C_sR_c\right)s + {}^1\!/_{L_sC_s}\left(\frac{R_c}{R_t} + 1\right)}$$

$$\frac{E_o(s)}{U(s)} = \frac{{}^1\!/_{L_sC_s}}{s^2 + 2\sqrt{\left({}^1\!/_{L_sC_s}\right)} \times \frac{\sqrt{\left({}^1\!/_{L_sC_s}\right)}}{2}\left(\frac{L_s}{R_t} + C_sR_c\right)s + \left({}^1\!/_{L_sC_s}\right)\left(\frac{R_c}{R_t} + 1\right)} = x(let)$$

Now by using Laplace transform in both sides of Eq. (2.2) we get,

$$U(s) = sMI(s) \Rightarrow I(s) = U(s)/sM \quad \ldots (2.6)$$

Integrator transfer function,

$$\frac{U_S(s)}{E_O(s)} = \frac{K_i}{1+sR_iC_i} \quad \ldots (2.7)$$

where R_iC_i is time constant of the integrator,

K_i is integrator constant.

we can write,

$$\frac{U_s(s)}{I(s)} = \frac{U_s(s)}{E_o(s)} \times \frac{E_o(s)}{I(s)}$$

From Eqn. (2.6) and (2.7) we get,

$$\frac{U_s(s)}{I(s)} = \frac{K_i}{1 + sR_iC_i} \times \frac{E_o(s)}{U(s)} \times sM$$

$$\text{Or, } \frac{U_S(s)}{I(s)} = \frac{sK_iM}{1+sR_iC_i} \times x$$

By putting the value of x,

$$\frac{U_s(s)}{I(s)} = \frac{sK_iM}{1 + sR_iC_i} \times \frac{{}^{1}/_{L_sC_s}}{s^2 + 2\sqrt{\left({}^{1}/_{L_sC_s}\right)} \times \frac{\sqrt{\left({}^{1}/_{L_sC_s}\right)}}{2}\left(\frac{L_s}{R_t} + C_sR_c\right)s + \left({}^{1}/_{L_sC_s}\right)\left(\frac{R_c}{R_t} + 1\right)}$$

In practical setting $R_t \gg R_s$

$$\therefore G(s) = \frac{U_s(s)}{I(s)} = \frac{sK_iM}{1+sR_iC_i} \times \frac{{}^{1}/_{L_sC_s}}{s^2 + 2\sqrt{\left({}^{1}/_{L_sC_s}\right)} \times \frac{\sqrt{\left({}^{1}/_{L_sC_s}\right)}}{2}\left(\frac{L_s}{R_t} + C_sR_c\right)s + \left({}^{1}/_{L_sC_s}\right)} \quad \ldots (2.8)$$

Comparing with standard second order system, $G(s) = \frac{\omega_n{}^2}{s^2+2\xi\omega_n s+\omega_n{}^2}$ we get,

$$\omega_n = \frac{1}{\sqrt{L_sC_s}}$$

$$\xi = \frac{\frac{1}{\sqrt{L_sC_s}}}{2}\left(\frac{L_s}{R_t} + C_sR_c\right)$$

where ω_n is the natural frequency of oscillation of the system,

ξ is the damping ratio of the system.

2.4 Amplitude Response of Rogowski coil

The response of amplitude of gain shows the damping conditions at different values of damping ratio ξ.

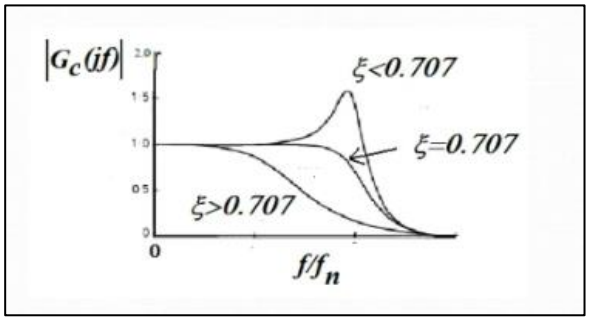

Fig. 2.5: Amplitude response of Rogowski coil

The amplitude response of 2nd order system in which current to be measured as input and output of integrator as ultimate output. Here the terminating resistance R_t has chosen such that the damping ratio has two ranges:

1. When $\xi < 0.707$

The arrangement of equivalent circuit of Rogowski coil followed by integrator and co axial cable has the two frequency limits, the lower limiting frequency f_l and upper limiting frequency f_u .The lower limiting frequency is equal to $\frac{3}{\tau}$, where τ is the time constant of the integrator and the upper frequency limit is less than the characteristics impedance of co axial cable. The resonance is occurring at resonating frequency f_r. In Fig. 2.6, the 2nd order system amplitude is 1.05 times of steady constant value at upper limiting frequency, and 0.95 times of steady constant value at lower limiting frequency. So, the value of damping ratio needs to be chosen at which the span of f_l to f_u is constant if this type of characteristics of arrangement performed then the Fourier components of a periodic signal lies between lower limiting frequency to upper limiting frequency leads to the ultimate output wave shape at integrator side would be replica of input current which need to be measured.

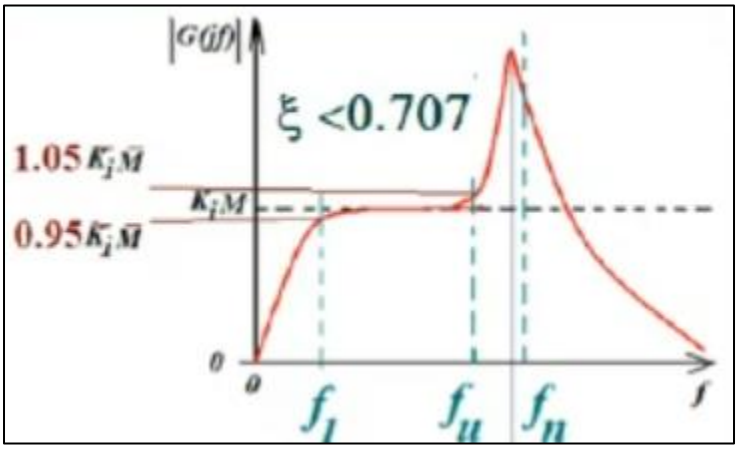

Fig. 2.6: Amplitude response of Rogowski coil for $\xi < 0.707$

2. When $\xi \geq 0.707$

If we consider this type of characteristics of arrangement, the lower limiting frequency will be governed by first order characteristics and but for upper limiting frequency if $\xi \geq 0.707$ then between lower limiting frequency and upper limiting frequency there will be no resonance frequency and the deviation in steady constant value would be 5% only.

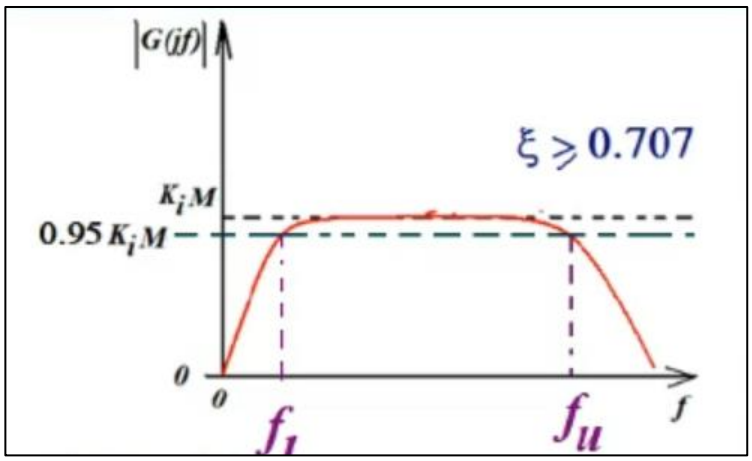

Fig. 2.7: Amplitude response of Rogowski coil for $\xi \geq 0.707$

2.5 Significance of Terminating Resistance

Terminating resistor R_t determines the damping ratio of the system, the damping ratio Eqn. (2.8) has Rogowski coil electrical parameters which are only dependent on its dimensions so damping ratio.

$$\omega_n = \frac{1}{\sqrt{L_s C_s}}$$

Where ω_n is the natural frequency of oscillation of the system.

$$\xi = \frac{\frac{1}{\sqrt{L_s C_s}}}{2}\left(\frac{L_s}{R_t} + C_s R_c\right)$$

Where ξ is the damping ratio of the system.

$$R_t = \frac{L_c}{2\xi\,\omega_n L_s C_s - C_s R_c}$$

For high frequency applications, $2£\omega_n L_s C_s \gg C_s R_c$

$$R_t = \frac{1}{2\xi\omega_n C_s} \quad \ldots (2.9)$$

For electrical parameter values of Rogowski coil with damping coefficient, terminating resistance R_t values are calculated in different values of damping ratio (ξ) from Eqn. (2.9) as shown in TABLE I.

TABLE I:

SL NO.	Damping Ratio (ξ)	Terminating resistance (R_t)
1	0.1	36.75kΩ
2	0.2	18.37kΩ
3	0.3	12.125kΩ
4	0.4	9.25kΩ

2.6 Measurement systems using Rogowski Coil

The signal in the form of output voltage in the output of Rogowski coil probe is proportional to the rate of change of current, to get the input current an integrator is needed to connect at output side. There are different types of integrator circuit in use like passive integrator such as R-C and R-L integrator, active integrator using op-amps etc. These integrated outputs are taken to the recording device oscilloscope with the help of co-axial cable to record the output waveform which is a replica of input current to analyze the front time and tail time.

2.6.1 Rogowski coil measurement system with passive integrator

Passive integrators generally are of two types, RC integrators and RL integrators. In this thesis only RC integrator is used. A R-C passive integrator consists of a resistor connected with capacitor in series as shown in Fig. (2.8). The values of R and C are determined by the relation $\omega_L \gg 1/RC$, where ω_L is the lowest frequency component of the signal to be integrated.

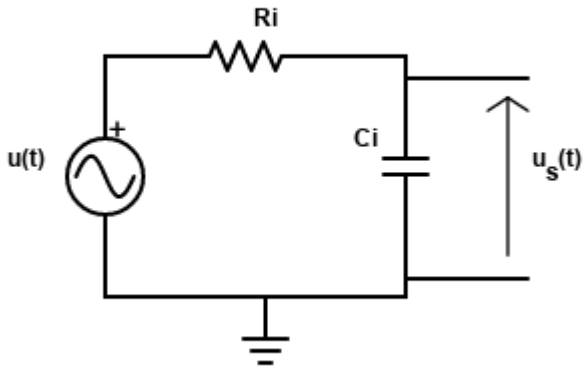

Fig.2.8: R-C passive integrator

By using voltage divider rule and by representing the circuit impedances in Laplace domain, we get the Laplace transform of the integrator output as:

$$\mathrm{U_s(s)} = \frac{1/\mathrm{sC_i}}{R_i + 1/\mathrm{sC_i}} \times \mathrm{U(s)}$$

$$\text{or, } \frac{\mathrm{U_s(s)}}{\mathrm{U(s)}} = \frac{1}{1 + \mathrm{s}R_i\mathrm{C_i}}$$

From Eqn. 2.2 using Laplace transformation, we get $\mathrm{U(s)} = \mathrm{sMI(s)}$.

Now,

$$\frac{\mathrm{U_s(s)}}{\mathrm{I(s)}} = \frac{\mathrm{sM}}{1 + \mathrm{s}R_i\mathrm{C_i}}$$

If $\omega_L R_i C_i \gg 1$, then

$$\frac{U_s(s)}{I(s)} \approx \frac{M}{R_i C_i} \quad \ldots (2.10)$$

2.6.2 Rogowski coil measuring system with active integrator

The output voltage of the Rogowski coil u(t) which is to be integrated to get a replica of input current can be obtained with the help of active integrator circuit. Here the operational amplifier is used to integrate the output voltage of the Rogowski coil. The loading effect on the Rogowski coil is inappreciable due to the high input impedance of the op-amp. Further, the loading effect of the subsequent circuit on the integrator is much less due to low output impedance of active integrator.

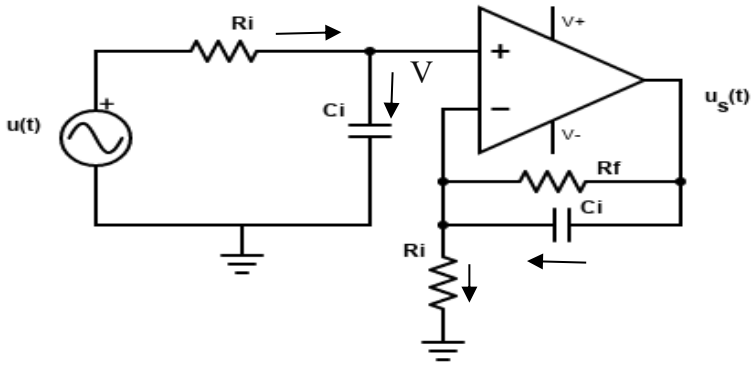

Fig. 2.9: Active integrator using non-inverting operational amplifier

Let the inverting terminal of op-amp is at potential 'V' and hence non-inverting terminal is also appears to be at the same potential 'V' due to virtual ground concept. Input current to op-amp is zero. Hence applying KCL at non-inverting terminal node we have

$$\frac{u(t)-V}{R_i} = C_i \frac{dV}{dt} \quad \ldots (2.11)$$

Now applying KCL at inverting terminal node we have

$$\frac{V}{R_i} = C_i \frac{d(u_s(t)-V)}{dt} + \frac{u_s(t)-V}{R_f}$$

Here, feedback resistance R_f is very large in MΩ range, so the term $\frac{u_s(t)-V}{R_f}$ is very small and can be neglected from the above equation.

So,
$$\frac{V}{R_i} = C_i \frac{d(u_s(t)-V)}{dt}$$

$$\text{or,} \frac{V}{R_i} = C_i \frac{du_s(t)}{dt} - C_i \frac{d\text{V}}{dt}$$

From Eqn. 2.7 by replacing the value of the term $C_i \frac{dV}{dt}$ in above equation we get,

$$\frac{V}{R_i} = C_i \frac{du_s(t)}{dt} - \frac{u(t)-V}{R_i}$$

$$\text{or, } \frac{V}{R_i} = C_i \frac{du_s(t)}{dt} - \frac{u(t)}{R_i} + \frac{V}{R_i}$$

$$\text{or, } C_i \frac{du_s(t)}{dt} = \frac{u(t)}{R_i}$$

By using Laplace transform in both sides we get,

$$sC_iU_s(s) = U(s)/R_i$$

$$\text{or, } \frac{U_s(s)}{U(s)} = \frac{1}{sC_iR_i} \qquad \ldots (2.12)$$

From Eqn. 2.2 using Laplace transformation, we get $\text{U(s)} = \text{sMI(s)}$.

By using the above U(s) value in Eqn. 2.8,

$$\frac{U_s(s)}{I(s)} = \frac{M}{C_i R_i} \quad \ldots (2.13)$$

So Rogowski coil with active integrator gives a gain of M/C_iR_i, same as with passive integrator.

- **Significance of R_f:**

We know that an op-amp has a very high open loop dc gain. At low frequencies impedance of the feedback capacitor, X_{C_i} is very high and a very high impedance can be assumed as an open circuit. Due to this reason even if there is very low input dc voltage, op-amp will be driven to saturation. Therefore, a very high resistance R_f is connected in parallel to the feedback capacitor so that the gain of the circuit is limited to a finite value (effectively very small).

2.7 Shielding of Rogowski coil

A Rogowski coil needs a metallic shielding to prevent electrostatic interference in practical application. When an object in earth potential in close proximity of Rogowski coil is present a parasitic capacitance between ground and R-coil formed and that ground capacitance will be distributed in nature throughout the R-coil. When an external voltage source appeared in the vicinity the parasitic capacitance also gets formed between the Rogowski coil and external voltage source, if change in voltage is fast then a circulating current or leakage current starts to flow through voltage source to Rogowski coil to ground then there will be a voltage drop occurs in different section of Rogowski coil. Due to voltage drops the ultimate output voltage will have an error so to minimize the ground or parasitic capacitance shielding is required.

2.8 PSPICE Modelling of Rogowski Coil

1. PSpice Lumped parameter model
2. PSpice Distributed parameter model.

2.8.1 PSPICE LUMPED PARAMETER MODEL:

The lumped parameter model [5] consists of concentrated passive elements in the circuit connected with the wire. The Rogowski coil consist of resistance, capacitance per unit length, inductance per unit length, the mutual inductance between the current carrying conductor and the coil and the parasitic capacitance. The equivalent circuit diagram of lumped parameter model of Rogowski coil is shown in Fig 2.10, where M and L_s are the mutual inductance and self-inductance, respectively, C_s is the shunt capacitance of the coil, R_c is the equivalent coil resistance, and R_t the terminal resistance. Simulation studies of Rogowski coil with the help PSPICE is performed to compare the output of the integrator and input current, in the time domain. The parasitic inter-turn capacitance is neglected.

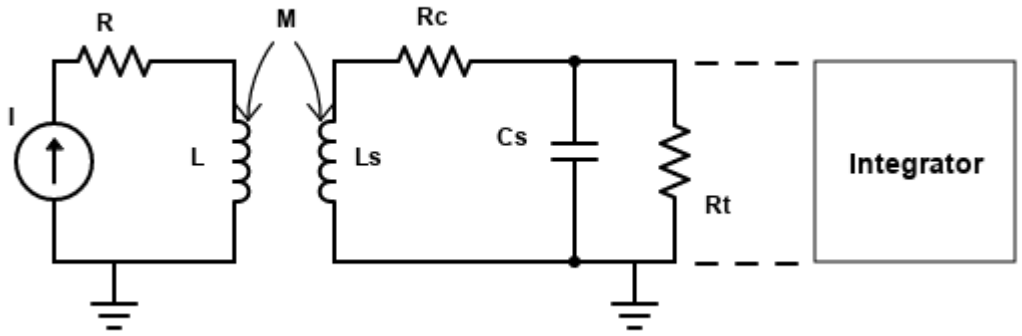

Fig. 2.10: Lumped parameter model of Rogowski coil

Since the capacitance to ground is distributed in nature, the lumped parameter model is not suitable for studying high frequency measurement so it can be transformed into distributed model for better insight.

2.8.1 PSPICE DISTRIBUTED PARAMETER MODEL:

The lumped model is not suitable for high frequency measurements as discussed above so it should be replaced by distributed model in Fig. 2.11, one of the distributed models is based on transmission line theory [6]. In this model the electrical distance of the coil is separated with n division ,each division contains series inductance $L_s = L_l/n$, $C_S = C_l/n, R_c = {}^{R_l}/_{n}$. The inter-turn capacitance is neglected due its small value.

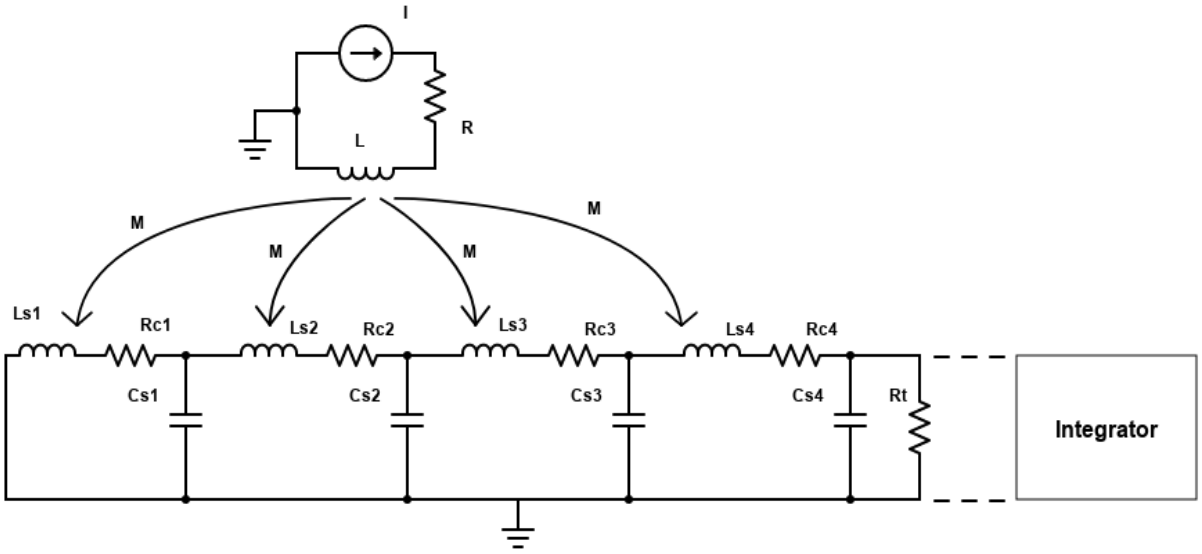

Fig. 2.11: Distributed parameter model

2.9 Merits and Demerits of Rogowski Coil

Although Rogowski coil can be used for measurement of high-speed pulse current without having bulky circuit for the arrangement, there are some merits and demerits of the proposed measurement system.

- ***MERITS:***

1. Due to the non-magnetic core, saturation does not take place and linearity comes even when high speed current subjected to the system for measurement
2. No danger of secondary opening
3. The size of Rogowski coil as compared to the conventional current transformer is small for measuring high amplitude input current.
4. The Rogowski coil responds in nano seconds for the fast-changing currents due to its low inductance value.
5. Construction cost of Rogowski coil is less.

- ***DEMERITS:***

1. If the Rogowski coil is used with an active integrator to integrate the output voltage to get the input current, the active integrator consists of op-amp which needs to be operated with external voltage dc (bias) source but in CT this arrangement is not required.
2. Rogowski coil cannot handle DC.
3. Sensitivity of Rogowski coil is low as compared to CT due to low permeability of the core.

2.10 Application of Rogowski Coil

Not only, the Rogowski coil is useful in conventional applications, but also, there are other cases where Rogowski coil is the best choice [11]. Because of non-geometric structure and capability in measuring high amplitude current it has various applications in laboratories, industrial

measurement instruments, and unconventional measuring systems [12]. In following, a brief overview of the Rogowski coil applications is represented.

In the power system protection, conventional CTs are being used for decades. These CTs were necessary for electromagnetic relays operation, due to the large power demand of these relays for proper operation. Nowadays, the relays are numeric and work with low power signals properly. As a consequence, the Rogowski coil can be used instead of CTs for fault detection in transmission lines and electrical machines [13]. Using Rogowski coil leads to fast response of the relays and flexibility of protection schemes [14], [15]. This matter has also opened new gates to the protection schemes fields [13]. For example, the Rogowski coil owing to wide frequency bandwidth can measure the travelling wave variation, which enables using travelling wave-based protection schemes fields [16]. Travelling wave-based algorithms is useful in fault location methods [17]. It is also possible to add the coil on distribution overhead lines without primary separation for high impedance fault detection [18]. Some of the CTs problems, such as CTs saturation, which lead to maloperations of the relays, are not the matter of concerns in the Rogowski coil. Numerous researches are focused on using the Rogowski coil instead of CTs in transmission and distribution substations [16], [11], [17]. The Rogowski coil is useful as an electronic current transducer in smart substations for protection and monitoring applications as well [19].

In applications where there is no normal geometrical structure, the Rogowski coil is one of the best options, due to its flexibility [20]. For instance, One Rogowski coil can be placed around the tower, for measuring the impulse current distribution in a wind turbine tower [21]. Measuring the leakage current of the system, which placed on earth, can be done by placing big Rogowski coils around all of the legs of that component. Using this method, the grounding resistance of overhead line towers can be measured, individually [17]. The coil can also be placed around high voltage bushings, for on line monitoring [16]. It is also useful for eddy current measurements in non-geometric structures [22].

The Rogowski coil has intrinsic insulation from main circuit. Using optical link between the coil and the measurement system has strengthened the coil for using in high voltage applications. This area can be developed vastly in the future.

Chapter 3: Investigation and Results

3.1 Introduction

In this chapter investigations and results are discussed in brief. The values of different components of Rogowski coil and required system parameters are stated and calculated. Finally, the simulation studies have been discussed.

3.2 Investigation

The current system using Rogowski coil is widely in use due to its linear characteristics and potential for inexpensiveness unlike the current transformer. The circuit arrangement of the coil with passive integrator is inexpensive as compared to active integrator for the measurement of the current. The output of integrator which is the replica of input current is taken to an oscilloscope with the help of co axial cable. Use of active integrator for integration of output voltage leads to more accuracy as compare to passive integrator due to less loading effect of the active integrator. For sensing of currents with very high frequency components, the constraint imposed by the bandwidth of the op-amp is overcome by opting for a passive integrator. The investigation and study in this chapter consist of two sections. In the first section a steep impulse current of 1/20μs is generated with the help of MATLAB programming to use in the simulation work. The second one consists of evaluating the time response of the Rogowski coil-based system for performance analysis. The performance analysis of Rogowski coil-based system is carried out by varying different system parameters for better understanding.

The PSPICE simulations have been carried out for both lumped and distributed parameter model with the calculated parameters of Rogowski coil, practical values of coaxial cable parameters, and the input impedance of oscilloscope for recording the output of the system.

3.3 Values of different parameters

- **Rogowski Coil**

The electrical parameters of a real-life Rogowski coil [23] are, self-resistance of coil $R_c = 129\Omega$, self-inductance of the coil $L_s = 2.08mH$, shunt-capacitance of the coil $C_s = 38.5pF$ and the mutual inductance between current carrying conductor and the coil is $M_c = 1.049\mu H$

- **Co axial cable**

The co axial cable used for transmitting the output waveforms to the oscilloscope are of different types with different parameters.

RG-7: Silver plated copper conductor gas-injected foamed high-density polyethylene insulation cable shown in fig 3.1.

Overall outer diameter: 8.128mm

Shielding: 95% braid copper

Characteristics impedance: 75Ω

Co axial capacitance: 52.8pF/m

Delay time: 3.97ns/m

Length of Co axial cable: 15m

Attenuation coefficient: 2.2967dB/100m at 5MHz

Fig 3.1: RG 7 Co axial cable

- **Oscilloscope**

The input impedance of the oscilloscope consists of resistance R_o and capacitance C_o are connected in parallel. The practical

Values of R_o and C_o are considered:

Input resistance of the oscilloscope R_o : 1 MΩ

Input capacitance of the oscilloscope C_o : 16pF

- **Integrator Parameters**

The passive and active integrators used to integrate the output voltage are series connection of resistor and capacitor for passive integrator and input resistance in active integrator with feedback capacitor. The values of resistor and capacitor for integrating circuit are calculated considering the input current waveform. The time of peak value of current has been considered as quarter cycle of a sine wave. So, the corresponding angular frequency has been considered as

$$\omega_L \gg \frac{1}{R_i C_i}$$

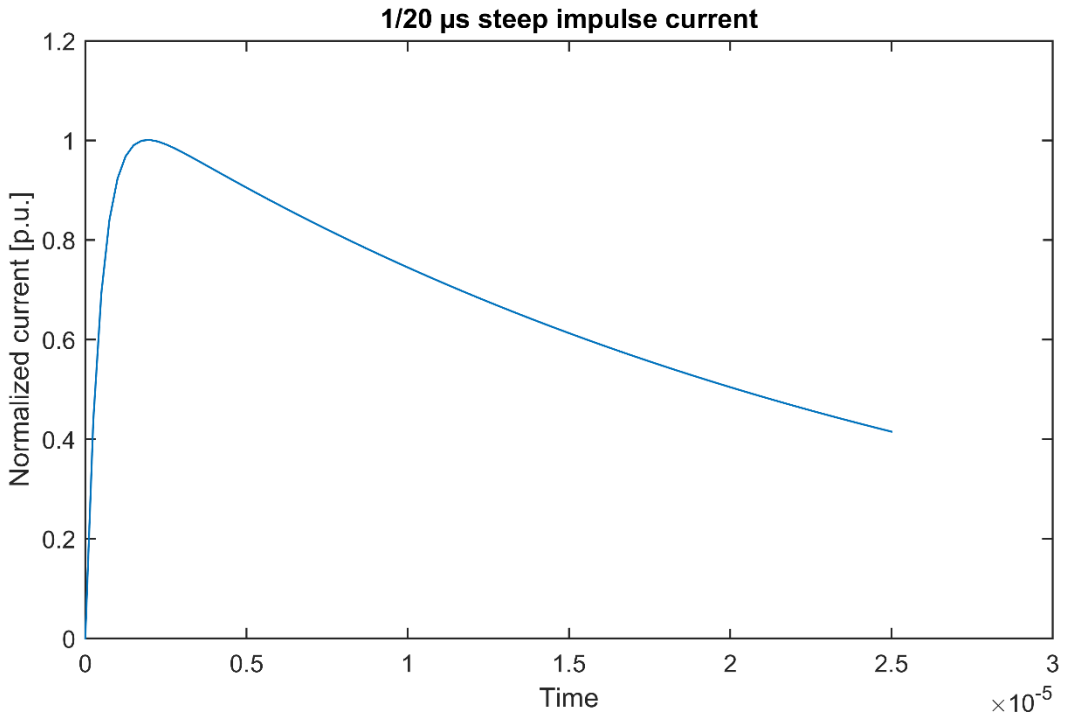

Fig 3.2: Input impulse current of 1/20μs wave shape

From below Eqn. (3.1) and Eqn. (3.2) we get the following values of front time and tail time of the input current waveform in Fig. (3.2).

$$T_f = 1.08\ \mu s$$

$$T_p = 20.11\ \mu s$$

Peak time (T_{peak}) is time when the current has reached to its peak value.

$T_{peak} = 1.99\mu s$, $\omega_L = \frac{2\pi}{4T_{peak}}$

$$\omega_L R_i C_i \gg 1$$

With above conditions, the integrator circuit parameters are calculated shown below.

Integrator resistance, $R_i = 10k\Omega$

Integrator capacitance, $C_i = 0.1\mu F$

3.4 Representation of standard exponential impulse current

The impulse wave shape as shown in fig is defined according to the IEC recommendation [7]. The value of the impulse current is normally defined by its peak value. Impulse current waveform characteristics [8] can be described using important parameters, namely the front time T_f and the time of half tail time T_p. The front time defined by 1.25 times of the interval between the instants when the impulse is 10% and 90% of the peak value. The front time can be calculated using (3.1) where $t_{0.1}$ and $t_{0.9}$ are at 10% and 90% of peak current respectively. The time to half value of an impulse current is the time interval between the virtual origin and the instant on the tail at which the current has decreased to half of the peak as shown in (3.2). In the simulation, we are using 1/20 μs waveshape

$$T_f = 1.25(t_{0.9} - t_{0.1}) \quad \ldots (3.1)$$

$$T_p = t_{0.5} \quad \ldots (3.2)$$

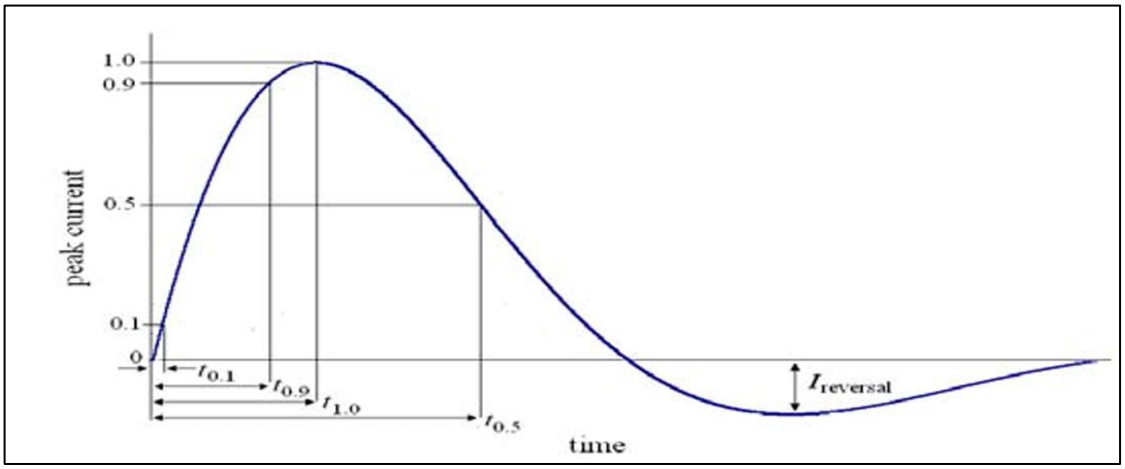

Fig 3.3: Standard exponential impulse current waveform

Here the polarities reversal of current after the current fallen to zero should not more than 20% of the peak value. The parameters of wave impulse current are defined in IEC or ANSI/IEEE as shown in table.

- **Tolerance of impulse current**

Wave shape (μs)	Front time T_f	Time to half T_p	Peak value	Polarity reversal
1/20	1μs ± 10%	20μs ± 10%	± 10%	20%
4/10	4μs ± 10%	10μs ± 10%	± 10%	20%
8/20	8μs ± 10%	20μs± 10%	± 10%	20%
30/80	30μs ± 10%	80μs ± 10%	± 10%	20%

The impulse current (without considering the polarity reversal) can be represented by the double exponential expression [8]

$$i(t) = I[e^{(-\alpha t)} - e^{(-\beta t)}] \quad \text{... (3.3)}$$

where α and β are constants, and need to be determined for the impulse waveform of current,

I is the peak value of impulse current waveform.

- **Expression for A factor**

In the previous double exponential expression formula, the constants α and β are usually difficult to fit the impulse waveform of the impulse current, for this reason an additional A factor [9] must be introduced for better accuracy. A factor is important to create the double exponential impulse waveforms with different parameters and amplitudes.

With respect to Eqn. (3.3), the modified formula for impulse current is written as

$$i(t) = AI[e^{(-\alpha t)} - e^{(-\beta t)}] \quad \text{… (3.4)}$$

and its derivative is

$$\frac{di(t)}{dt} = AI(-\alpha e^{-\alpha t} + \beta e^{-\beta t}) \quad \text{… (3.5)}$$

At the peak value I, Eqn. (3.5) should satisfy the following condition.

$$\frac{di(t_{max})}{dt} = AI\left(-\alpha e^{-\alpha t_{max}} + \beta e^{-\beta t_{max}}\right) = 0 \qquad \ldots (3.6)$$

Where t_{max} is the time from the beginning of the current to its peak value.

From Eqn. (3.5) the t_{max} can be expressed.

$$t_{max} = \frac{(\ln \beta - \ln \alpha)}{(\beta - \alpha)} \qquad \ldots (3.7)$$

Substituting Eqn (3.7) into Eqn. (3.4) yields

$$i(t_{max}) = AI(e^{-\alpha t_{max}} - e^{-\beta t_{max}}) \qquad \ldots (3.8)$$

The expression for A can be given as

$$A(\alpha, \beta) = \ 1/(e^{-\alpha \frac{\ln \beta - \ln \alpha}{\beta - \alpha}} - e^{-\beta \frac{\ln \beta - \ln \alpha}{\beta - \alpha}}) \qquad \ldots (3.9)$$

By putting the values of α & β from Eqn. (3.10) and Eqn. (3.11) into Eqn. (3.9) we get,

$$A = 1.1$$

- **Expression for α and β parameters**

The expression for the formula constants is important for determining the wave shape of the current. The relation between the formula constants and front time and tail is non-linear. For this reason, the expression to determine the formula constants as [10] are given below.

$$\alpha = \frac{1}{T_p}[4.0616 - 26.963\frac{T_f}{T_p} - 28.909(\frac{T_f}{T_p})^2 + 598.99(\frac{T_f}{T_p})^3 - 1273.2(\frac{T_f}{T_p})^4]^{\frac{-1}{4}}$$

$$\beta = \frac{1}{\alpha T_f^2}[6.222 * 10^{-5} + 1.495\frac{T_f}{T_p} - 2.087(\frac{T_f}{T_p})^2 + 8.418(\frac{T_f}{T_p})^3 - 4.649(\frac{T_f}{T_p})^4]$$

By putting the values of T_f and T_p from above calculated values of T_f and T_p in above equations we get,

$$\alpha = 38976.6\ s^{-1} \quad \ldots (3.10)$$

$$\beta = 2100000 s^{-1} \quad \ldots (3.11)$$

To get accurate waveform of input impulse current from MATLAB, α and β values are needed to be changed slightly. By keeping α constant β is changed using trial and error method.

- **MATLAB Program to generate input impulse current waveform:**

```
A=1.1;
a=38976.6;
b=2100000;
I=1;
t=[0:0.25e-6:25e-6];
x1= exp(-a*t);
x2= exp(-b*t);
i=A*I*(x1-x2);
crnt=[t' i'];
```

3.5 Simulation Circuit Arrangement:

The simulation circuit arrangements have been shown in fig (3.4) to fig (3.15).

LUMPED PARAMETER MODEL

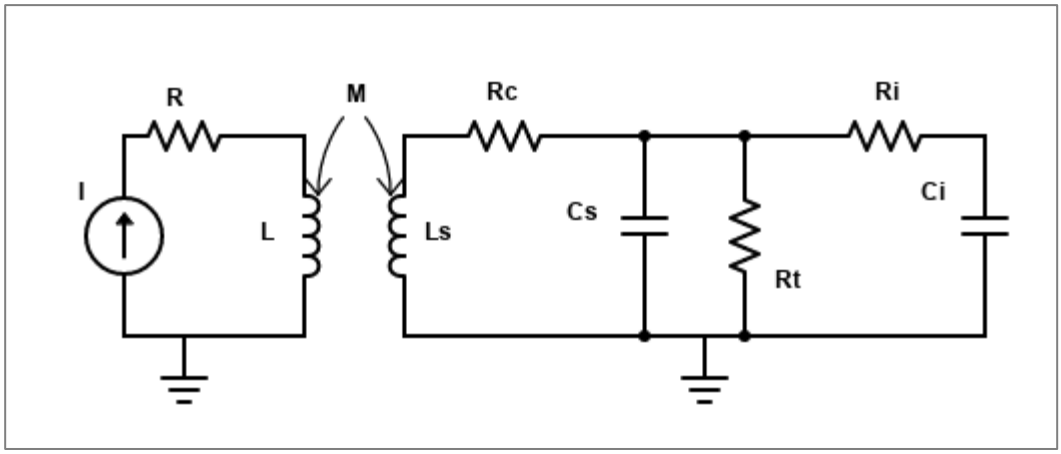

Fig 3.4: Lumped parameter model with passive integrator

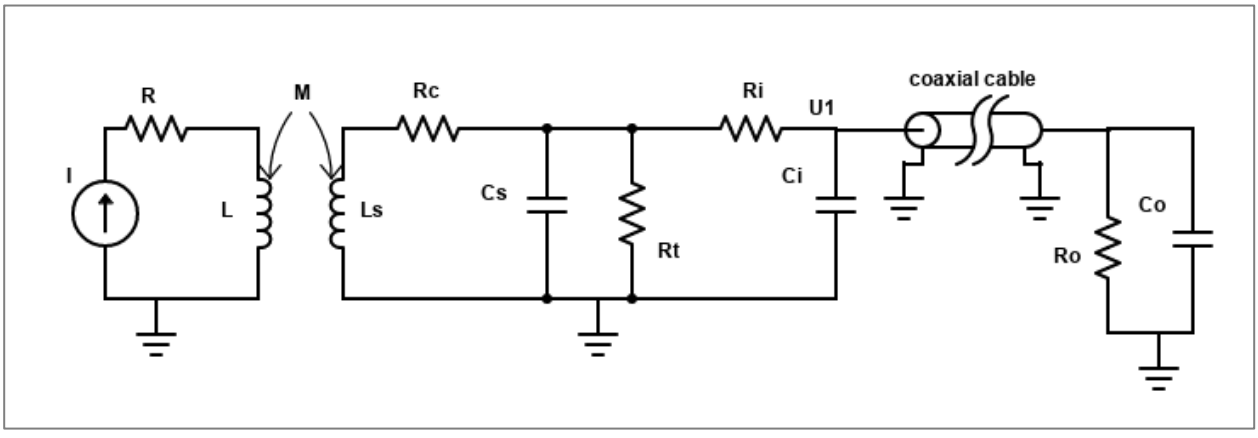

Fig 3.5: Lumped parameter model with passive integrator with coaxial cable connected to Oscilloscope

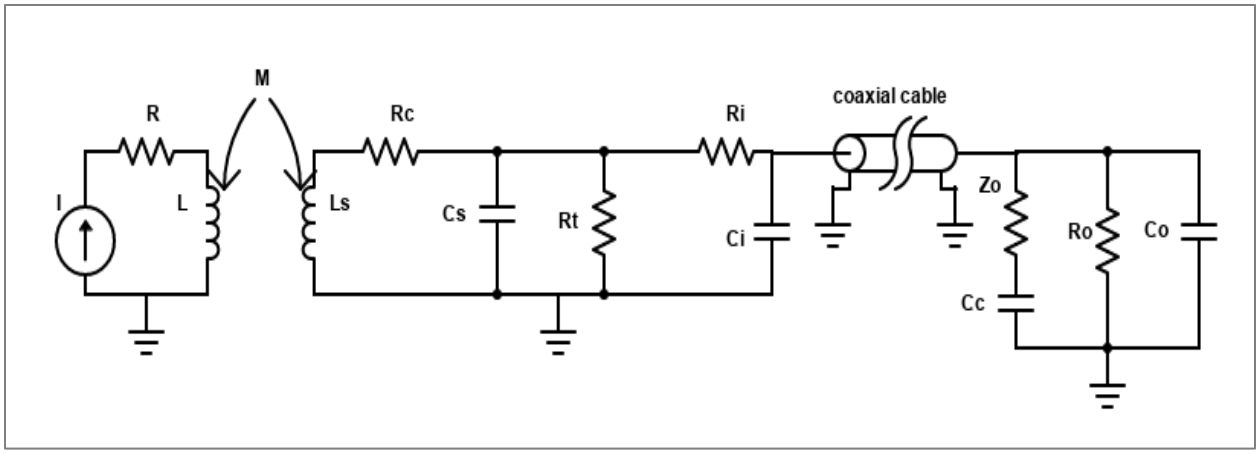

Fig 3.6: Lumped parameter model with passive integrator with coaxial cable terminated at series RC matching impedance connected to Oscilloscope

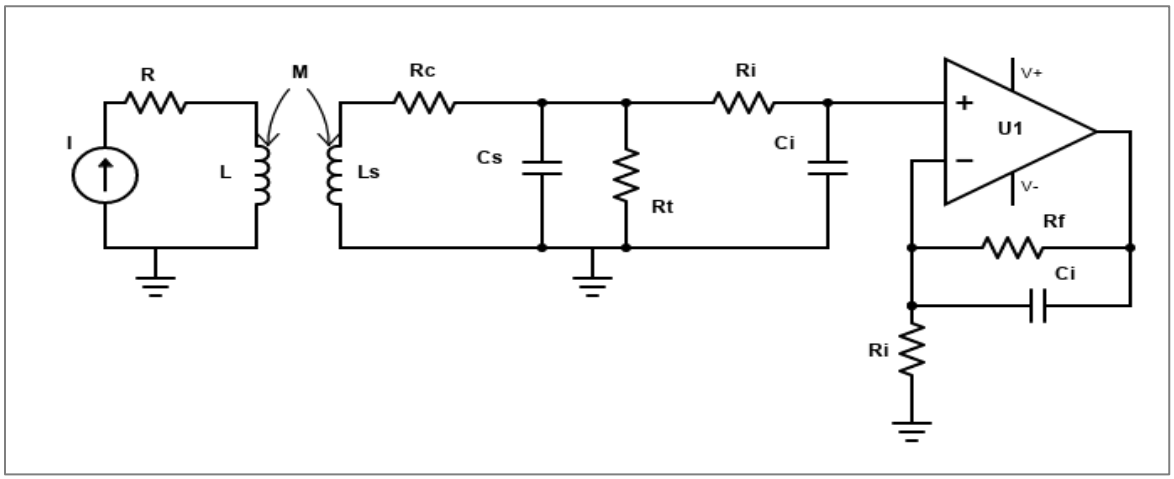

Fig 3.7: Lumped parameter model with active integrator

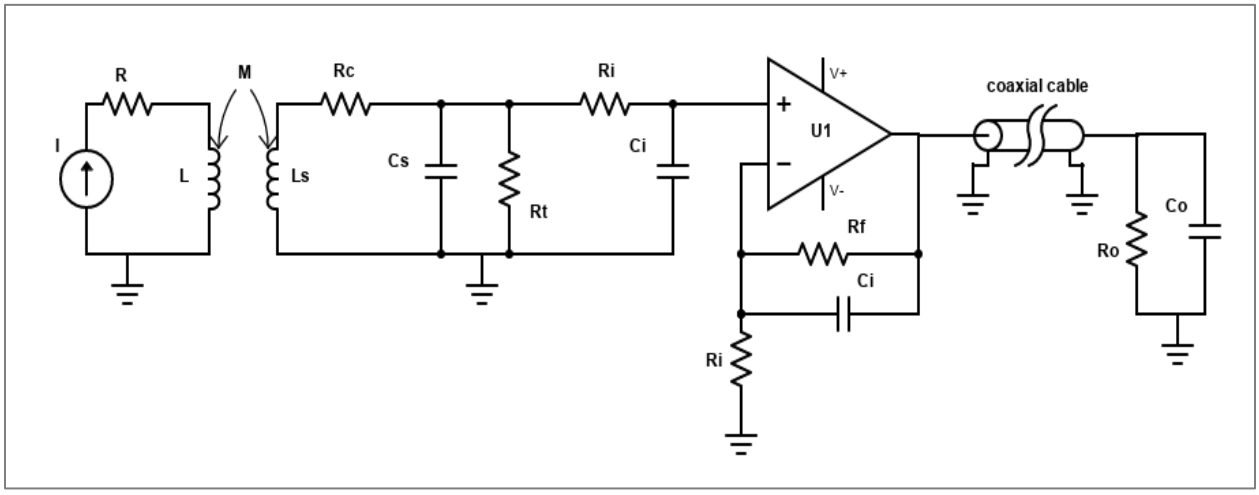

Fig 3.8: Lumped parameter model with active integrator with coaxial cable connected to Oscilloscope

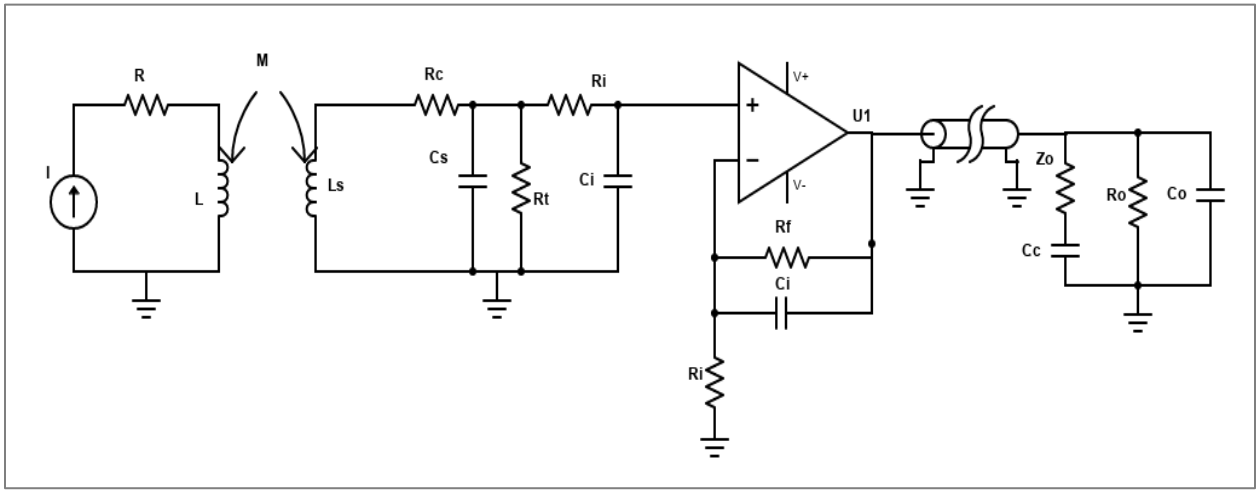

Fig 3.9: Lumped parameter model with active integrator with coaxial cable terminated at series RC matching impedance connected to Oscilloscope

DISTRIBUTED PARAMETER MODEL

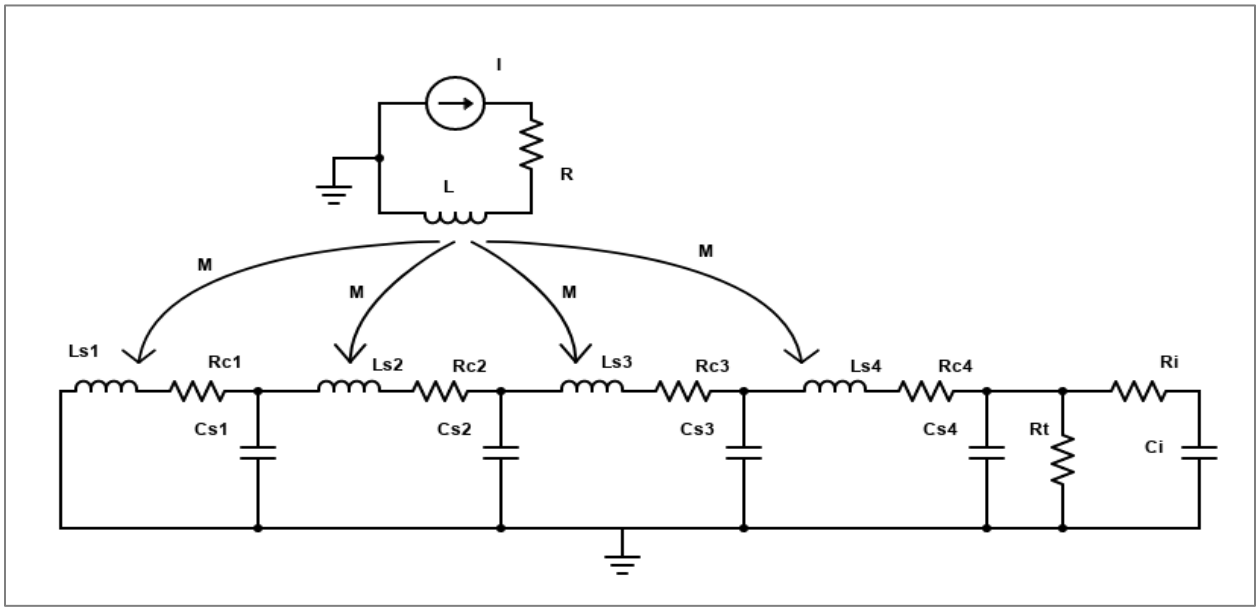

Fig 3.10: Distributed Parameter Model With passive integrator

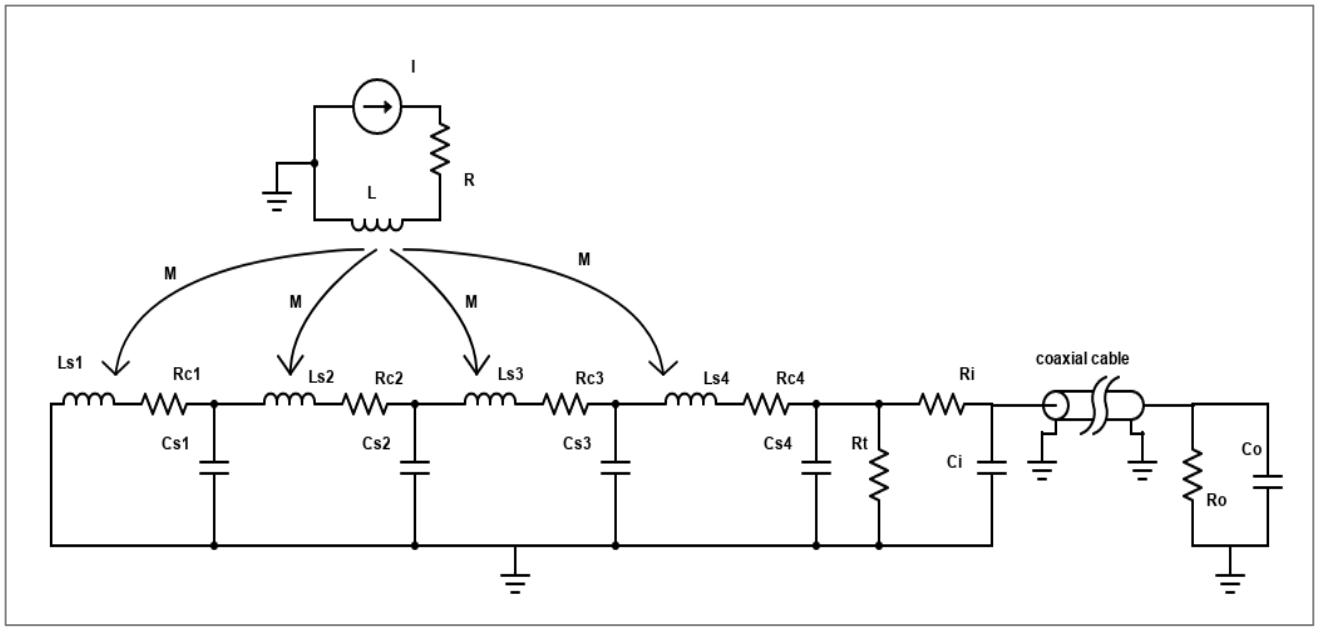

Fig 3.11: Distributed Parameter Model passive integrator with coaxial cable connected to Oscilloscope

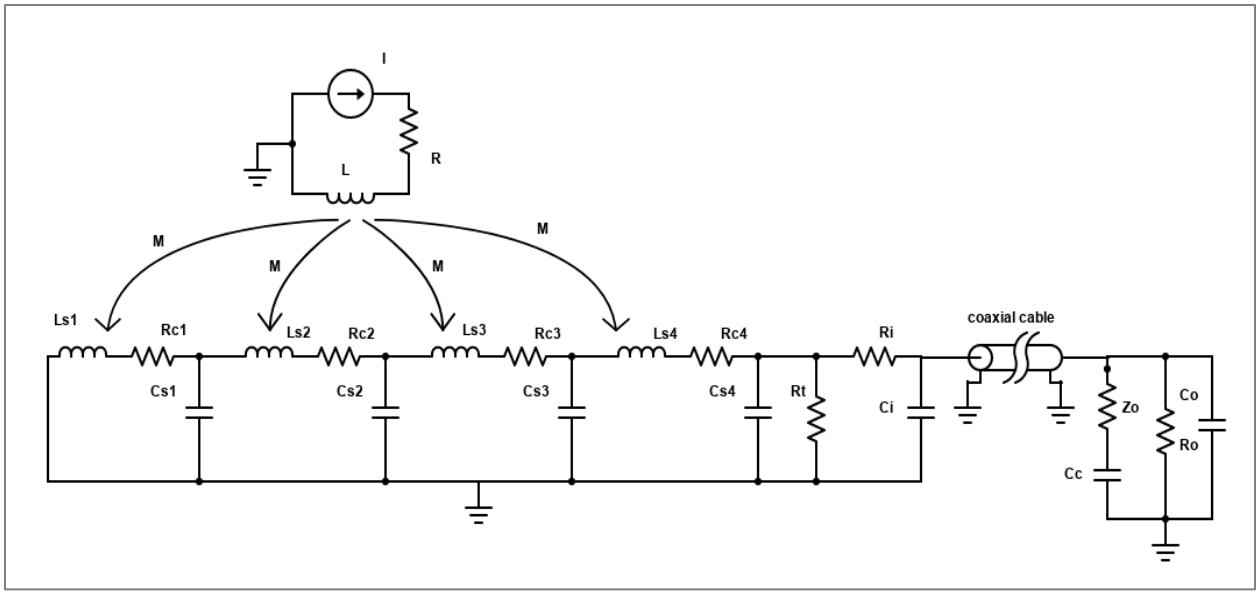

Fig 3.12: Distributed parameter model with passive integrator with coaxial cable terminated at series RC matching impedance connected to Oscilloscope

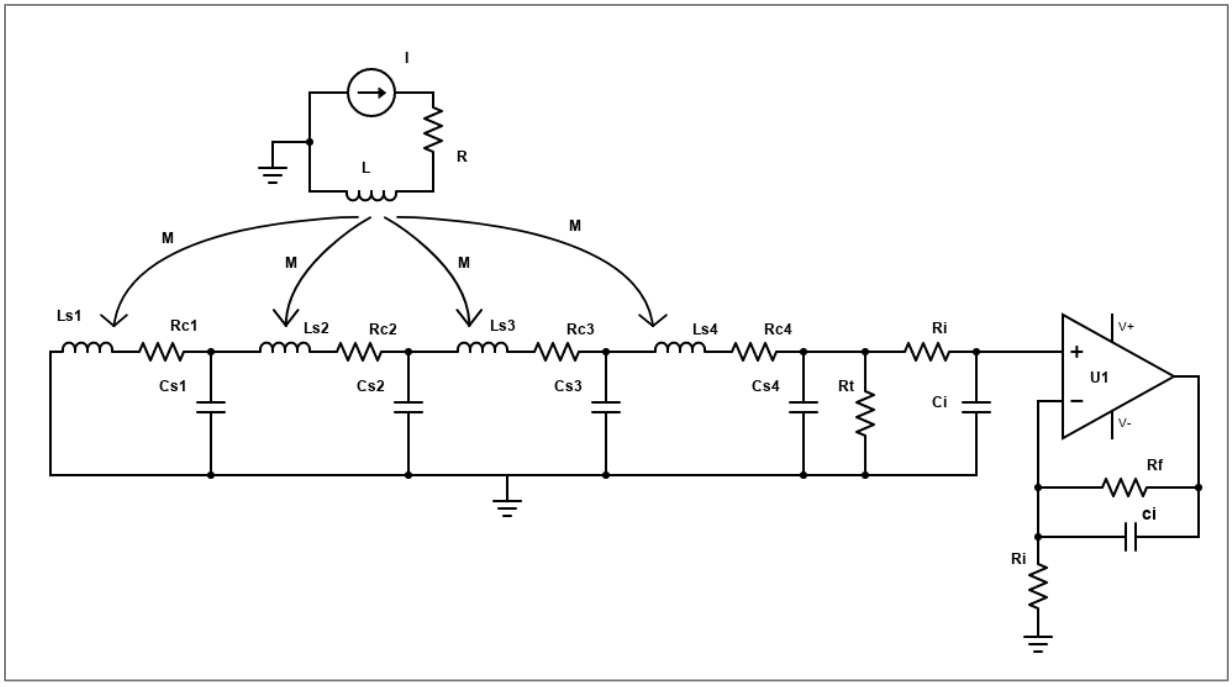

Fig 3.13: Distributed Parameter Model with active integrator

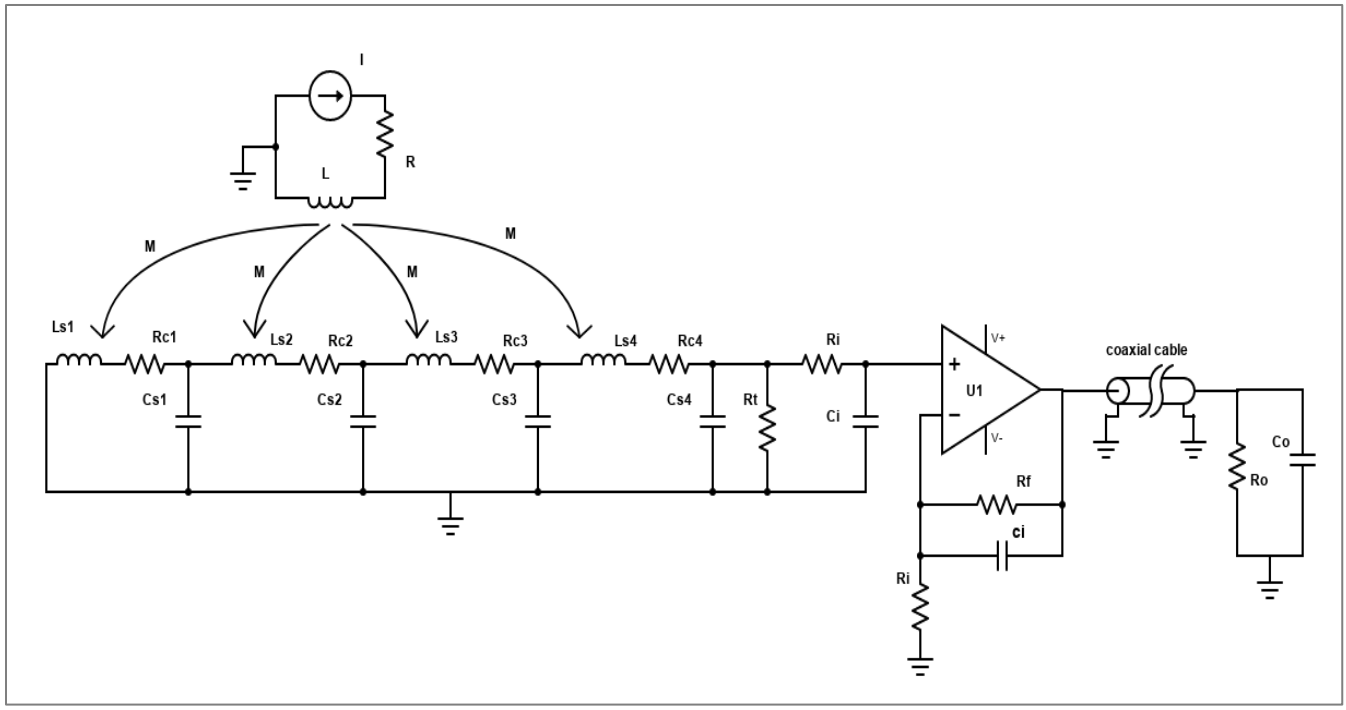

Fig 3.14: Distributed Parameter Model active integrator with coaxial cable connected to Oscilloscope

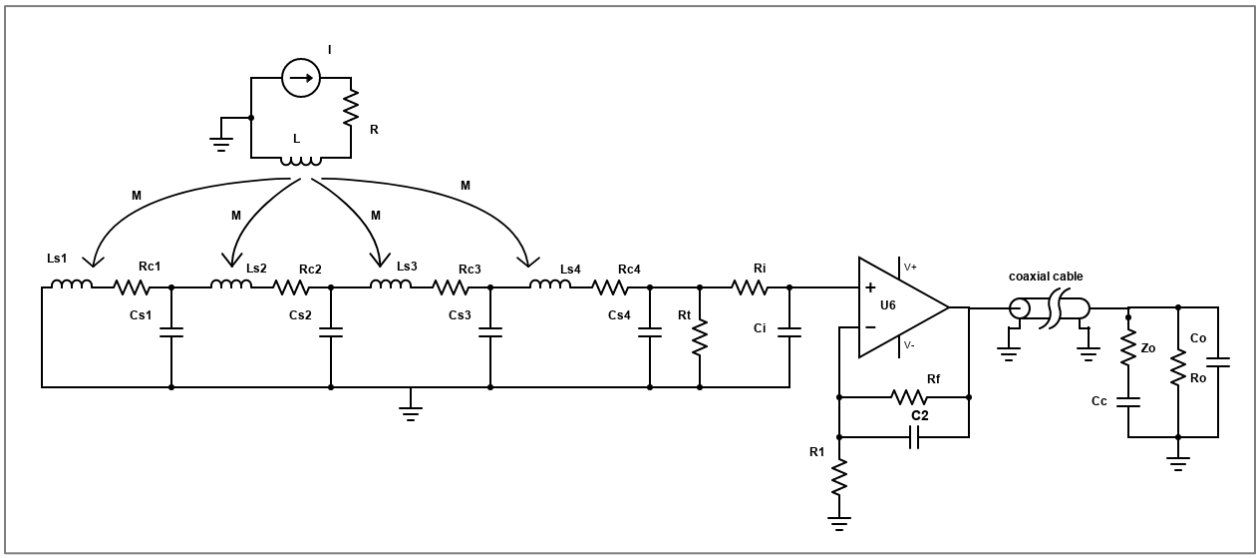

Fig 3.15: Distributed parameter model with active integrator with coaxial cable terminated at series RC matching impedance connected to Oscilloscope

3.6 Simulation Results

The above circuits from Fig. 3.4 to Fig. 3.15 are simulated in PSPICE using 1/20 μs impulse input current from Fig. 3.2 as input. The simulated output waveforms are generated using different terminating resistance from Table no … Percentage error of front time and tail time of output waveform from front time and tail time of the input impulse waveform is obtained for different terminating resistance error analysis.

3.6.1 Simulation Output configurations

- **Lumped Parameter Model: [Circuit arrangements Fig 3.4 to Fig 3.9]**

1.***Time response of Lumped Parameter Model with passive integrator***

For different values of terminating resistance, the simulation has been done. The output waveforms are:

1. R_t: 36.75k**Ω Fig.**3.12
2. R_t: 18.37k**Ω Fig.**3.13
3. R_t: 12.125k**Ω Fig.**3.14
4. R_t: 9.25k**Ω Fig.**3.15

2. ***Time response of Lumped parameter model with passive integrator with coaxial cable connected to Oscilloscope:***

For different values of terminating resistance, the simulation has been done. The output waveforms are:

1. R_t: 36.75k**Ω Fig.**3.16
2. R_t: 18.37k**Ω Fig.**3.17
3. R_t: 12.125k**Ω Fig.**3.18
4. R_t: 9.25k**Ω Fig.**3.19

3. ***Time response of Lumped parameter model with passive integrator with coaxial cable terminated at series RC matching impedance connected to Oscilloscope:***

For different values of terminating resistance, the simulation has been done. The output waveforms are:

1. R_t: 36.75k**Ω** **Fig.**3.20
2. R_t: 18.37k**Ω** **Fig.**3.21
3. R_t: 12.125k**Ω** **Fig.**3.22
4. R_t: 9.25k**Ω** **Fig.**3.23

4. ***Time response of Lumped parameter model with active integrator:***

For different values of terminating resistance, the simulation has been done. The output waveforms are:

1. R_t: 36.75k**Ω** **Fig.**3.24
2. R_t: 18.37k**Ω** **Fig.**3.25
3. R_t: 12.125k**Ω** **Fig.**3.26
4. R_t: 9.25k**Ω** **Fig.**3.27

5. ***Time response of Lumped parameter model with active integrator with coaxial cable connected to Oscilloscope:***

For different values of terminating resistance, the simulation has been done. The output waveforms are:

1. R_t: 36.75k**Ω** **Fig.**3.28
2. R_t: 18.37k**Ω** **Fig.**3.29
3. R_t: 12.125k**Ω** **Fig.**3.30
4. R_t: 9.25k**Ω** **Fig.**3.31

6. ***Time response of Lumped parameter model with active integrator with coaxial cable terminated at series RC matching impedance connected to Oscilloscope*****:**

For different values of terminating resistance, the simulation has been done. The output waveforms are:

1. R_t: 36.75k**Ω** **Fig.**3.32
2. R_t: 18.37k**Ω** **Fig.**3.33
3. R_t: 12.125k**Ω** **Fig.**3.34
4. R_t: 9.25k**Ω** **Fig.**3.35

- **Distributed Parameters Model:** [**Circuit arrangements Fig 3.10 to Fig 3.15**]

7. ***Time response of Distributed parameter model with passive integrator:***

For different values of terminating resistance, the simulation has been done. The output waveforms are:

1. R_t: 36.75k**Ω** **Fig.**3.36
2. R_t: 18.37k**Ω** **Fig.**3.37
3. R_t: 12.125k**Ω** **Fig.**3.38
4. R_t: 9.25k**Ω** **Fig.**3.39

8. ***Time response of Distributed parameter model with passive integrator with coaxial cable connected to Oscilloscope:***

For different values of terminating resistance, the simulation has been done. The output waveforms are:

1. R_t: 36.75k**Ω** **Fig.**3.40
2. R_t: 18.37k**Ω** **Fig.**3.41
3. R_t: 12.125k**Ω** **Fig.**3.42
4. R_t: 9.25k**Ω** **Fig.**3.43

9. ***Time response of Distributed parameter model with passive integrator with coaxial cable terminated at series RC matching impedance connected to Oscilloscop*e*:***

For different values of terminating resistance, the simulation has been done. The output waveforms are:

1. R_t: 36.75k**Ω** **Fig.**3.44
2. R_t: 18.37k**Ω** **Fig.**3.45
3. R_t: 12.125k**Ω** **Fig.**3.46
4. R_t: 9.25k**Ω** **Fig.**3.47

10. ***Time response of Distributed parameter model with active integrator:***

For different values of terminating resistance, the simulation has been done. The output waveforms are:

1. R_t: 36.75k**Ω** **Fig.**3.48
2. R_t: 18.37k**Ω** **Fig**.3.49
3. R_t: 12.125k**Ω** **Fig.**3.50
4. R_t: 9.25k**Ω** **Fig.**3.51

11. ***Time response of Distributed parameter model with active integrator with coaxial cable connected to Oscilloscope:***

For different values of terminating resistance, the simulation has been done. The output waveforms are:

1. R_t: 36.75k**Ω** **Fig.**3.52
2. R_t: 18.37k**Ω** **Fig**.3.53
3. R_t: 12.125k**Ω** **Fig.**3.54
4. R_t: 9.25k**Ω** **Fig**.3.55

12. ***Time response of Distributed parameter model with active integrator with coaxial cable terminated at series RC matching impedance connected to Oscilloscop*e*:***

For different values of terminating resistance, the simulation has been done. The output waveforms are:

1. R_t: 36.75k**Ω** **Fig.**3.56
2. R_t: 18.37k**Ω** **Fig.**3.57
3. R_t: 12.125k**Ω** **Fig.**3.58
4. R_t: 9.25k**Ω** **Fig.**3.59

3.6.2 Output Waveforms

I. LUMPED PARAMETER MODEL

I. (a) With passive integrator

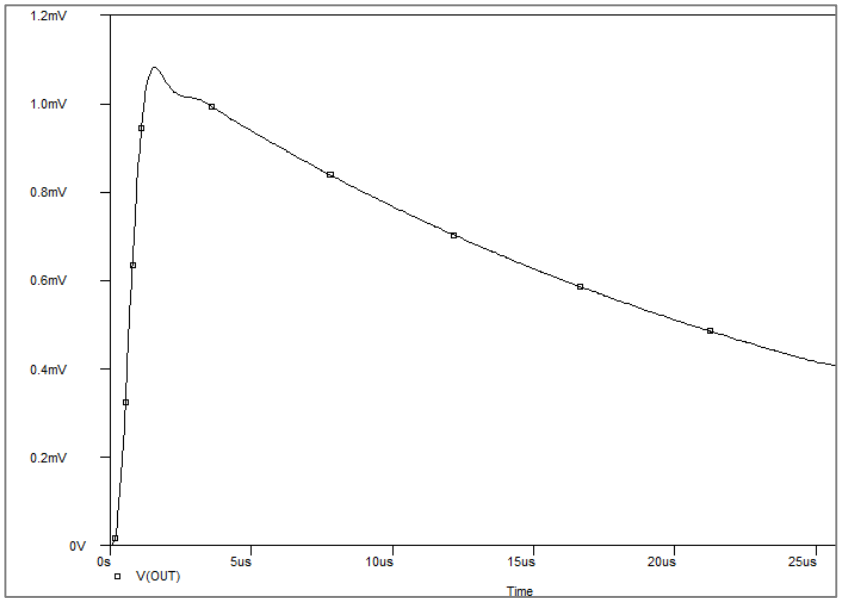

Fig. 3.12: Output waveform from simulation considering $R_t = 36.75\text{k}\Omega$

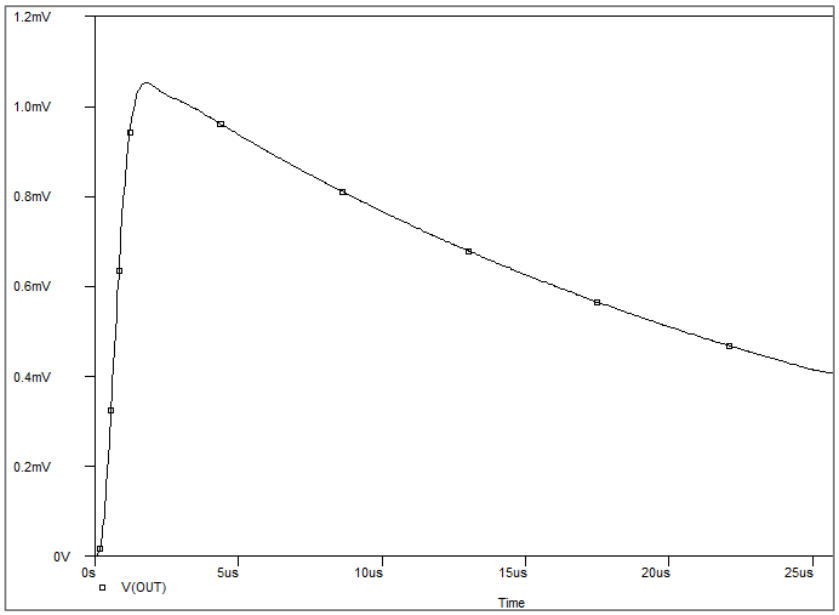

Fig. 3.13: Output waveform from simulation considering $R_t = 18.37\text{k}\Omega$

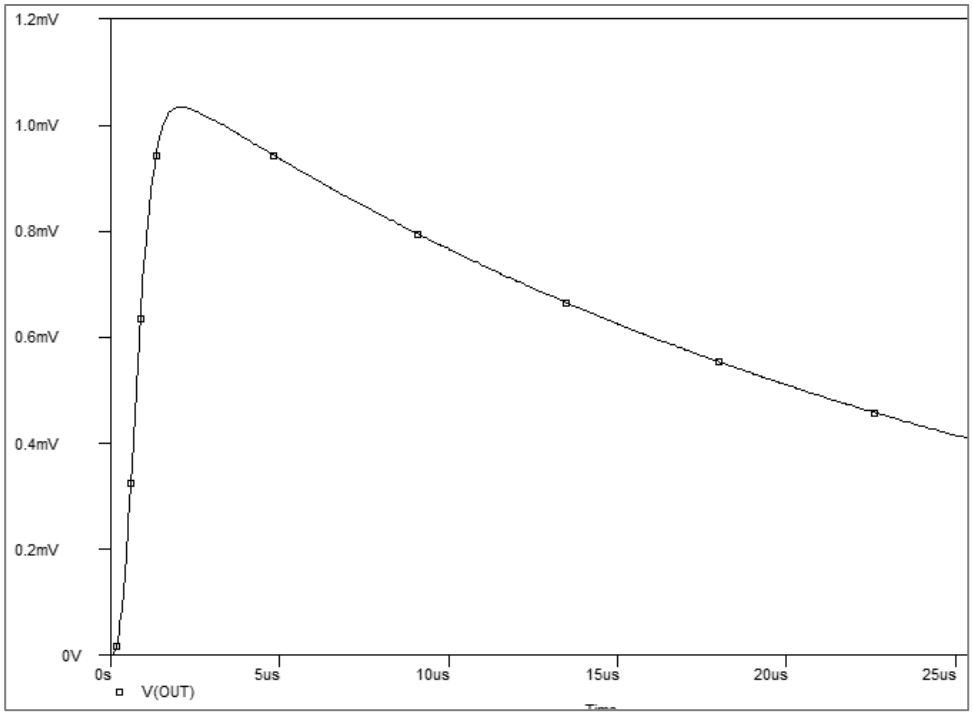

Fig. 3.14: Output waveform from simulation considering $R_t = 12.125\text{k}\Omega$

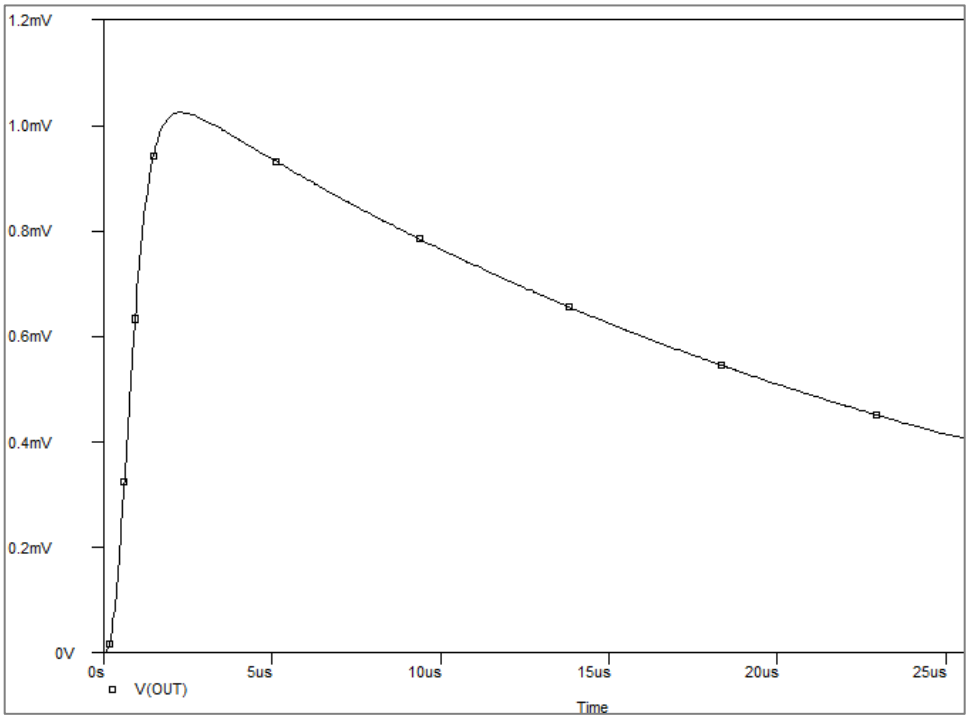

Fig. 3.15: Output waveform from simulation considering $R_t = 9.25\text{k}\Omega$

I. (b) With passive integrator with coaxial cable connected to Oscilloscope

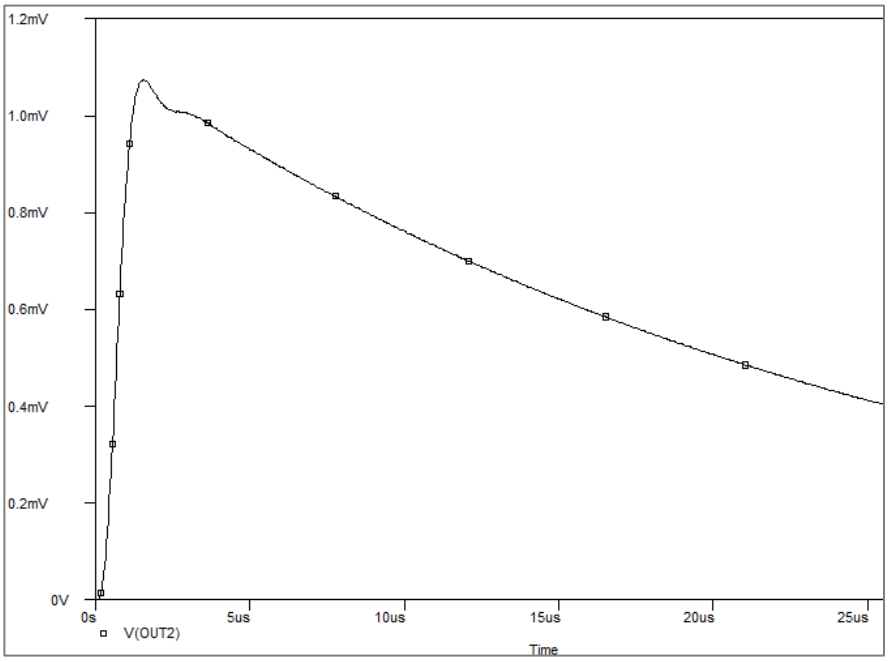

Fig. 3.16: Output waveform from simulation considering $R_t = 36.75\text{k}\Omega$

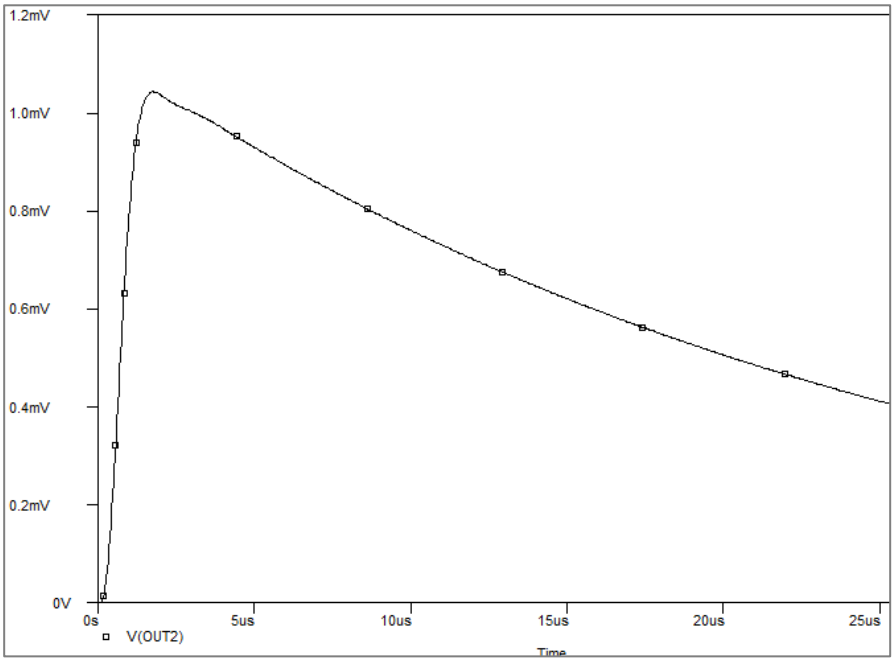

Fig. 3.17: Output waveform from simulation considering $R_t = 18.37\text{k}\Omega$

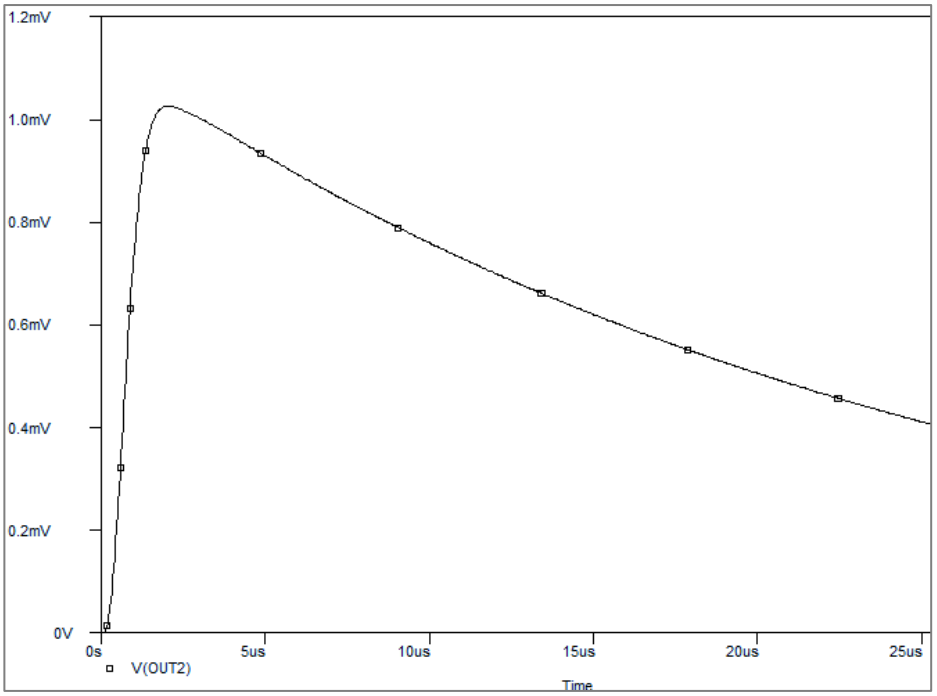

Fig. 3.18: Output waveform from simulation considering $R_t = 12.125\text{k}\Omega$

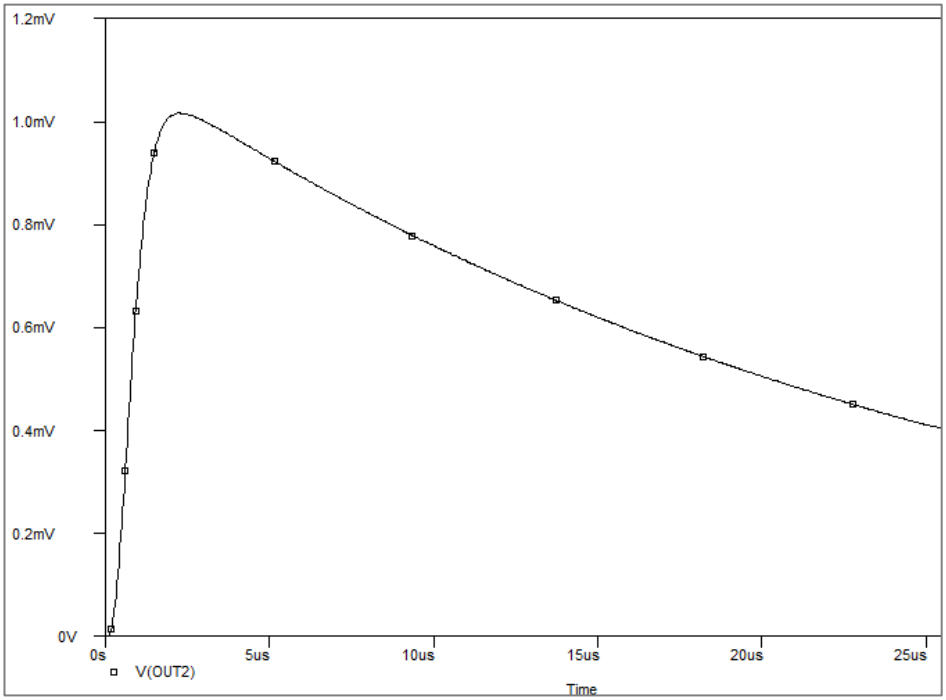

Fig. 3.19: Output waveform from simulation considering $R_t = 9.25\text{k}\Omega$

I. (c) With passive integrator with coaxial cable terminated at series RC matching impedance connected to Oscilloscope

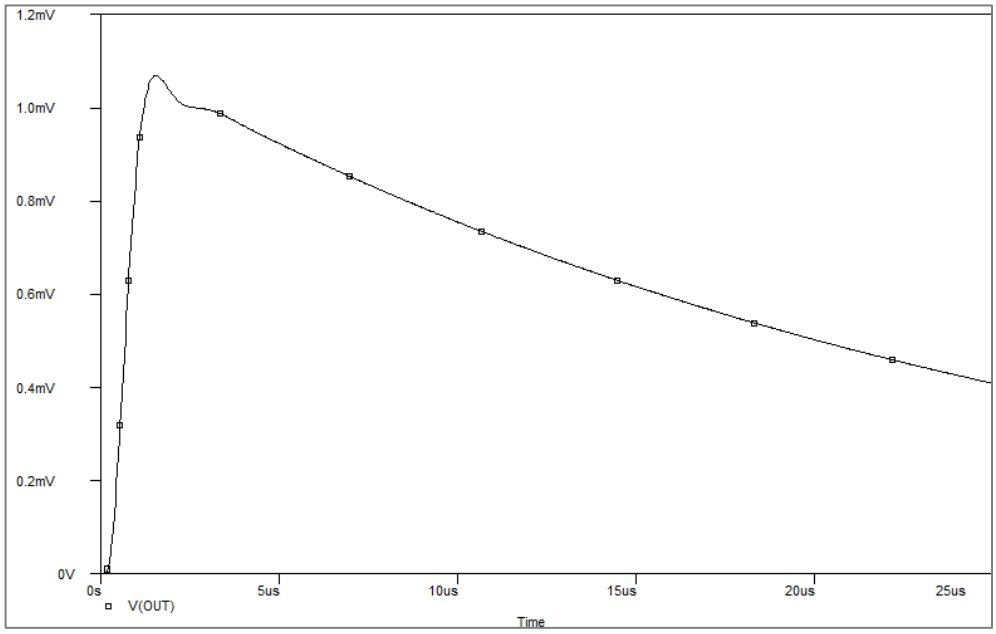

Fig. 3.20: Output waveform from simulation considering $R_t = 36.75\text{k}\Omega$

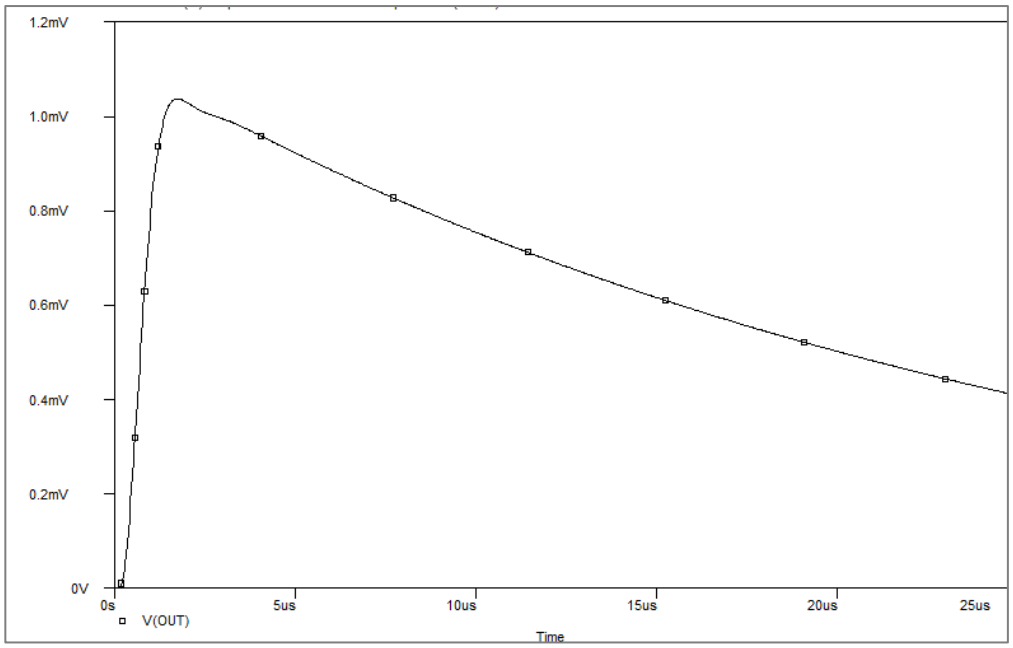

Fig. 3.21: Output waveform from simulation considering $R_t = 18.37\text{k}\Omega$

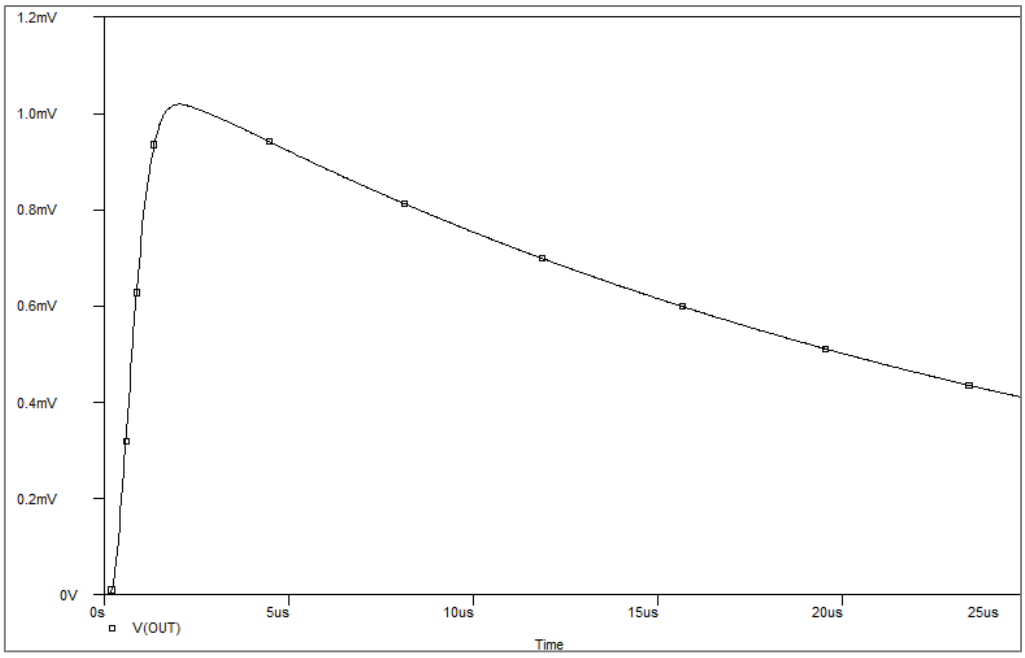

Fig. 3.22: Output waveform from simulation considering $R_t = 12.125\text{k}\Omega$

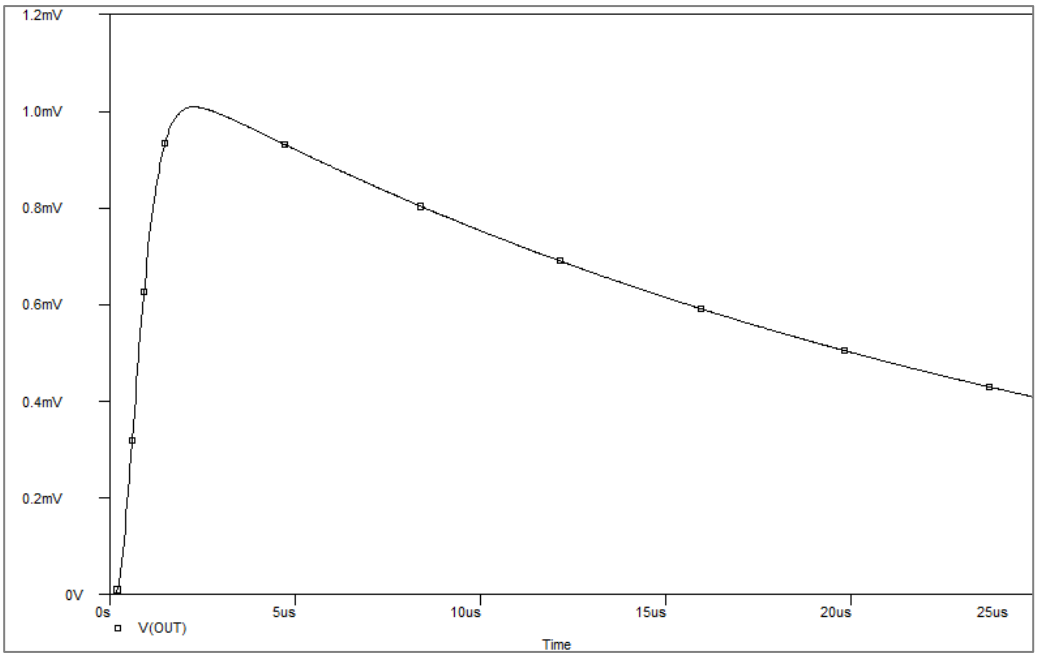

Fig. 3.23: Output waveform from simulation considering $R_t = 9.25\text{k}\Omega$

I. (d) With active integrator

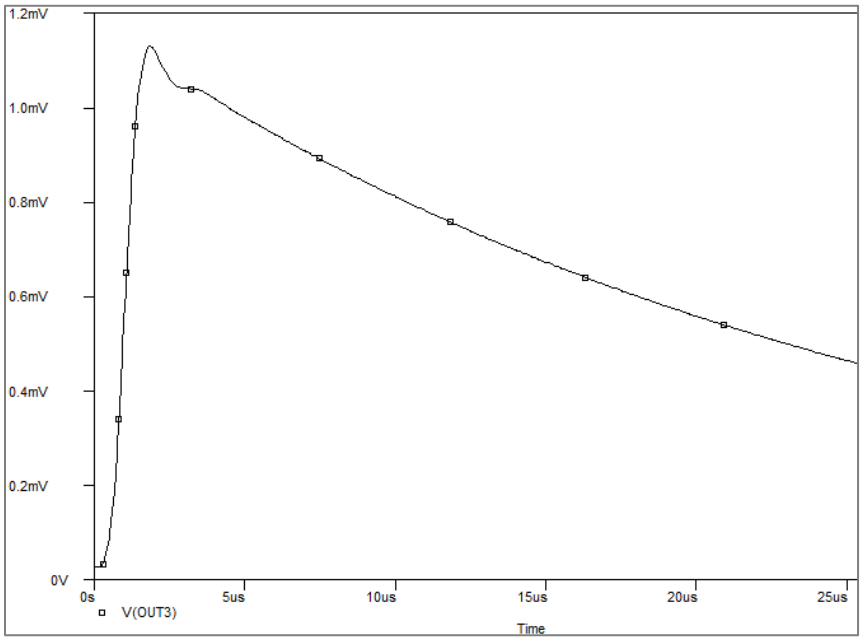

Fig. 3.24: Output waveform from simulation considering $R_t = 36.75\text{k}\Omega$

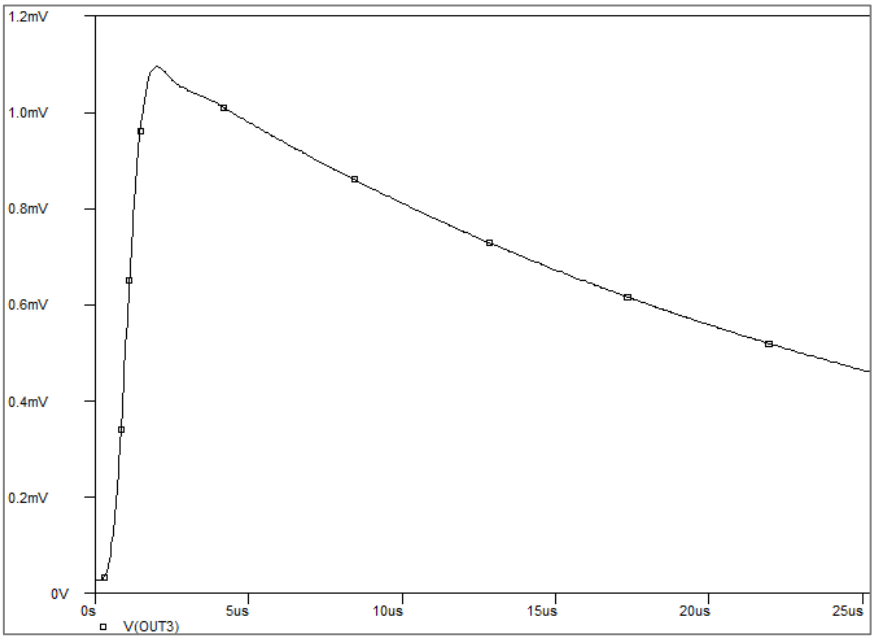

Fig. 3.25: Output waveform from simulation considering $R_t = 18.37\text{k}\Omega$

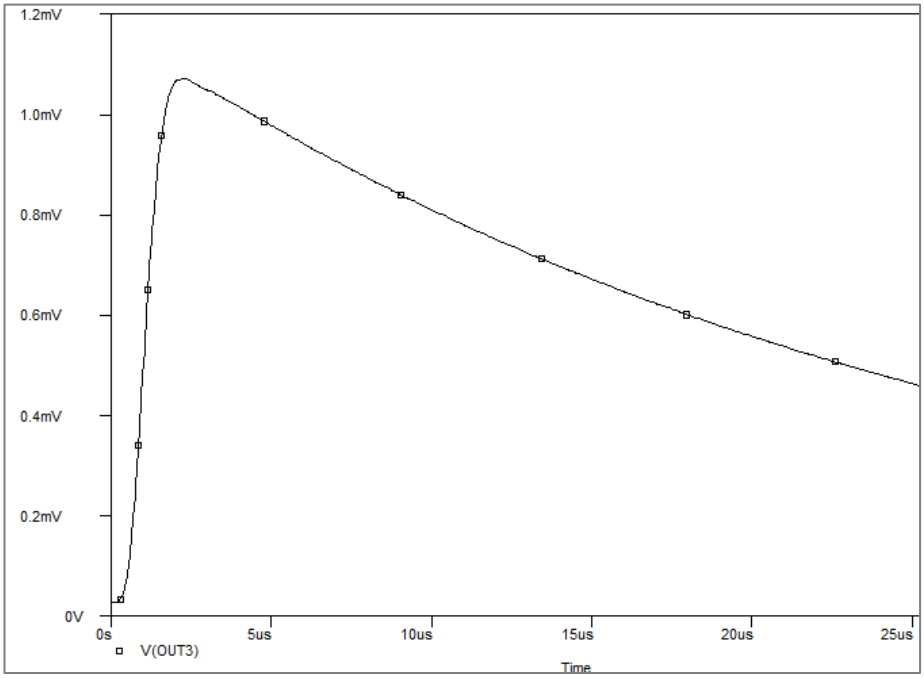

Fig. 3.26: Output waveform from simulation considering $R_t = 12.125\text{k}\Omega$

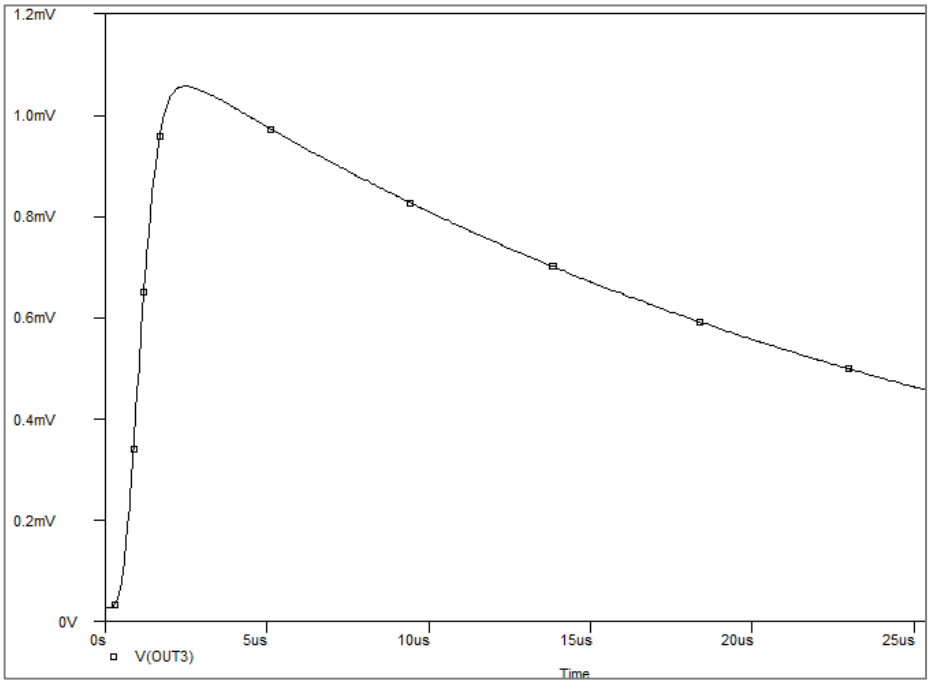

Fig. 3.27: Output waveform from simulation considering $R_t = 9.25\text{k}\Omega$

I. (e) With active integrator with coaxial cable connected to Oscilloscope

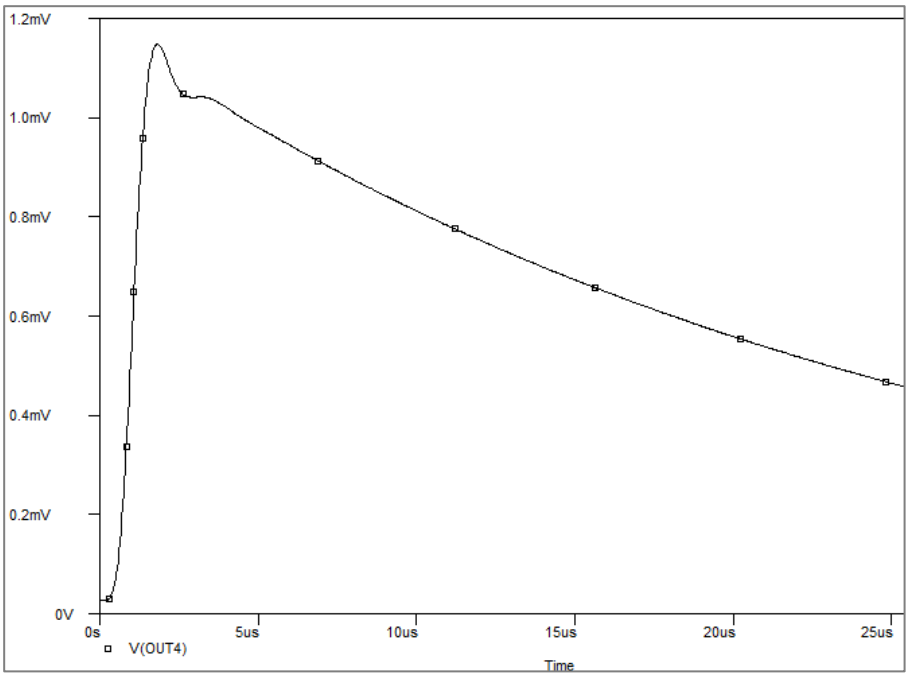

Fig. 3.28: Output waveform from simulation considering $R_t = 36.75\text{k}\Omega$

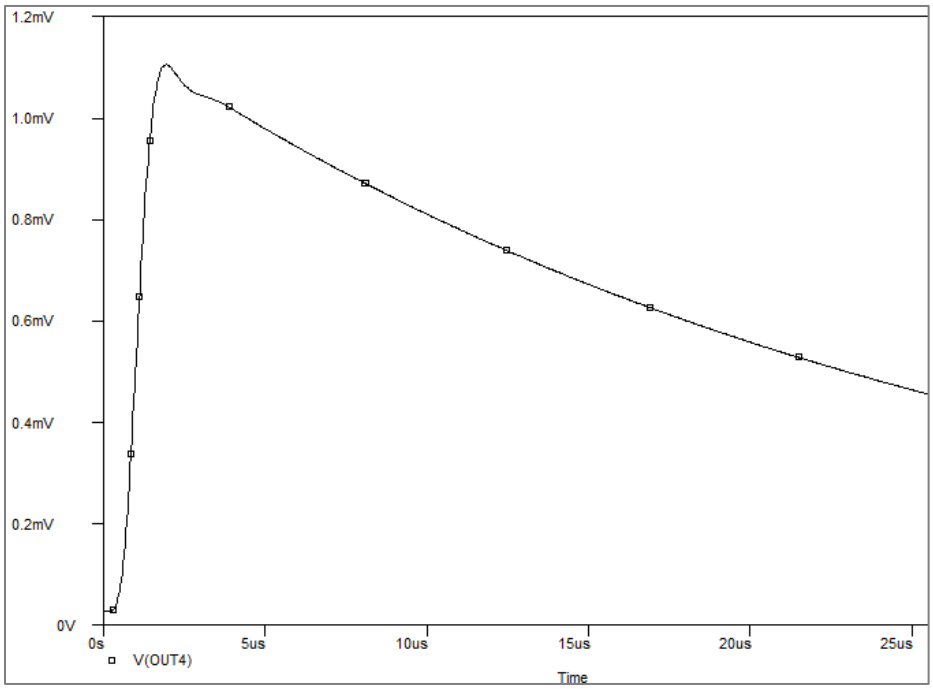

Fig. 3.29: Output waveform from simulation considering $R_t = 18.37\text{k}\Omega$

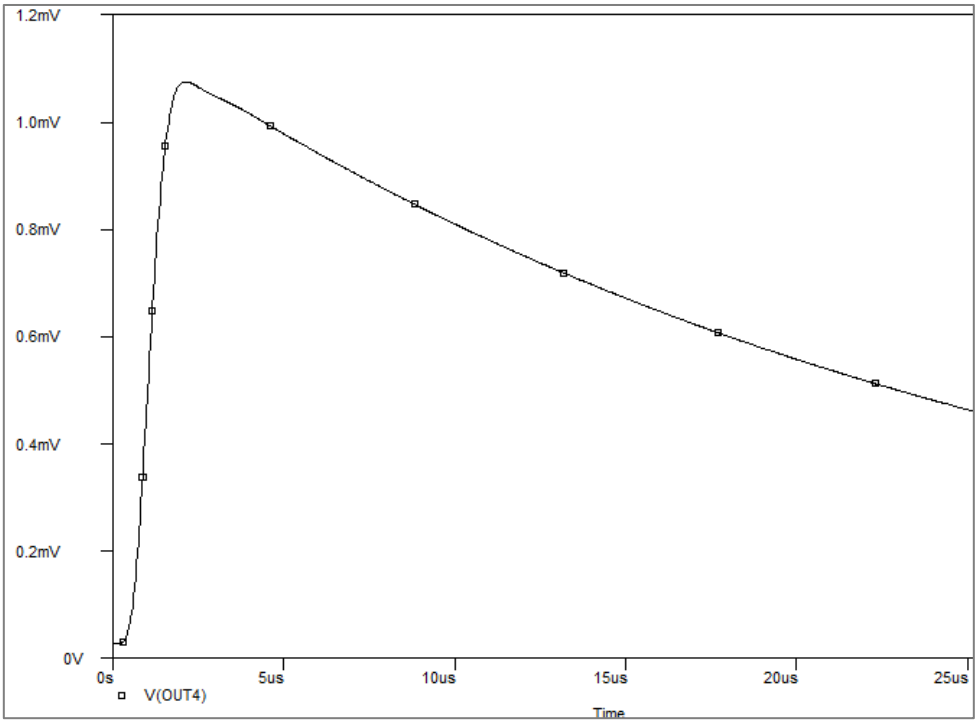

Fig. 3.30: Output waveform from simulation considering $R_t = 12.125\text{k}\Omega$

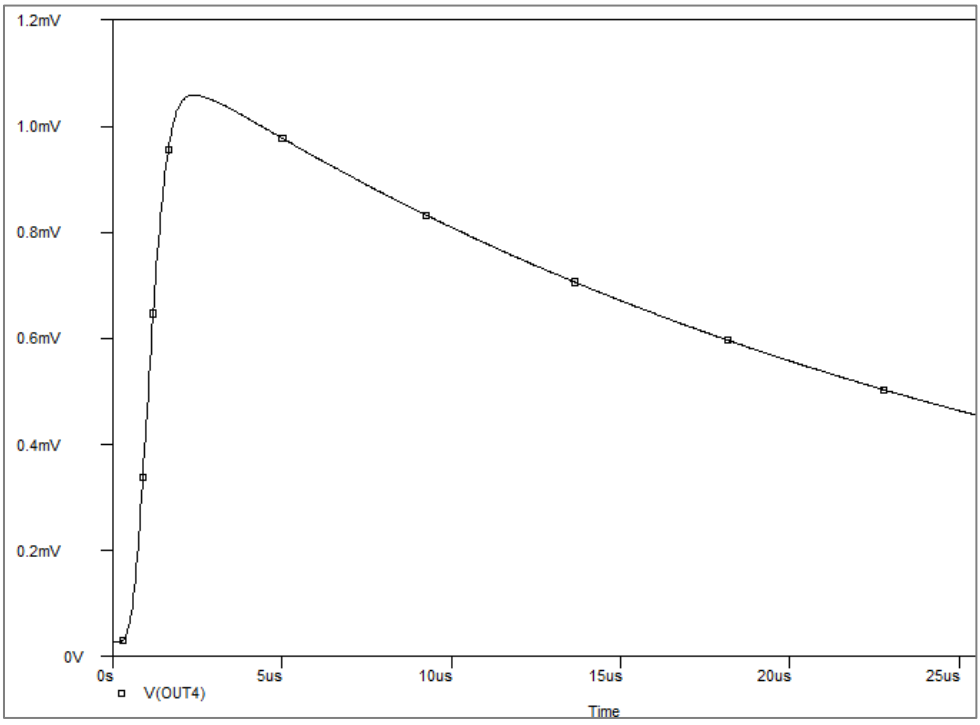

Fig. 3.31: Output waveform from simulation considering $R_t = 9.25\text{k}\Omega$

I. (f) With active integrator with coaxial cable terminated at series RC matching impedance connected to Oscilloscope

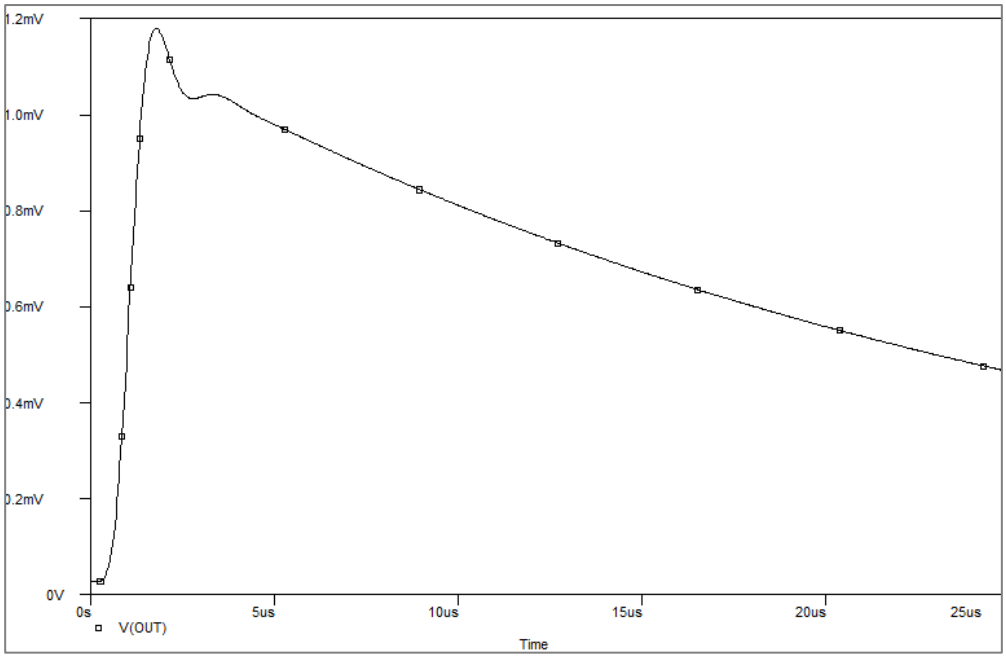

Fig. 3.32: Output waveform from simulation considering $R_t = 36.75\text{k}\Omega$

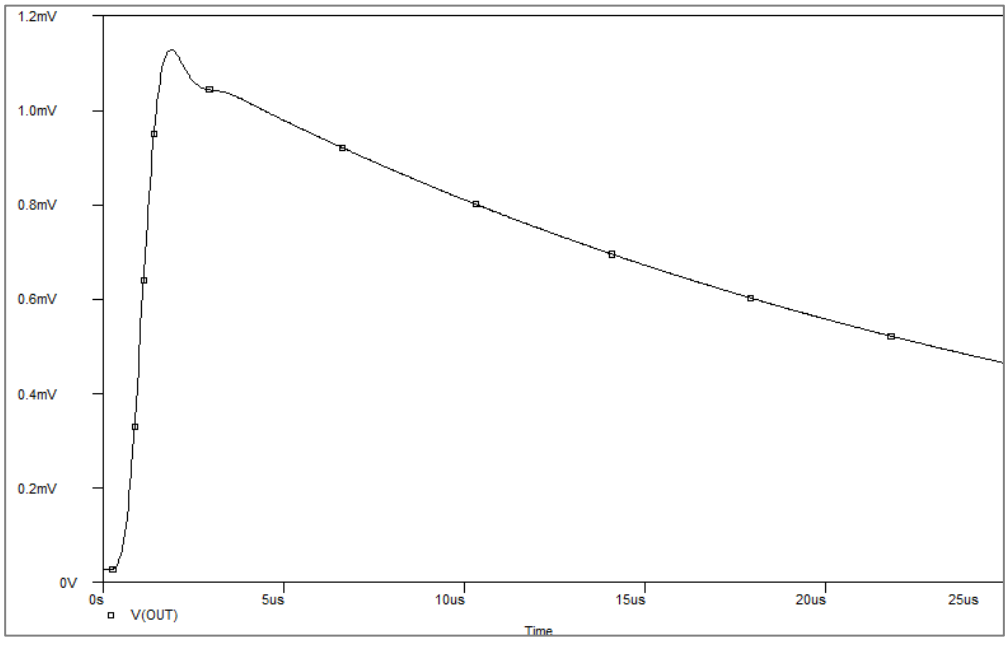

Fig. 3.33: Output waveform from simulation considering $R_t = 18.37\text{k}\Omega$

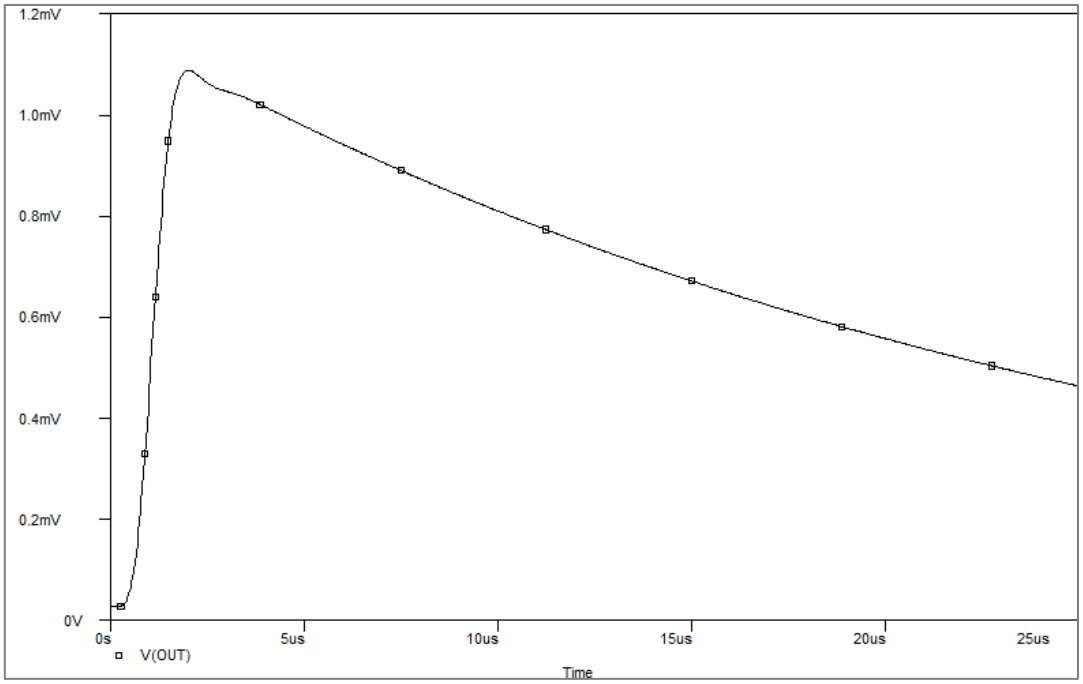

Fig. 3.34: Output waveform from simulation considering $R_t = 12.125\text{k}\Omega$

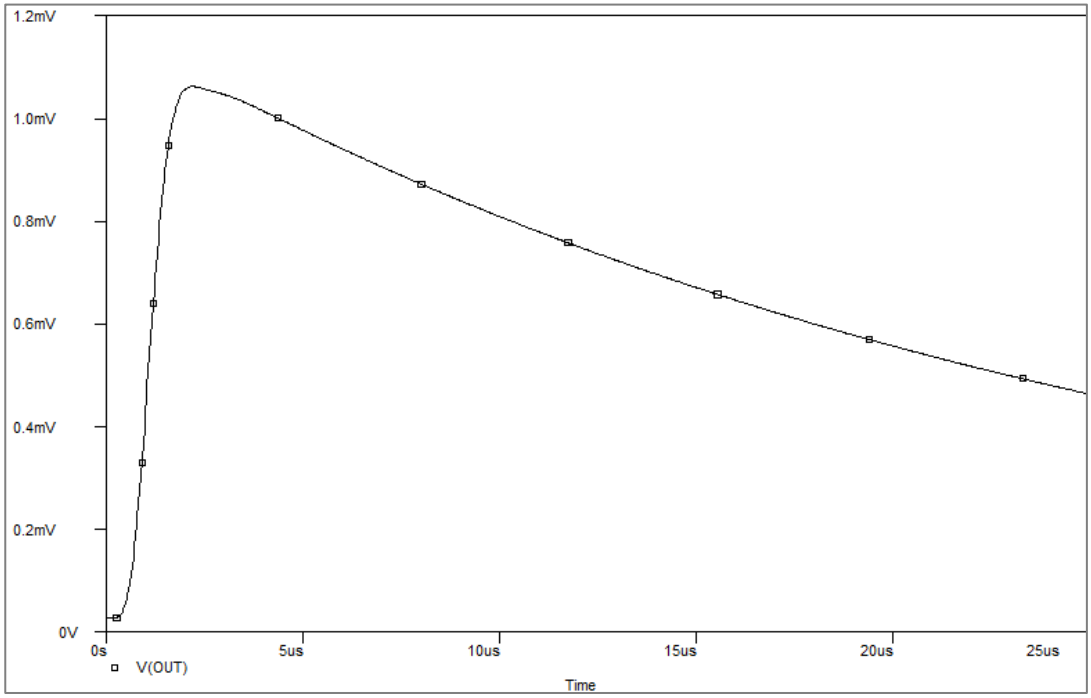

Fig. 3.35: Output waveform from simulation considering $R_t = 9.25\text{k}\Omega$

II. Distributed PARAMETER MODEL

II. (a) With passive integrator

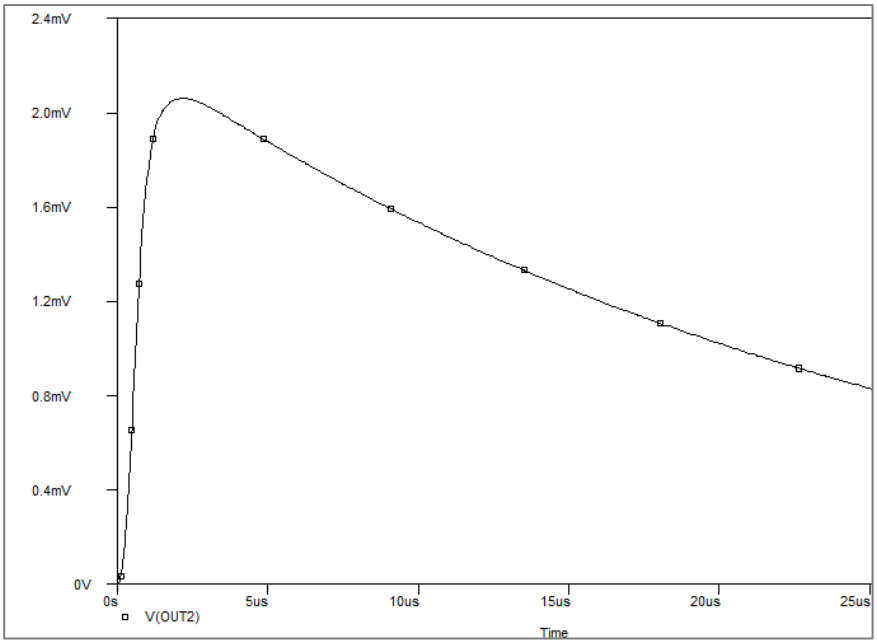

Fig. 3.36: Output waveform from simulation considering $R_t = 36.75\text{k}\Omega$

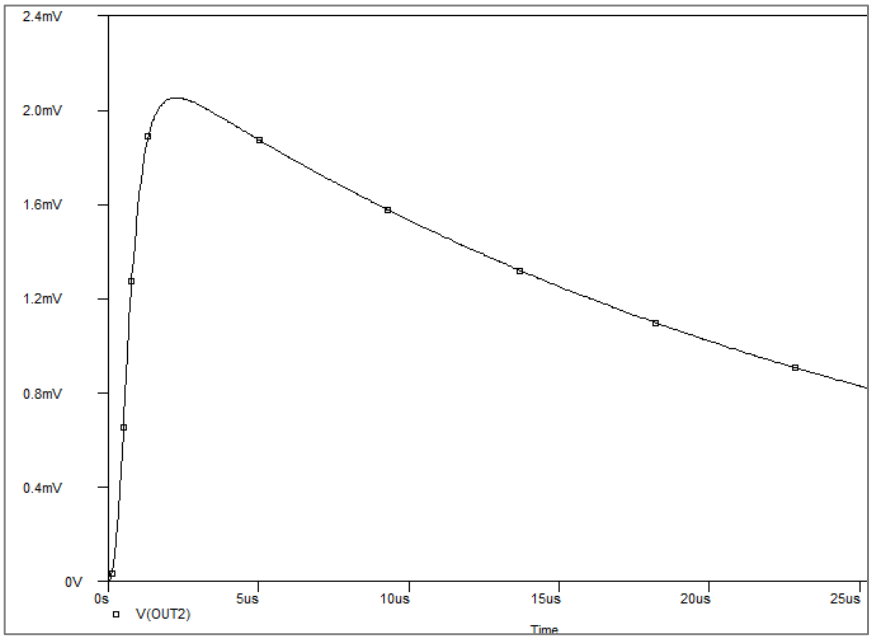

Fig. 3.37: Output waveform from simulation considering $R_t = 18.37\text{k}\Omega$

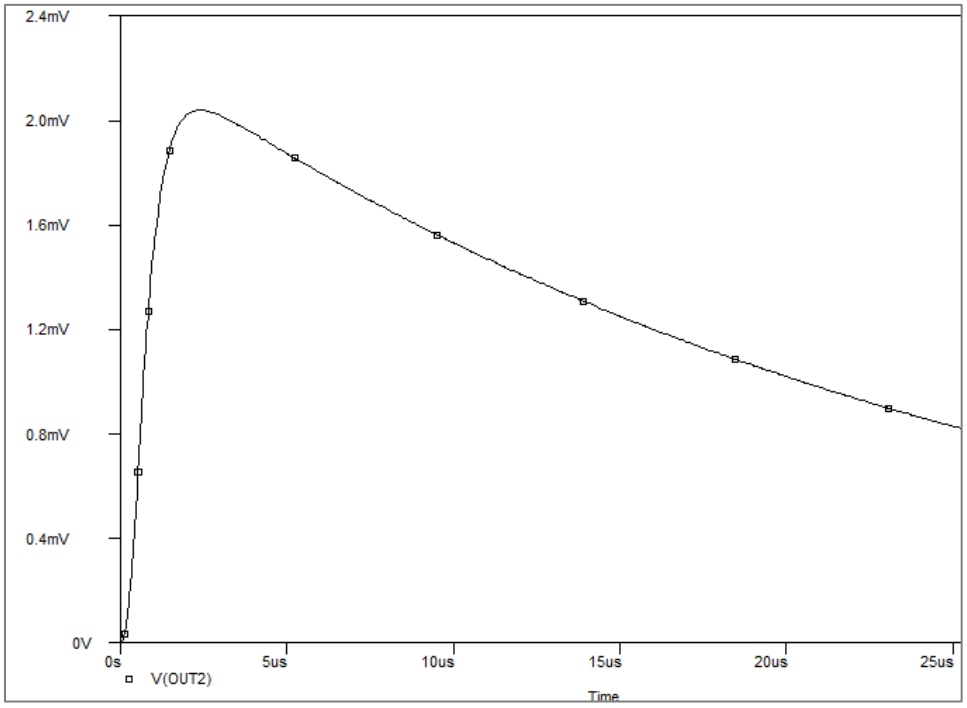

Fig. 3.38: Output waveform from simulation considering $R_t = 12.125\text{k}\Omega$

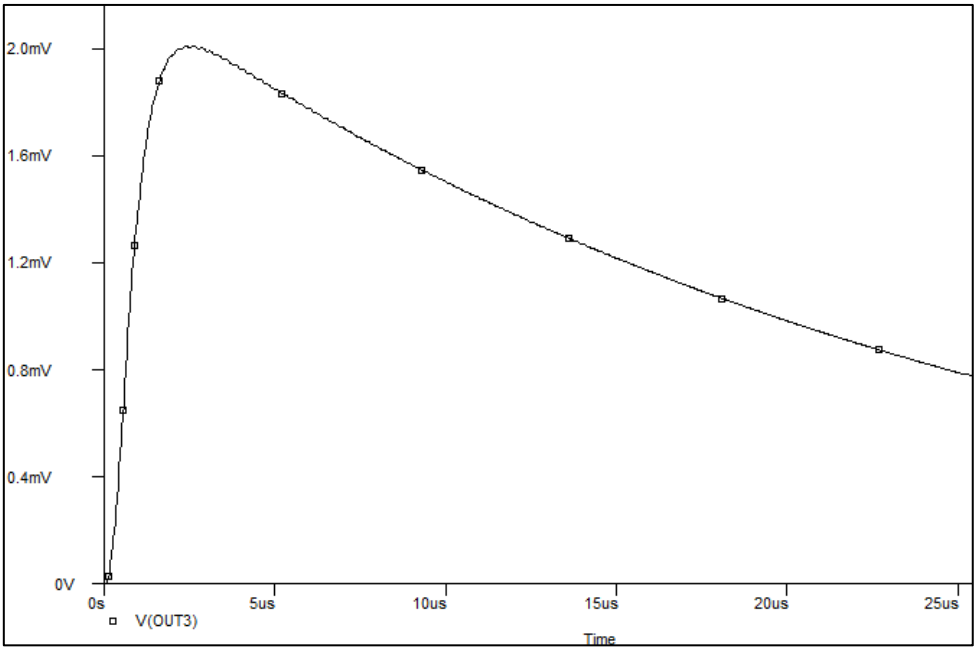

Fig. 3.39: Output waveform from simulation considering $R_t = 9.25\text{k}\Omega$

II. (b) With passive integrator with coaxial cable connected to Oscilloscope

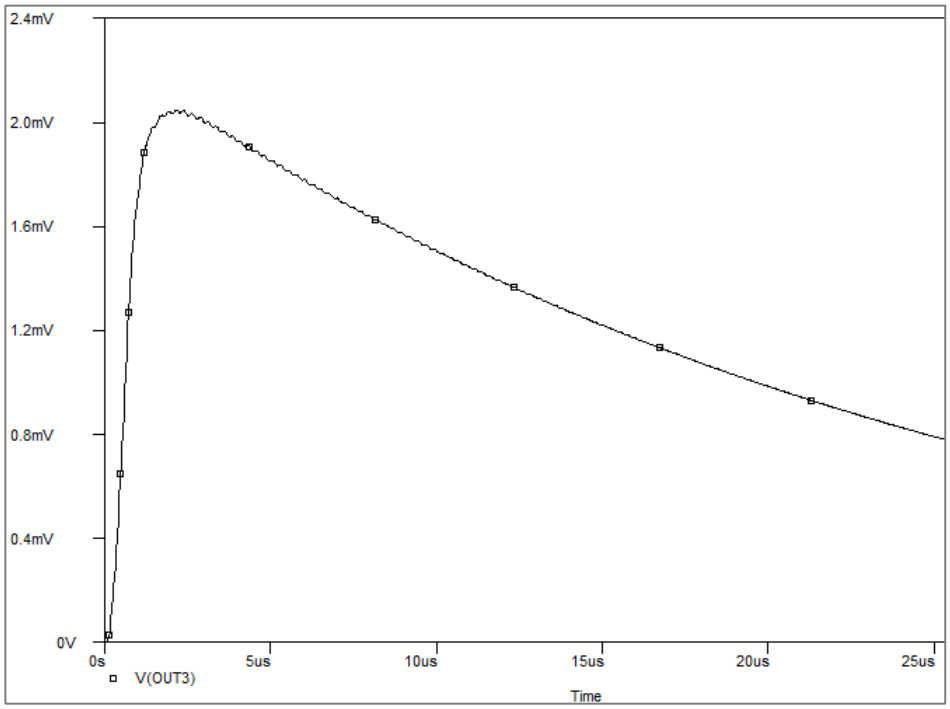

Fig. 3.40: Output waveform from simulation considering $R_t = 36.75\text{k}\Omega$

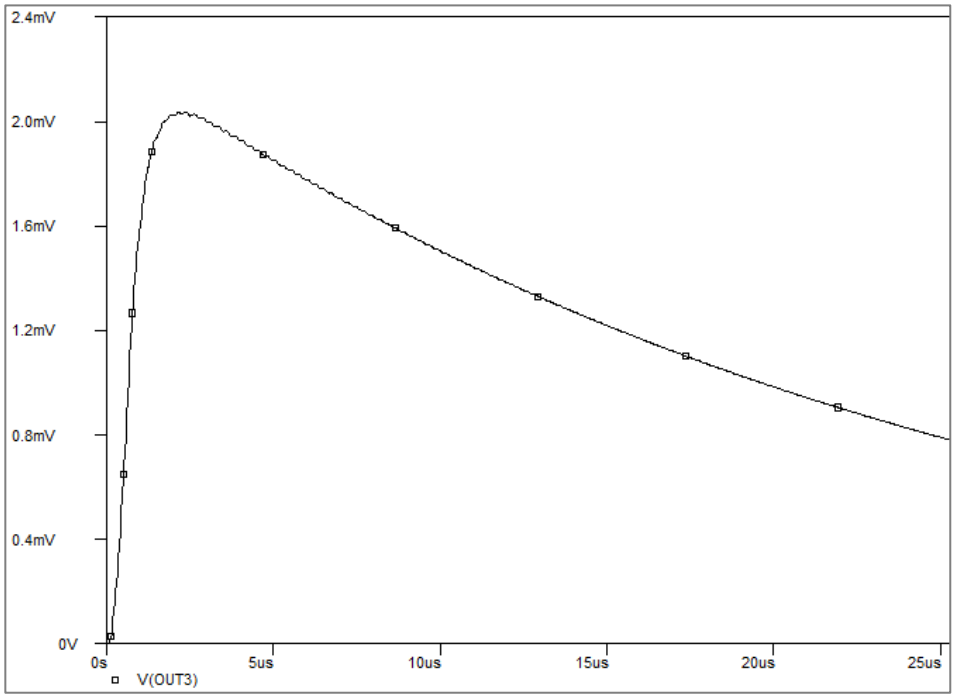

Fig. 3.41: Output waveform from simulation considering $R_t = 18.37\text{k}\Omega$

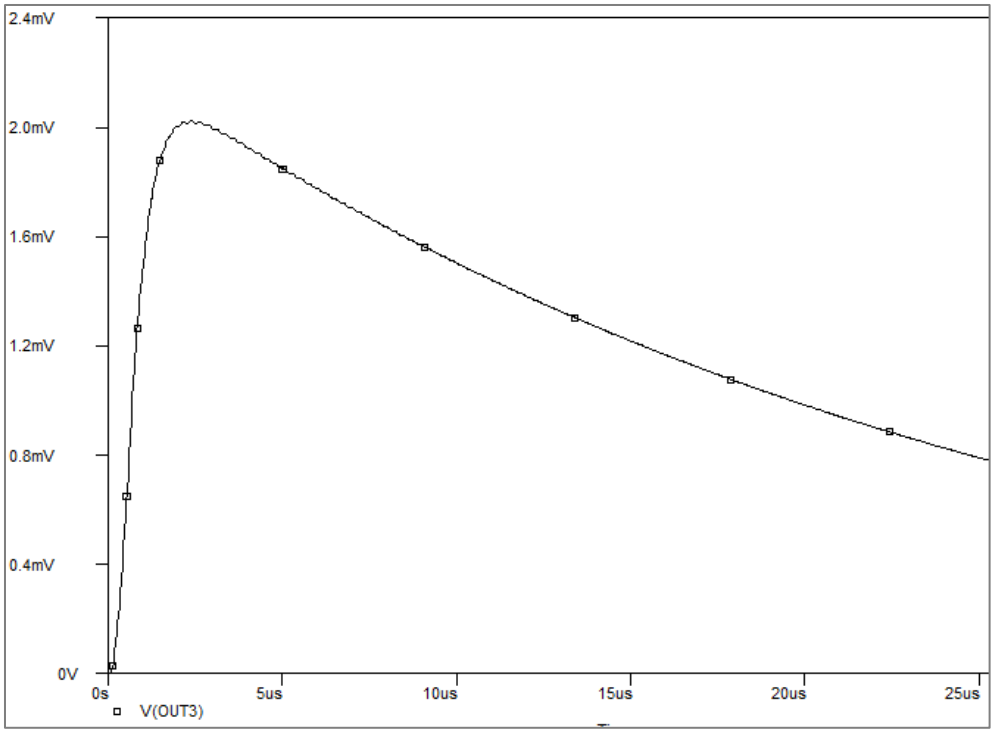

Fig. 3.42: Output waveform from simulation considering $R_t = 12.125\text{k}\Omega$

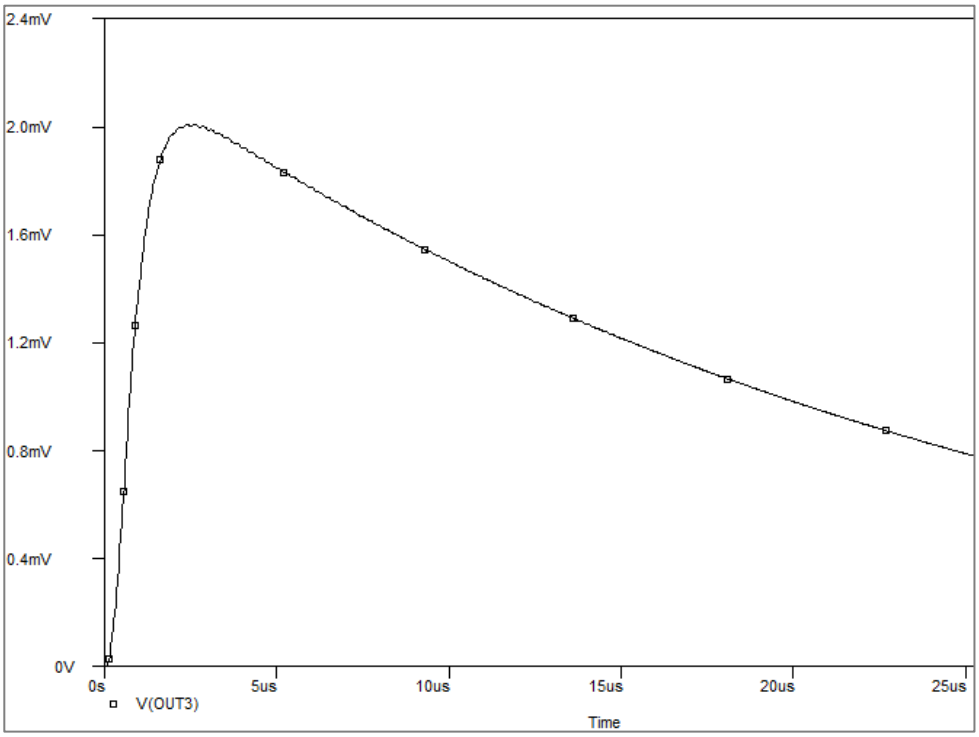

Fig. 3.43: Output waveform from simulation considering $R_t = 9.25\text{k}\Omega$

II. (c) With passive integrator with coaxial cable terminated at series RC matching impedance connected to Oscilloscope

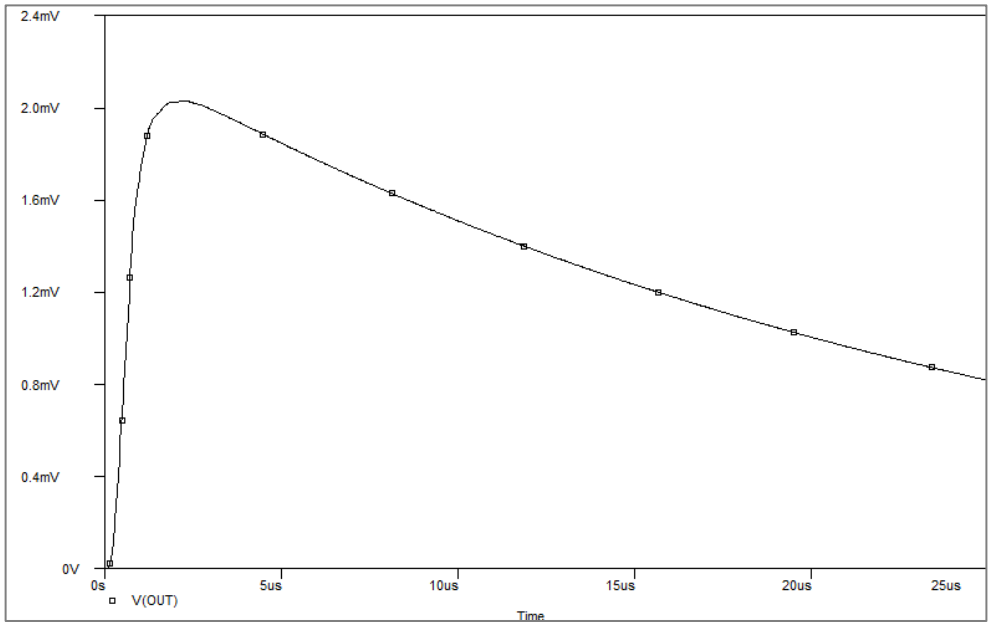

Fig. 3.44: Output waveform from simulation considering $R_t = 36.75\text{k}\Omega$

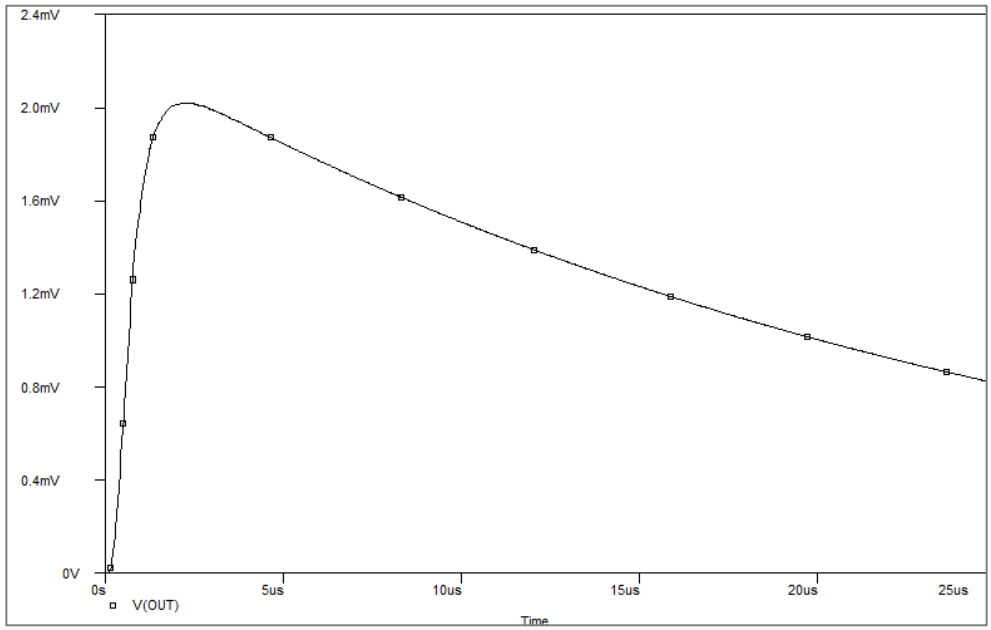

Fig. 3.45: Output waveform from simulation considering $R_t = 18.37\text{k}\Omega$

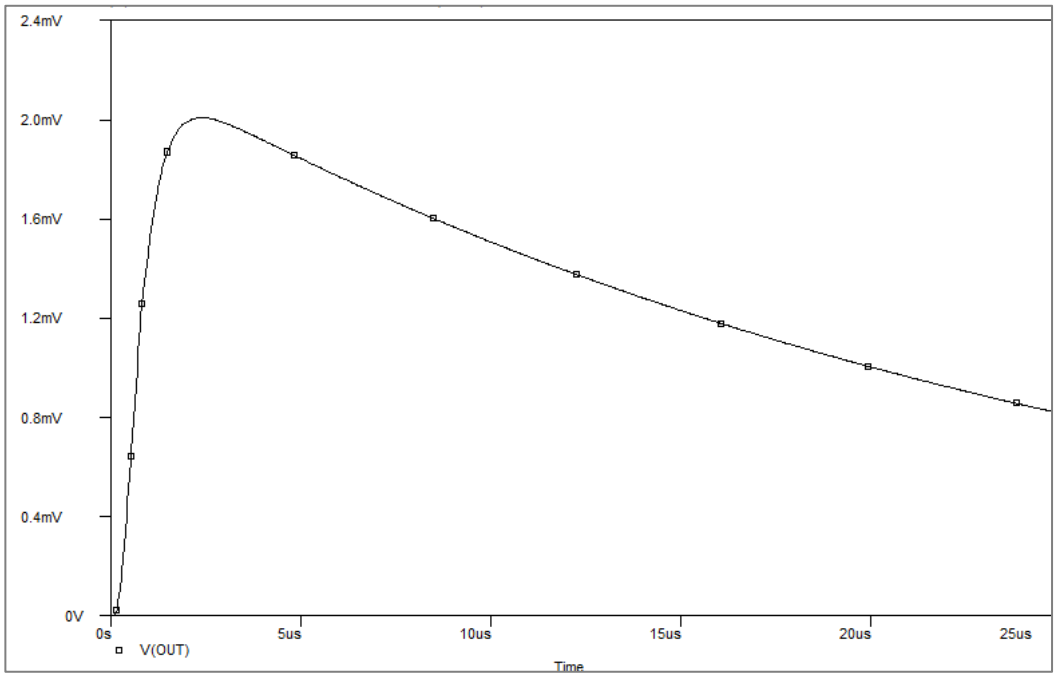

Fig. 3.46: Output waveform from simulation considering $R_t = 12.125\text{k}\Omega$

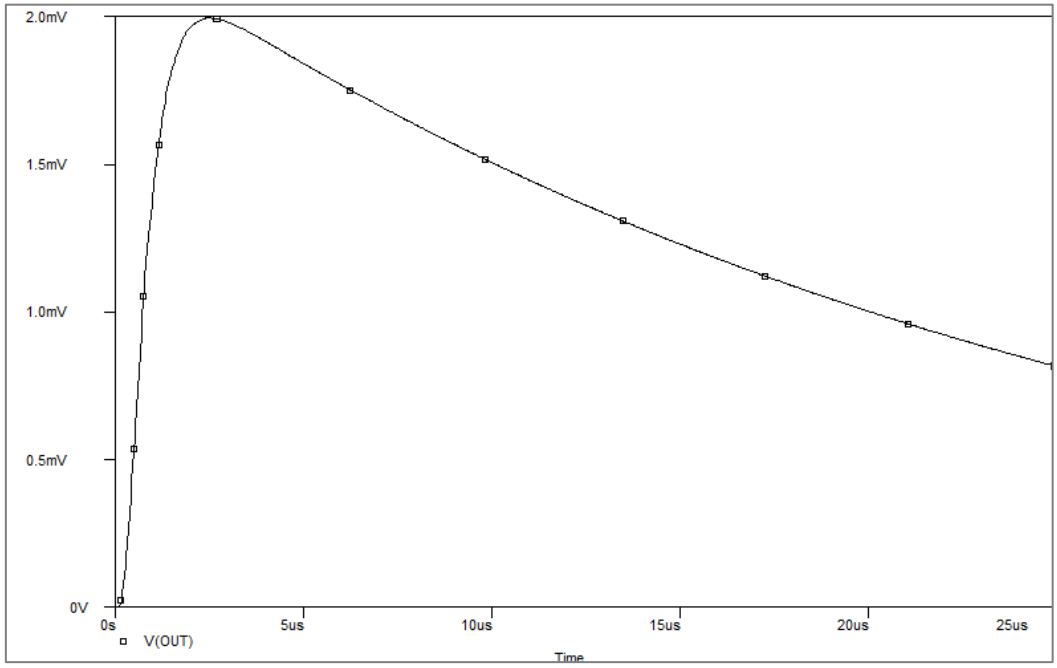

Fig. 3.47: Output waveform from simulation considering $R_t = 9.25\text{k}\Omega$

II. (d) With active integrator

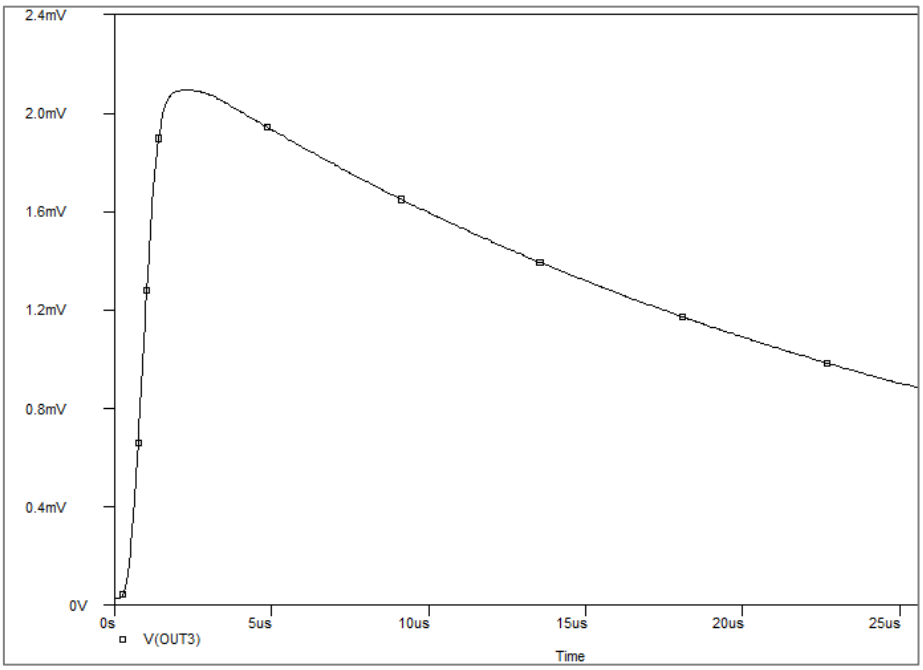

Fig. 3.48: Output waveform from simulation considering $R_t = 36.75\text{k}\Omega$

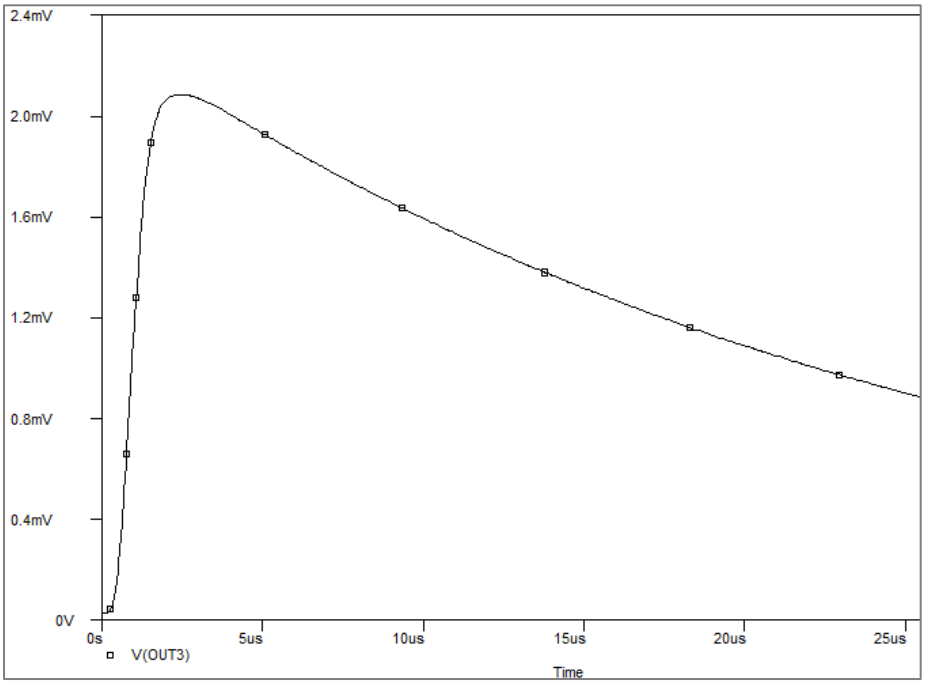

Fig. 3.49: Output waveform from simulation considering $R_t = 18.37\text{k}\Omega$

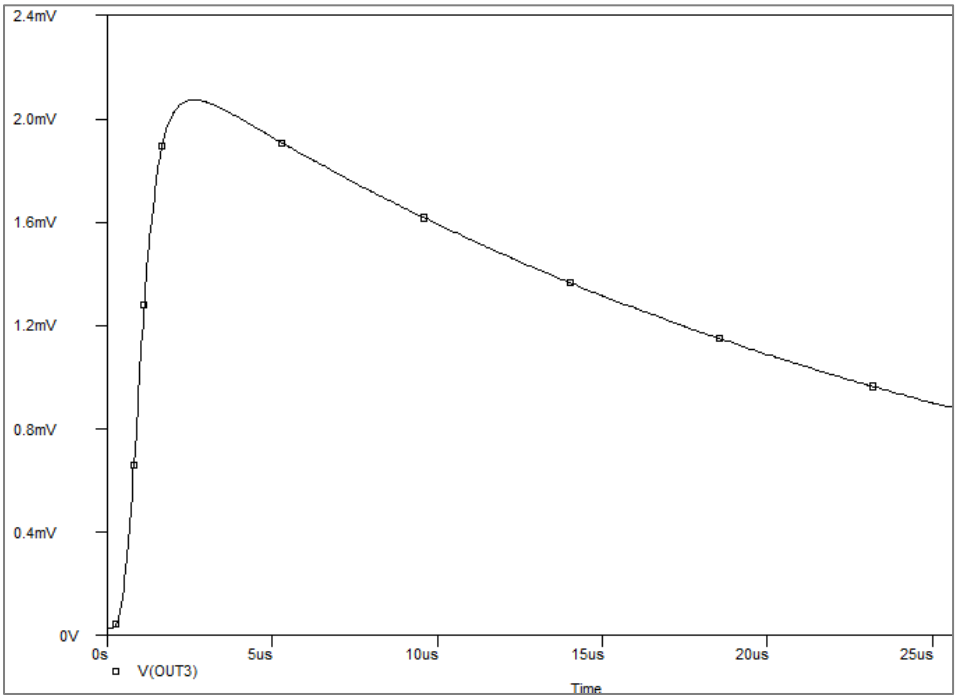

Fig. 3.50: Output waveform from simulation considering $R_t = 12.125\text{k}\Omega$

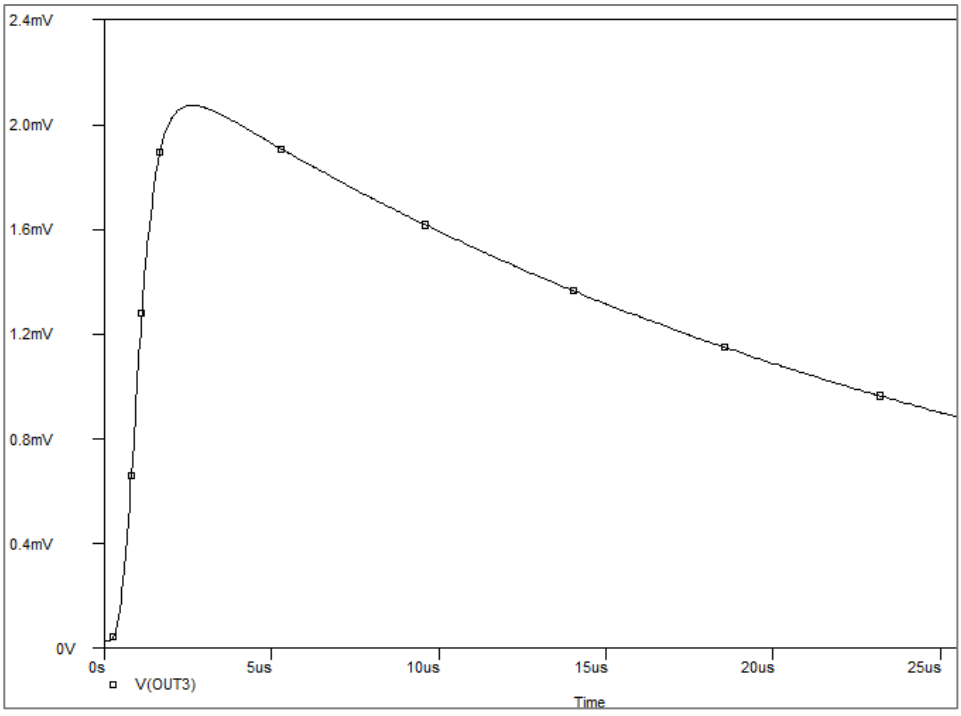

Fig. 3.51: Output waveform from simulation considering $R_t = 9.25\text{k}\Omega$

II. (e) With active integrator with coaxial cable connected to Oscilloscope

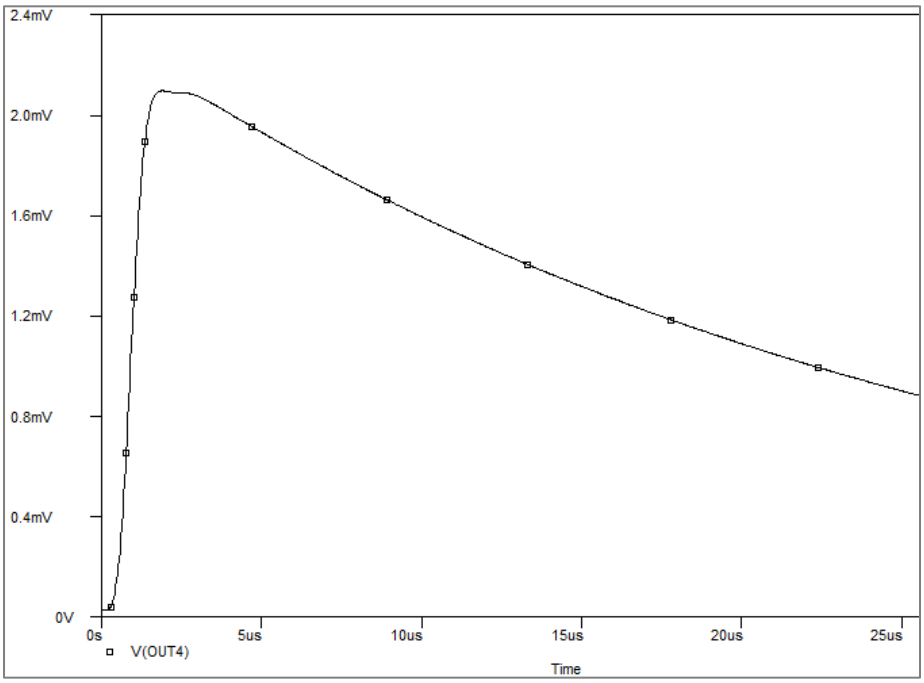

Fig. 3.52: Output waveform from simulation considering $R_t = 36.75\text{k}\Omega$

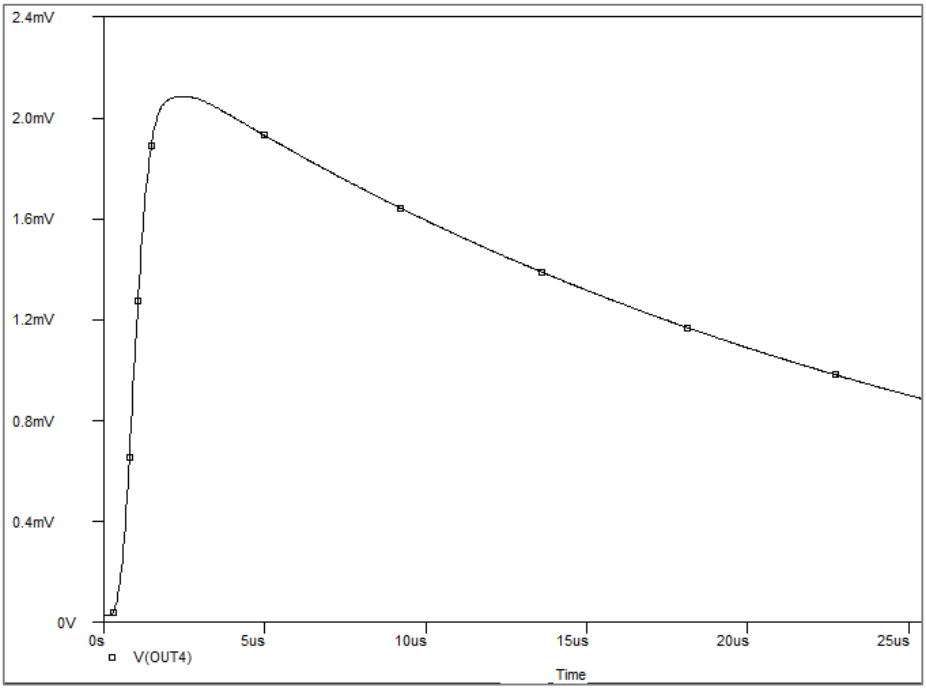

Fig. 3.53: Output waveform from simulation considering $R_t = 18.37\text{k}\Omega$

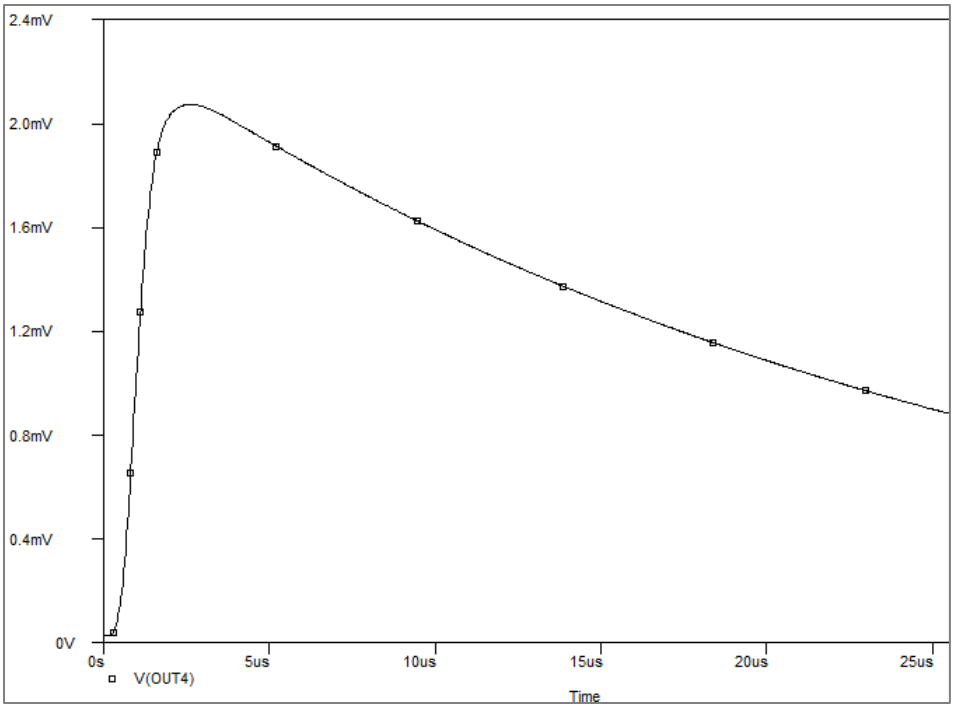

Fig. 3.54: Output waveform from simulation considering $R_t = 12.125\text{k}\Omega$

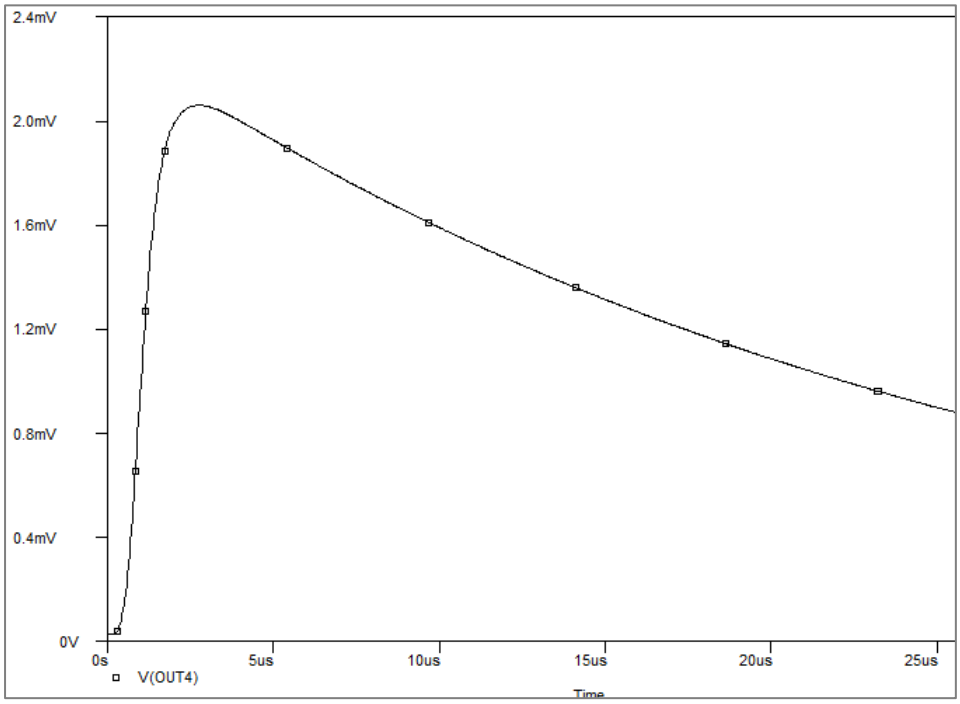

Fig. 3.55: Output waveform from simulation considering $R_t = 9.25\text{k}\Omega$

II. (e) With active integrator with coaxial cable terminated at series RC matching impedance connected to Oscilloscope

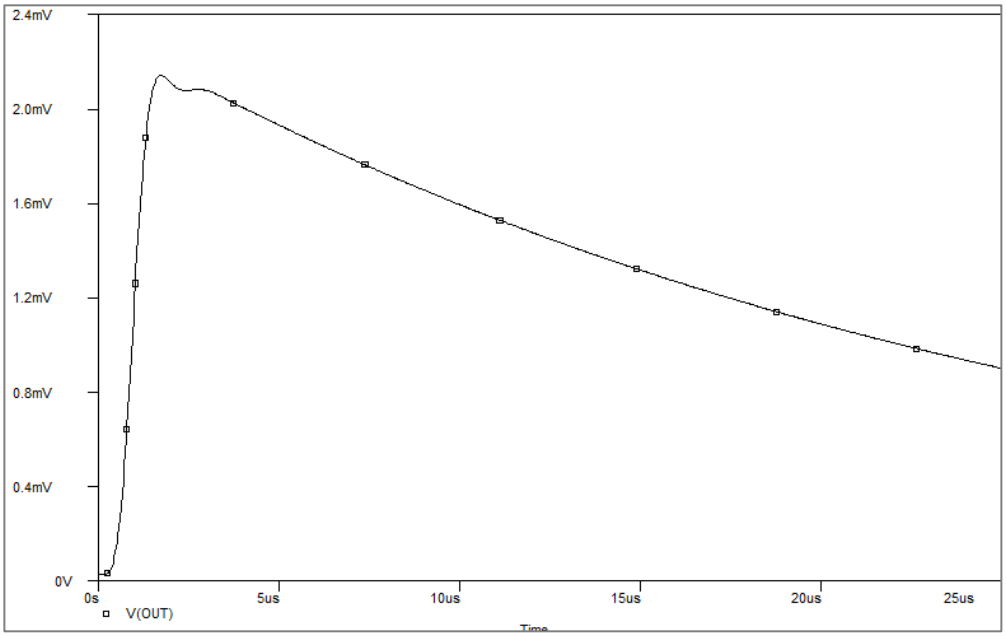

Fig. 3.56: Output waveform from simulation considering $R_t = 36.75\text{k}\Omega$

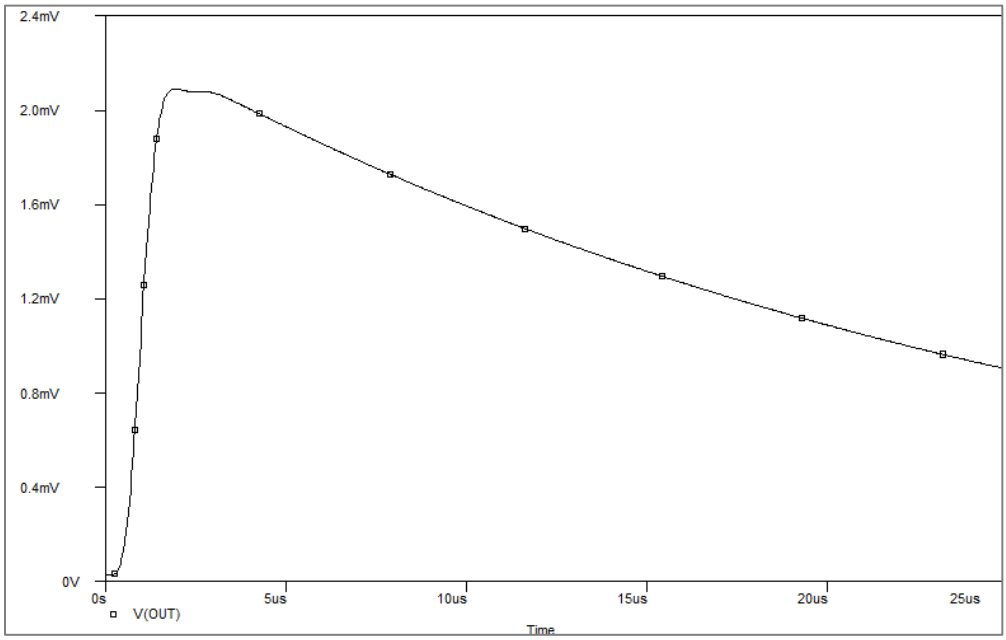

Fig. 3.57: Output waveform from simulation considering $R_t = 18.37\text{k}\Omega$

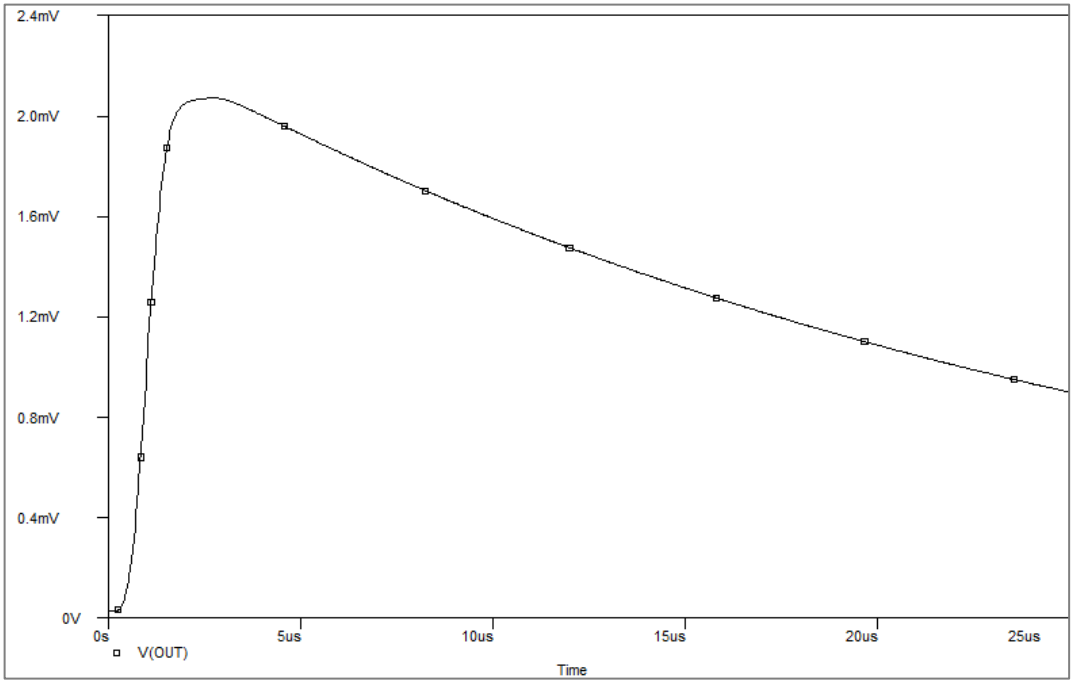

Fig. 3.58: Output waveform from simulation considering $R_t = 12.125\text{k}\Omega$

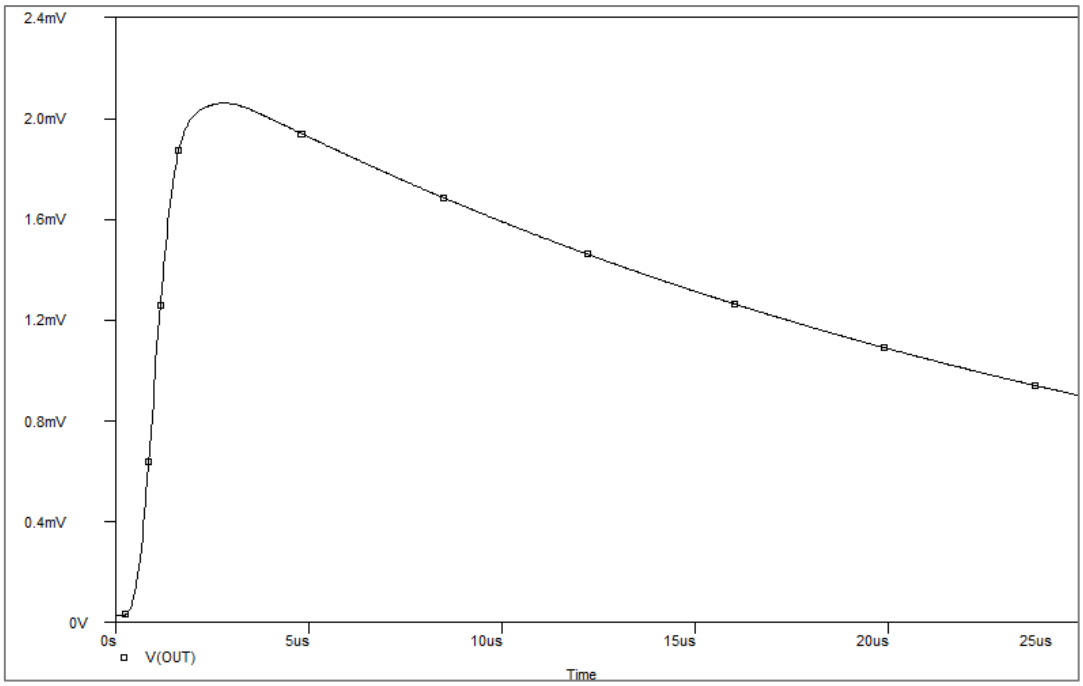

Fig. 3.59: Output waveform from simulation considering $R_t = 9.25\text{k}\Omega$

3.6.3 Error Analysis:

The percentage error of front time and tail time of the above output waveforms as compared to the input waveform at four different terminating resistance values table. I. have been obtained below.

I. LUMPED PARAMETER MODEL

I. (a) With passive integrator

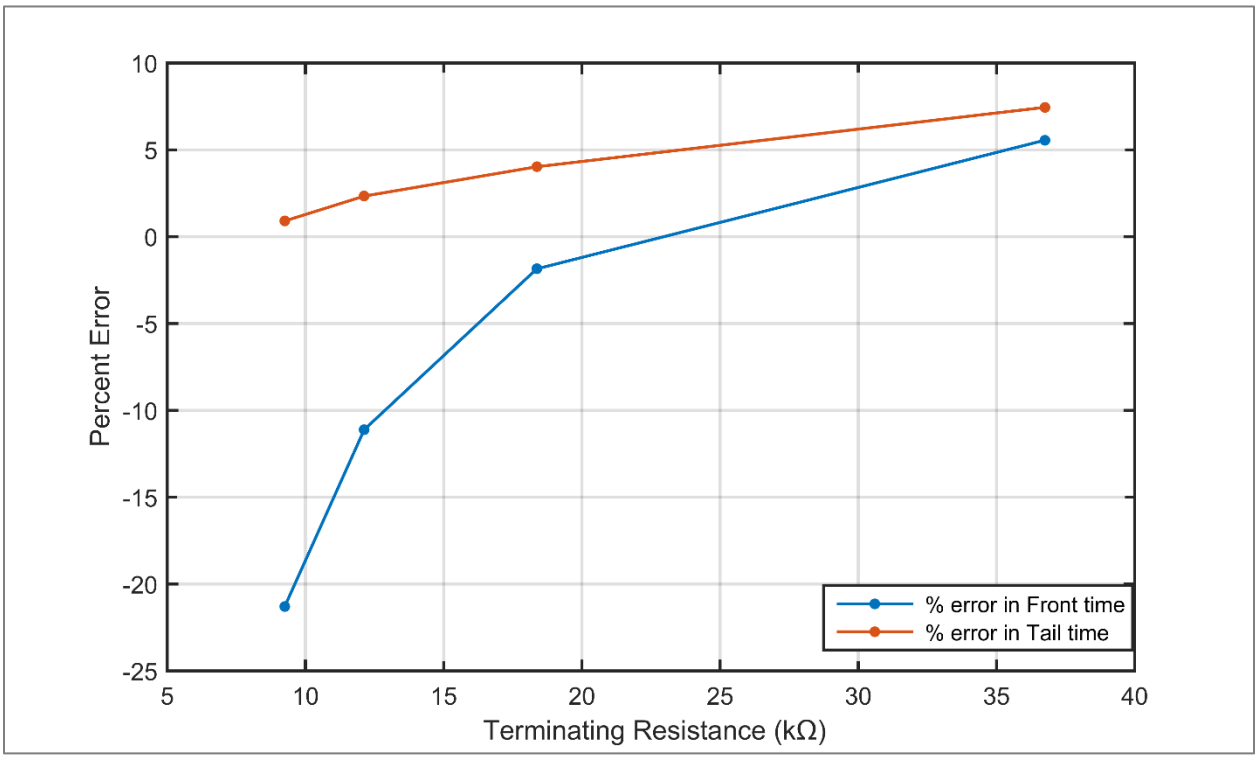

Fig I. (a): Percentage error of Front time and Tail time of output from input

I. (b) With passive integrator with coaxial cable connected to Oscilloscope

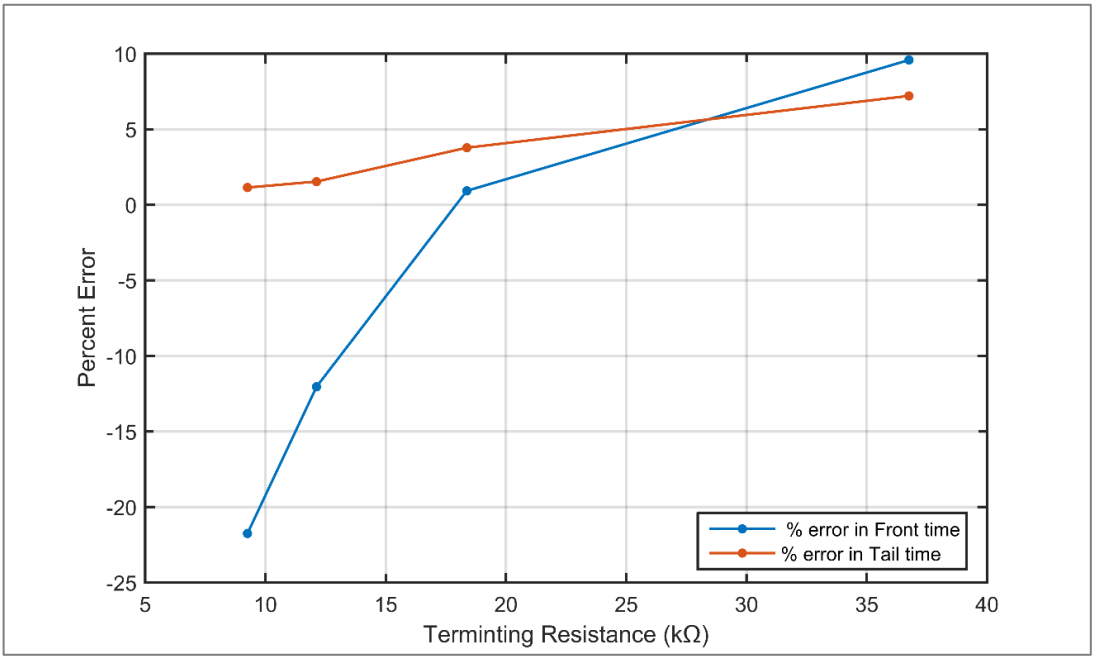

Fig I. (b): Percentage error of Front time and Tail time of output from input

I. (c) With active integrator with coaxial cable terminated at series RC matching impedance connected to Oscilloscope

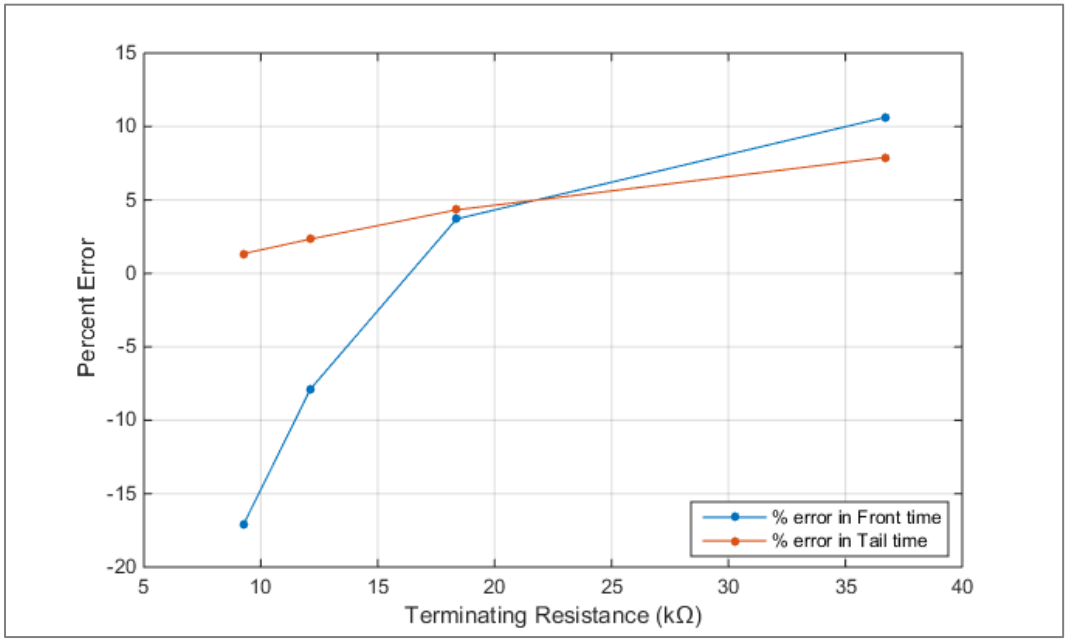

Fig I. (c): Percentage error of Front time and Tail time of output from input

I. (d) With active integrator

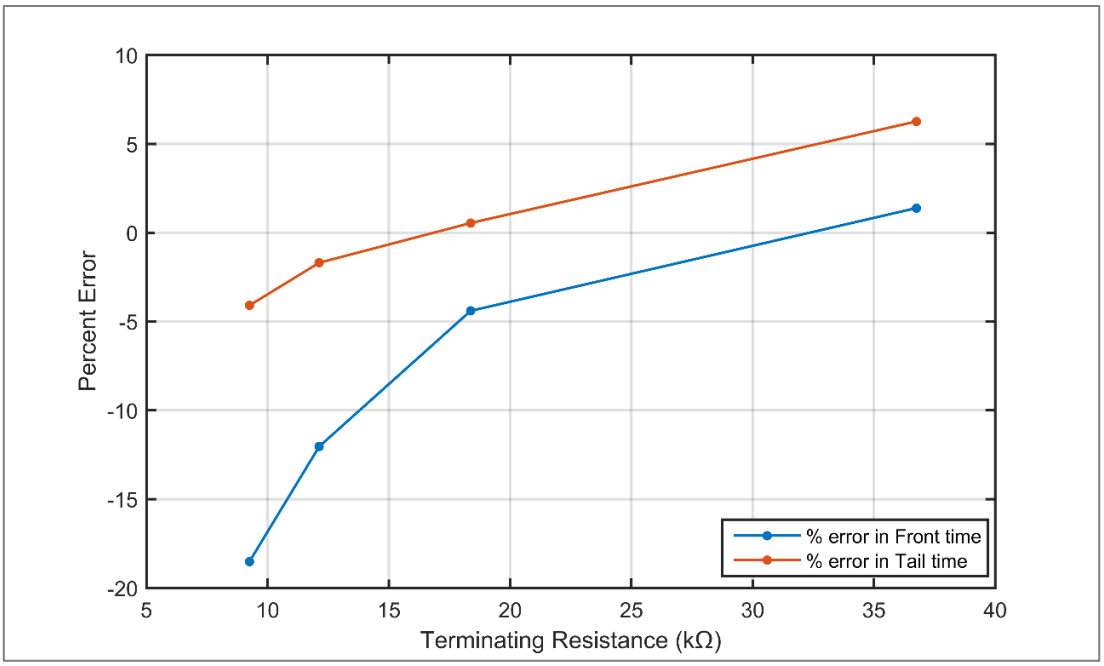

Fig I. (d): Percentage error of Front time and Tail time of output from input

I. (e) With active integrator with coaxial cable connected to Oscilloscope

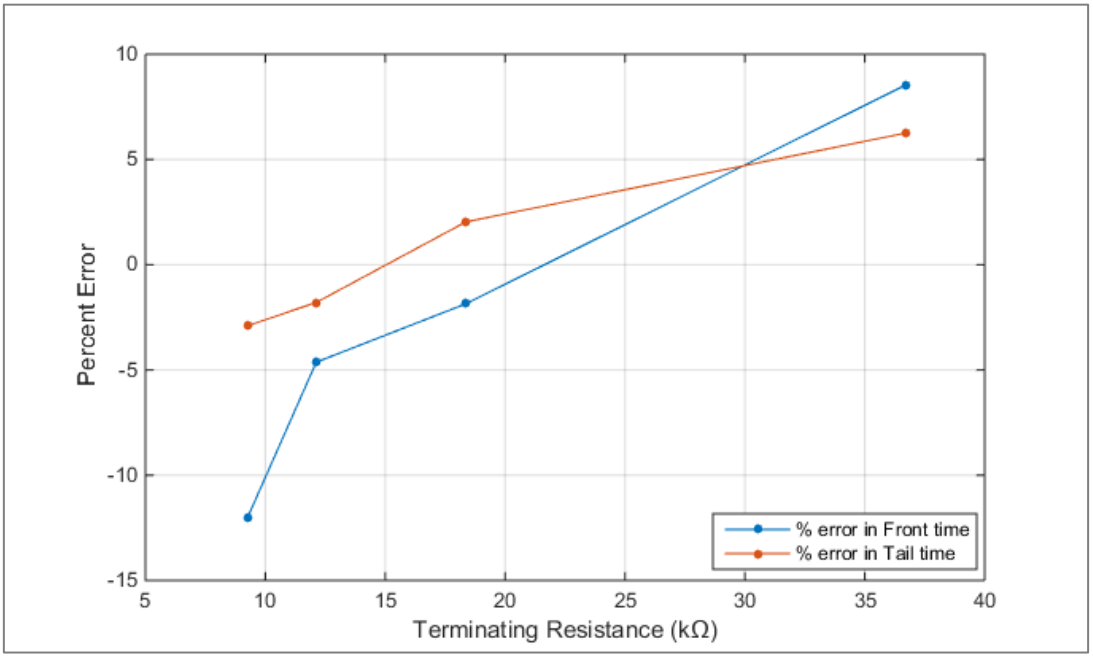

Fig. I. (e) Percentage error of Front time and Tail time of output from input

I. (f) With active integrator with coaxial cable terminated at series RC matching impedance connected to Oscilloscope

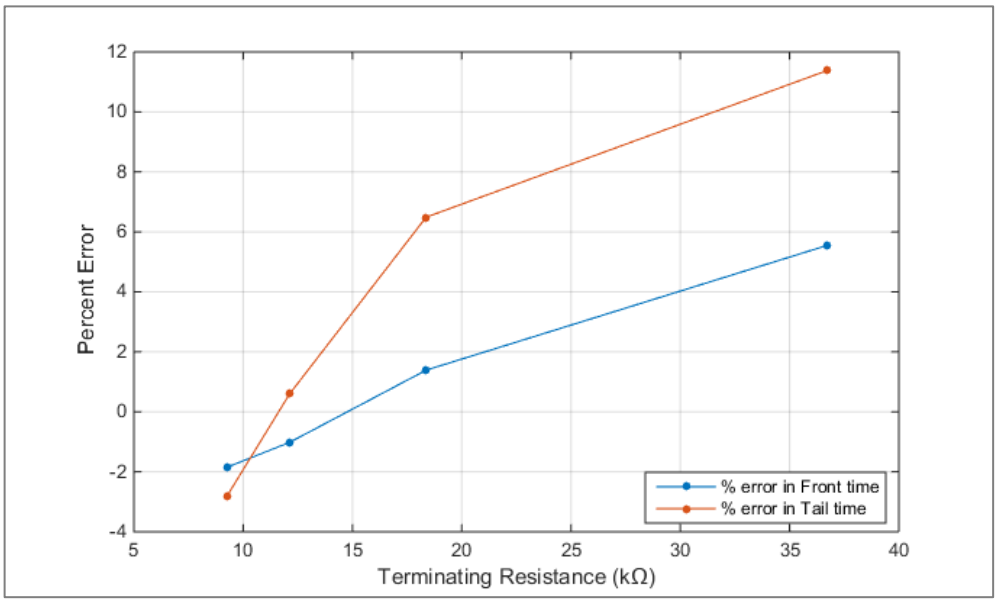

Fig. I. (f) Percentage error of Front time and Tail time of output from input

II. DISTRIBUTED PARAMETER MODEL

II. (a) With passive integrator

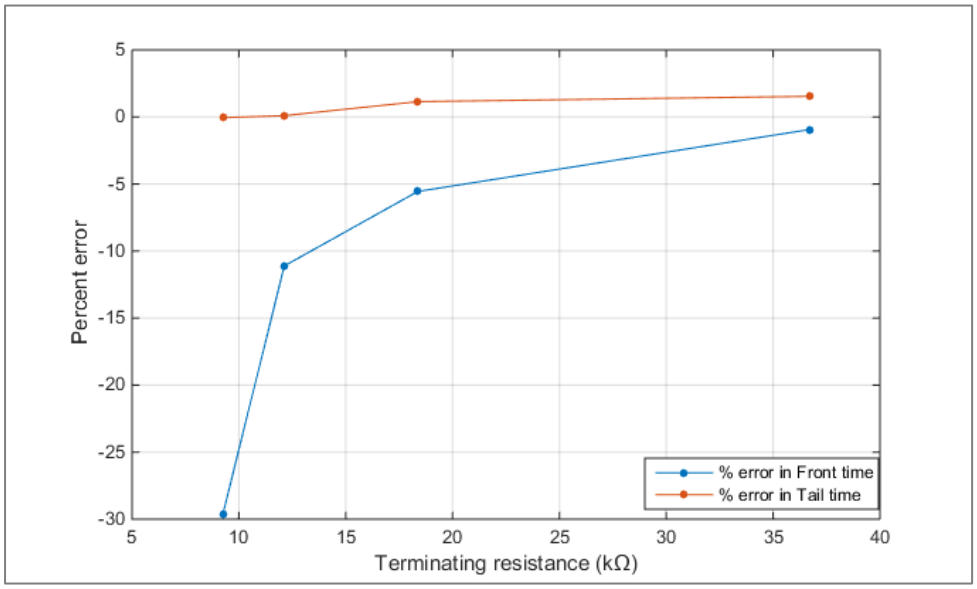

Fig. II. (a): Percentage error in Front Time and Tail Time of the output from input

II. (b) With passive integrator with coaxial cable connected to Oscilloscope

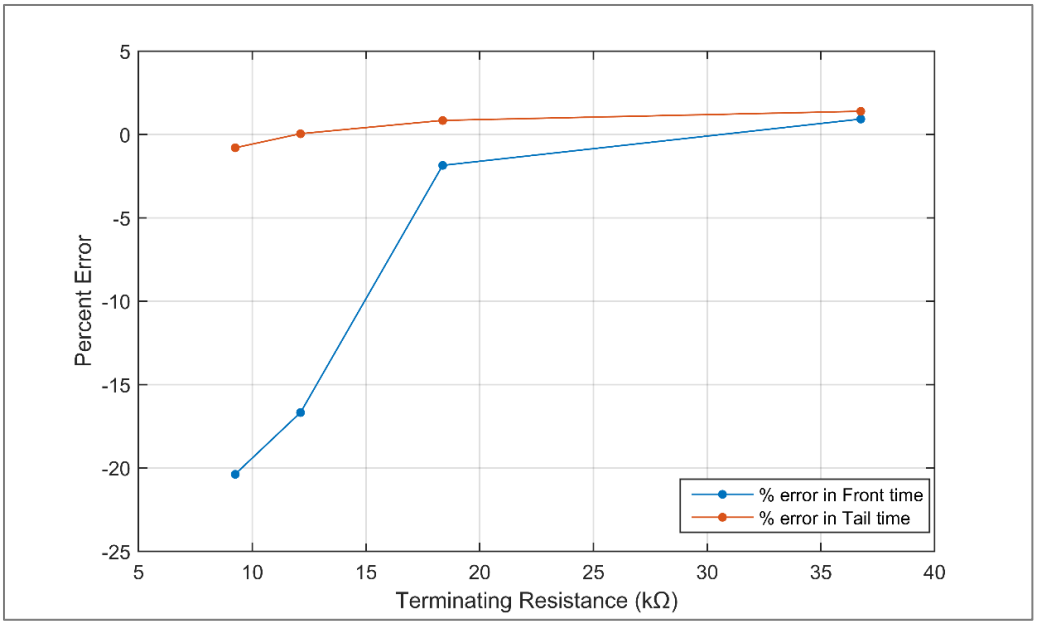

Fig. II. (b): Percentage error in Front Time and Tail Time of the output from input

II. (c) With passive integrator with coaxial cable terminated at series RC matching impedance connected to Oscilloscope

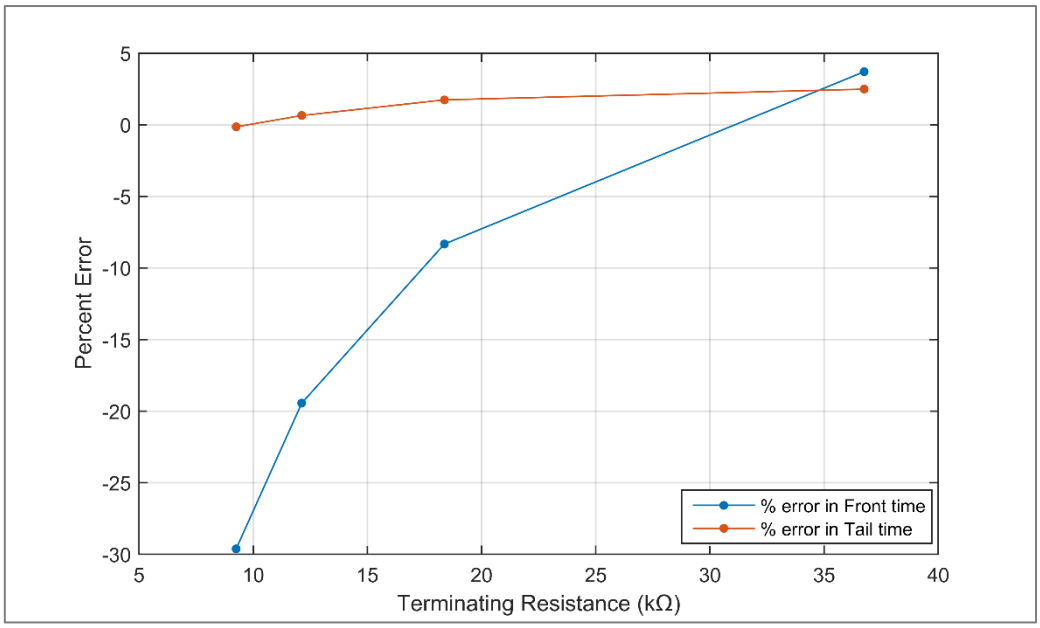

Fig. II. (c): Percentage error in Front Time and Tail Time of the output from input

II. (d) With active integrator

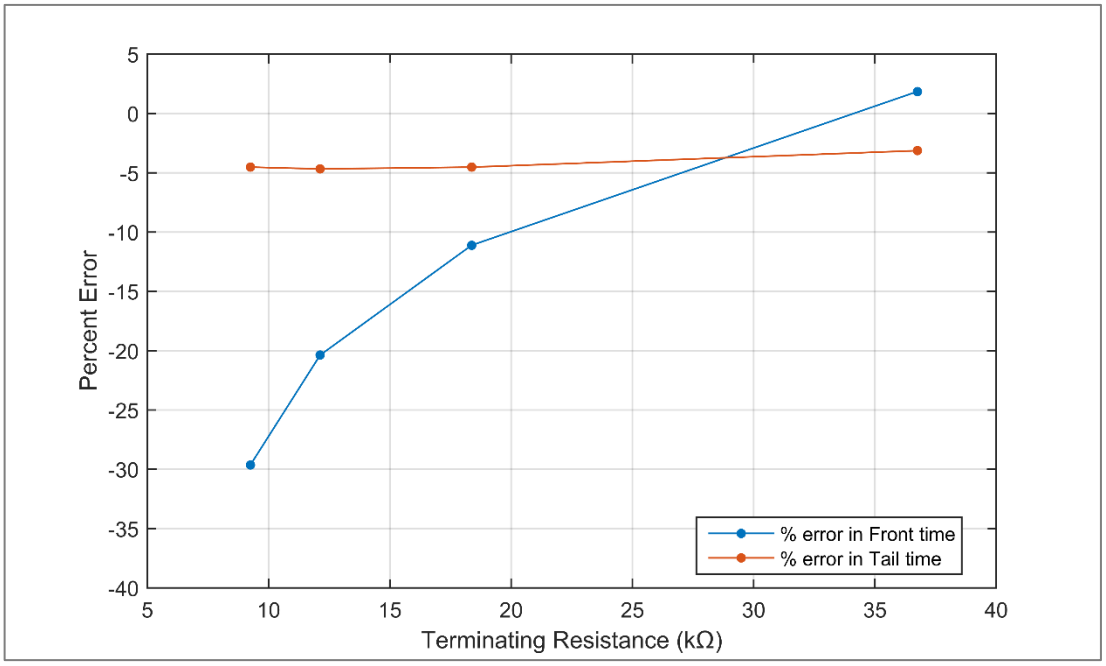

Fig II. (d): Percentage error in Front Time and Tail Time of the output from input

II. (e) With active integrator with coaxial cable connected to Oscilloscope

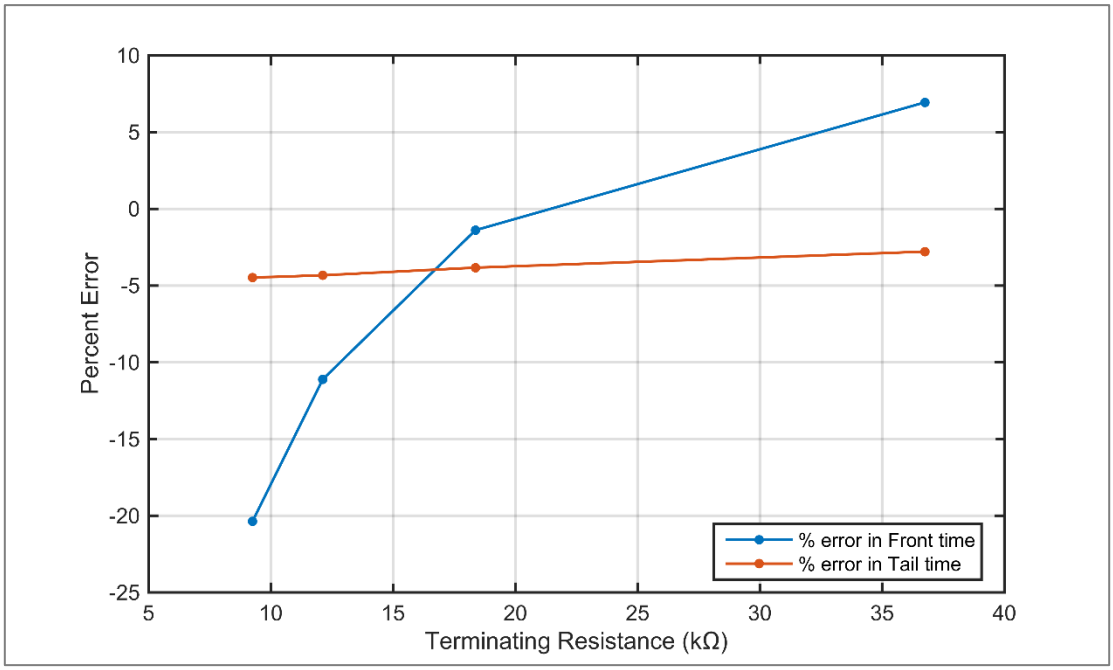

Fig. II (e): Percentage error in Front Time and Tail Time of the output from input

II. (f) With active integrator with coaxial cable terminated at series RC matching impedance connected to Oscilloscope

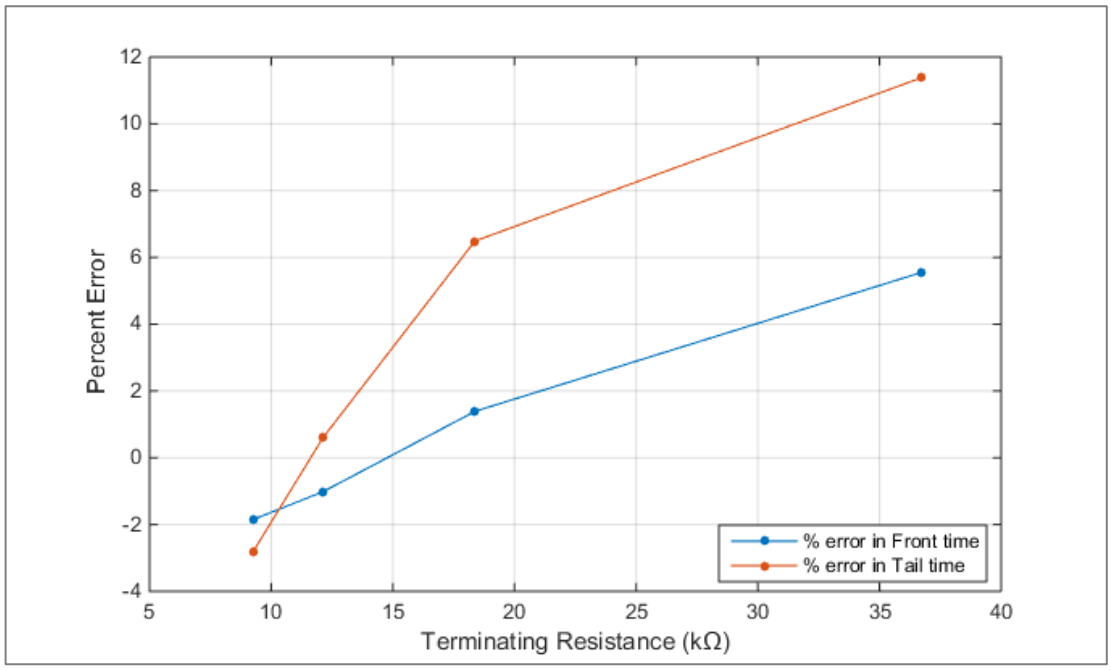

Fig. II (f): Percentage error in Front Time and Tail Time of the output from input

3.7 Discussion:

The impulse current of 1/20μs waveshape has been generated with the help of MATLAB. The front time at which the current reached to its peak value is 1.08μs and the time at which the peak current comes to its half value termed as tail time which is 20.11μs for the simulation. The integrator impedance has been chosen such that the frequency of the current is much greater than inverse of time constant of the system. The response of the impulse current has been performed in different conditions such as:

- Simulation results of all the circuit arrangements show that with increasing value of ξ, the values of corresponding front time and tail time increases. The reason is that with increasing zeta, damping increases which causes the system to lag.
- For ξ= 0.3 and 0.4, errors in front time are more than $\pm$10% in all the cases except that of lumped model with active integrator connected to oscilloscope. On the other hand, for ξ = 0.1 and 0.2, errors are considerably good in comparison to ξ greater than 0.2 where error in front time and tail time are well below$\pm$10%.
- Overall, the best results are observed in the case of distributed model with passive integrator connected to oscilloscope, with ξ=0.1& 0.2 where error in front time and error in tail time both are within $\pm$2%.
- For lumped model the best results obtained with active integrator with coaxial cable terminated at series RC matching impedance connected to oscilloscope with ξ=0.3 where error in front time and error in tail time both are within $\pm$1%.

Chapter 4: CONCLUSION

Conclusion

In this thesis, a simulation study has been carried out taking lumped and also partially distributed model of Rogowski coil considering passive and active integrator. For better performance analysis, simulations have been carried out for four different terminating resistance i.e., damping conditions. Simulation results show that as expected, distributed parameter model gives a better portrayal of the performance than lumped model in terms of getting the input current replica in the final output. Also, errors in front time and tail time of the output from that of the input, are well below ±10% which is a decent result. This distributed model with optimal parameters of the additional components used, can be utilized for performance analysis of various current measurement system employing Rogowski coil. It is obvious that subdividing the model into more lumped-parameter sections, would yield still better simulation results.

Despite the fact, this coil is invented decades ago; there are different fields, in which the research about the Rogowski coil is still continuing. By manipulating the associated parameters of the models, an approach can be taken into consideration for simulation to obtain better performance of these models of the Rogowski coil.

Appendix

Table 1: Lumped parameter model with passive integrator

Parameter symbol	Parameter Specifications
$\boldsymbol{R_i}$	10kΩ Resistance
$\boldsymbol{C_i}$	0.1μF Capacitor
$\mathbf{L_S}$	2.08mH Inductor
$\mathbf{C_S}$	38.5pF Capacitor
$\mathbf{R_C}$	119Ω Resistance
M	1.049μH Inductor
R	1mΩ Resistance
L	0.65nH Inductor
I	IPWL_FILE

Table 2: Lumped parameter model with passive integrator connected to oscilloscope

Parameter symbol	Parameter Specifications
$\boldsymbol{R_i}$	10kΩ Resistance
$\boldsymbol{C_i}$	0.1μF Capacitor
$\mathbf{L_S}$	2.08mH Inductor
$\mathbf{C_S}$	38.5pF Capacitor
$\mathbf{R_C}$	119Ω Resistance
M	1.049μH Inductor
R	1mΩ Resistance
L	0.65nH Inductor
I	IPWL_FILE
$\mathbf{R_O}$	1MΩ Resistance
$\mathbf{C_O}$	16pF Capacitor
$\mathbf{Z_O}$	75Ω Resistance

Table 3: Lumped parameter model with active integrator

Parameter symbol	Parameter Specifications
$\boldsymbol{R_i}$	10kΩ Resistance
$\boldsymbol{C_i}$	0.1μF Capacitor
L_S	2.08mH Inductor
C_S	38.5pF Capacitor
R_C	119Ω Resistance
M	1.049μH Inductor
R	1mΩ Resistance
L	0.65nH Inductor
I	IPWL_FILE
Rf	2.2MΩ Resistance

Table 4: Lumped parameter model with active integrator connected to oscilloscope

Parameter symbol	Parameter Specifications
$\boldsymbol{R_i}$	10kΩ Resistance
$\boldsymbol{C_i}$	0.1μF Capacitor
L_S	2.08mH Inductor
C_S	38.5pF Capacitor
R_C	119Ω Resistance
M	1.049μH Inductor
R	1mΩ Resistance
L	0.65nH Inductor
I	IPWL_FILE
R_O	1MΩ Resistance
C_O	16pF Capacitor
Z_O	75Ω Resistance
Rf	2.2MΩ Resistance

Table 5: Distributed parameter model with passive integrator

Parameter symbol	Parameter Specifications
$\boldsymbol{R_i}$	10kΩ Resistance
$\boldsymbol{C_i}$	0.1μF Capacitor
$\mathbf{L_{S1}}$, $\mathbf{L_{S2}}$, $\mathbf{L_{S3}}$, $\mathbf{L_{S4}}$	0.52mH Inductor
$\mathbf{C_{S1}}$, $\mathbf{C_{S2}}$, $\mathbf{C_{S3}}$, $\mathbf{C_{S4}}$	9.625pF Capacitor
$\mathbf{R_{c1}}$, $\mathbf{R_{c2}}$, $\mathbf{R_{c3}}$, $\mathbf{R_{c4}}$	29.75Ω Resistance
M	1.049μH Inductor
R	1mΩ Resistance
L	0.65nH Inductor
I	IPWL_FILE

Table 6: Distributed parameter model with passive integrator connected to Oscilloscope.

Parameter symbol	Parameter Specifications
$\boldsymbol{R_i}$	10kΩ Resistance
$\boldsymbol{C_i}$	0.1μF Capacitor
$\mathbf{L_{S1}}$, $\mathbf{L_{S2}}$, $\mathbf{L_{S3}}$, $\mathbf{L_{S4}}$	0.52mH Inductor
$\mathbf{C_{S1}}$, $\mathbf{C_{S2}}$, $\mathbf{C_{S3}}$, $\mathbf{C_{S4}}$	9.625pF Capacitor
$\mathbf{R_{c1}}$, $\mathbf{R_{c2}}$, $\mathbf{R_{c3}}$, $\mathbf{R_{c4}}$	29.75Ω Resistance
M	1.049μH Inductor
R	1mΩ Resistance
L	0.65nH Inductor
I	IPWL_FILE
$\mathbf{R_O}$	1MΩ Resistance
$\mathbf{C_O}$	16pF Capacitor
$\mathbf{Z_O}$	75Ω Resistance

Table 7: Distributed parameter model with active integrator

Parameter symbol	Parameter Specifications
$\boldsymbol{R_i}$	10kΩ Resistance
$\boldsymbol{C_i}$	0.1μF Capacitor
$\mathbf{L_{S1}}$, $\mathbf{L_{S2}}$, $\mathbf{L_{S3}}$, $\mathbf{L_{S4}}$	0.52mH Inductor
$\mathbf{C_{S1}}$, $\mathbf{C_{S2}}$, $\mathbf{C_{S3}}$, $\mathbf{C_{S4}}$	9.625pF Capacitor
$\mathbf{R_{c1}}$, $\mathbf{R_{c2}}$, $\mathbf{R_{c3}}$, $\mathbf{R_{c4}}$	29.75Ω Resistance
M	1.049μH Inductor
R	1mΩ Resistance
L	0.65nH Inductor
I	IPWL_FILE
Rf	2.2MΩ Resistance

Table 8: Distributed parameter model with active integrator connected to Oscilloscope.

Parameter symbol	Parameter Specifications
$\boldsymbol{R_i}$	10kΩ Resistance
$\boldsymbol{C_i}$	0.1μF Capacitor
$\mathbf{L_{S1}}$, $\mathbf{L_{S2}}$, $\mathbf{L_{S3}}$, $\mathbf{L_{S4}}$	0.52mH Inductor
$\mathbf{C_{S1}}$, $\mathbf{C_{S2}}$, $\mathbf{C_{S3}}$, $\mathbf{C_{S4}}$	9.625pF Capacitor
$\mathbf{R_{c1}}$, $\mathbf{R_{c2}}$, $\mathbf{R_{c3}}$, $\mathbf{R_{c4}}$	29.75Ω Resistance
M	1.049μH Inductor
R	1mΩ Resistance
L	0.65nH Inductor
I	IPWL_FILE
$\mathbf{R_O}$	1MΩ Resistance
$\mathbf{C_O}$	16pF Capacitor
$\mathbf{Z_O}$	75Ω Resistance
Rf	2.2MΩ Resistance

References

[1].David Jarry-Bolduc and Branislav Djokic 'Hydro generator sudden short circuit testing'.

[2]. Reza Sadeghi, Haider Samet, Teymoor Ghanbari and Darioush Daryabar 'Designing and manufacturing of electric arc furnace currents measurement system in Mobarakeh Steel Company by printed circuit board-type Rogowski coils.

[3]. Eric Vourc'h , Yu Wang , Pierre-Yves Joubert , Bertrand Revol1 , André Couderette, Lionel Cima 'Neel effect current sensors'.

[4]. Yannai Namia-Cohen, Yossi Sharon, Bagrat Khachatryan and Dima Cheskis' DC low current Hall effect measurements.

[5]. Zhou LI, Qiaogen ZHANG, Fenglian LIU and Xiaoya TAN 'Design of Rogowski coil with external integrator for measurement of lightning current up to 400kA'.

[6]. Valentinas Dubickas and Hans Edin 'High frequency model of the Rogowski coil with a small number of turns.'

[7] E. M. Abdel-Salam, "High Voltage Generation", in High Voltage
Engineering, M. Khalifa, New York: Marcel Dekker, 2000, pp.519-566.

[8]. N.H Halim, A. Azmi, Y.Yahya, F.Abdullah, M. Othman, and M.S. Laili The 5th international power engineering and optimization conference 'Development of A small scale standard lightning Impulse current Generator'.

[9]. Wang Jia and Zhang Xiaoqing 'Double Exponential Expression of Lightning Current Waveforms'.

[10]. Yuewu Shi, Wei Zhizhen Zhu, and Xin Nie 'The parameter Estimation of Double Exponential Pulse Based on a least infinity Norm Fitting Method'.

[11]. J.-P. Dupraz, A.Fanget, W. Grieshaber, and G. Montillet, "Rogowski coil: Exceptional current measurement tool for almost any application," in power engineering society General meeting, 2007.IEEE, June 2007, pp. 1-8.

[12]. A. Marinescu, "A calibration laboratory for Rogowski coil used in energy systems and power electronics," in optimization of electrical and electronic equipment (OPTIM), 2010 12th International conference on, May 2010, pp 913-919.

[13]. O. Poncelas, J.Rosero, J.Cusido, J. Ortega, and L. Romeral, " Motor fault detection using a Rogowski sensor without an integrator," Industrial Electronics, IEEE Transactions on, vol. 58,no.1, pp, 122-128,Jan 2009.

[14]. L. Kojovic, "PCB Rogowski coils benefit relay protection,' computer applications I power, IEEE, vol 15, no.3 pp. 50-53,Jul 2002

[15]. Y. Hongwei, Y. Dahai, Y. Xianggen and L. Weibo, "Study of a novel CT for short-circuited current measurement," in Transmission and Distribution conference and exhibition: Asia and Pacific, 2005 IEEE/PES, 2005 pp.1-5.

[16]. C. Xianghu, Z. Xiangjun, D.Feng, and L.Ling, "Novel PCB sensor based on Rogowski coil transmission lines fault detection," in Power energy Society General meeting, 2009.

[17]. X.Minjiang, G. Houlei, Z. Baoguang, W. Chengzhang, and T. Chun," Analysis on transfer characteristics of Rogowski coil trasducer to travelling wave,". In advance power systemautomation and protection (APAP) , 2011 International Conference on, vol. 2, Oct 2011.

[18]. G . Hashmi, M. Lehtonen, and A.ELHAFFAR, " Modelling of Rogowski coil for on-line PD monitoring in covered-conductor overhead distribution networks," Pulse, vol. 1,p. P2, 2007

[19]. S. Wang, X. Cao, and L.Chen, " Study of ECT based on Rogowski coil used in smart substation," in Power Engineering and Optimization Conference (PEOCO), 2013 IEEE 7th International, June 2013.

[20]. M. Chiampi, G. Crotti, and A.Morando, "Evaluation of flexible Rogowski coil performances in power frequency applications," Intrumentation and Measurement, IEEE Transactions on, vol.60,no.3.

[21]. K. Yamamoto, N.Ueda, A. Ametani, and D. Natsuno, "A study of lightning current distribution at a wind turbine foot: Influence on current measurements using a Rogowski coil,"

[22]. N. R. Prakash, K. Flora, R. Babu , R. Gangradey, and H.Patel, "Design and development of Rogowski Coil sensors for eddy current measurement on toroidal vessel," Journal of fusion energy , vol.32, no.2.

[23] J. Hlavacek, R. Prochazka, M. Knenicky, K. Draxler and R. Styblikova, "Influence of Rogowski coil shielding to measurement results," *2016 17th International Scientific Conference on Electric Power Engineering (EPE)*, 2016, pp. 1-5.